Centro Fermi
Museo Storico della Fisica e Centro Studi e Ricerche Enrico Fermi

K^-

Investigation of the low-energy kaons hadronic interactions in light nuclei by AMADEUS

Dr. Kristian Piscicchia*

Museo Storico della Fisica e Centro Studi e Ricerche Enrico Fermi
INFN, Laboratori Nazionali di Frascati

12 March 2014, the Galileo Galilei Institute for Theoretical Physics , Arcetri, Florance

*kristian.piscicchia@lnf.infn.it

Study of Strongly Interacting Matter
HadronPhysics3

INFN
Istituto Nazionale di Fisica Nucleare

Framework:
Low-Energy QCD with Strange Quarks

K^-

Strangeness in baryonic matter:

- role of strangeness in EoS of neutron stars

- hyperon-nucleon and hyperon-hyperon interactions role in the investigation of dense baryonic matter

- new constraints from 2 solar masses neutron stars, very stiff Equation of State required!

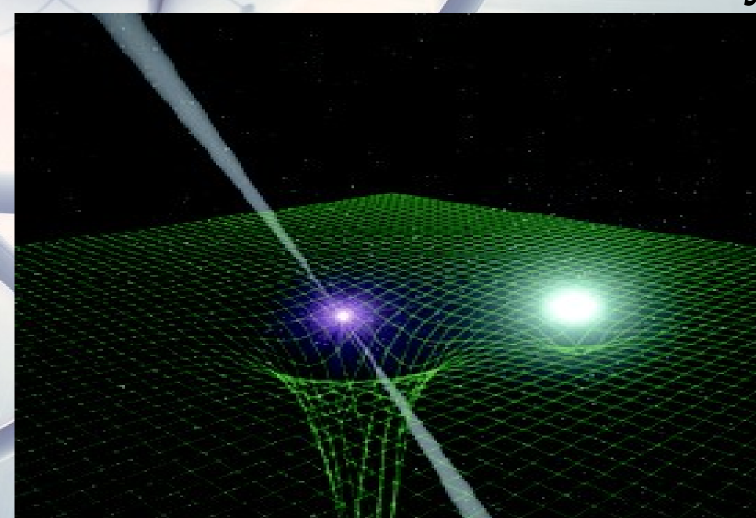

But

- the basic ingredient .. namely $\bar{K}N$ interaction still unclear and mysterious from the experimental point of view.

K^-

Framework: Low-Energy QCD with Strange Quarks

Approached by the investigation of the antikaon-nucleon interaction

Important constraints:

- **K^-N threshold physics (shift and with of kaonic atoms levels measured by SIDDHARTA)**
- **$\Sigma\pi$ mass spectra**
- **Nature and properties of the $\Lambda(1405)$ considered as K^-N quasibound state embedded in the $\Sigma\pi$ continuum**

K^-

Framework:
Low-Energy QCD
with Strange Quarks

CHIRAL PERTURBATION THEORY
Interacting systems of NAMBU-GOLDSTONE BOSONS
(pions, kaons) coupled to BARYONS

$$\mathcal{L}_{eff} = \mathcal{L}_{mesons}(\Phi) + \mathcal{L}_B(\Phi, \Psi_B)$$

works well for low-energy pion-pion and pion-nucleon interactions

... but NOT for systems with strangeness S = –1

BECOUSE Λ(1405) just below K^-N threshold (1432 MeV)

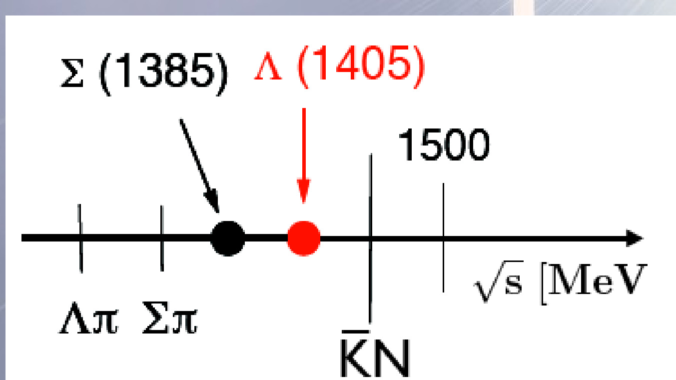

——>

Solutions:

- **Non-perturbative Coupled Channels approach based on Chiral SU(3) Dynamics**
- **phenomenological $\bar{K}N$ and NN potentials**

Scientific case Λ(1405)

K^-

Λ(1405) : mass = $1405.1^{+1.3}_{-1.0}$ MeV, width = 50 ± 2 MeV

I = 0, S = -1 , J^p = 1/2$^-$, Status: ** , strong decay into Σπ**

Its nature has been a puzzle for decades: three quark state, unstable $\overline{K}N$ bound state, penta-quark, two poles??

First experimental evidence:

M. H. Alston, et al., Phys. Rev. Lett. 6 (1961) 698

$K^- p \rightarrow \pi\pi\pi\Sigma$

Λ(1405)

Λ(1116)

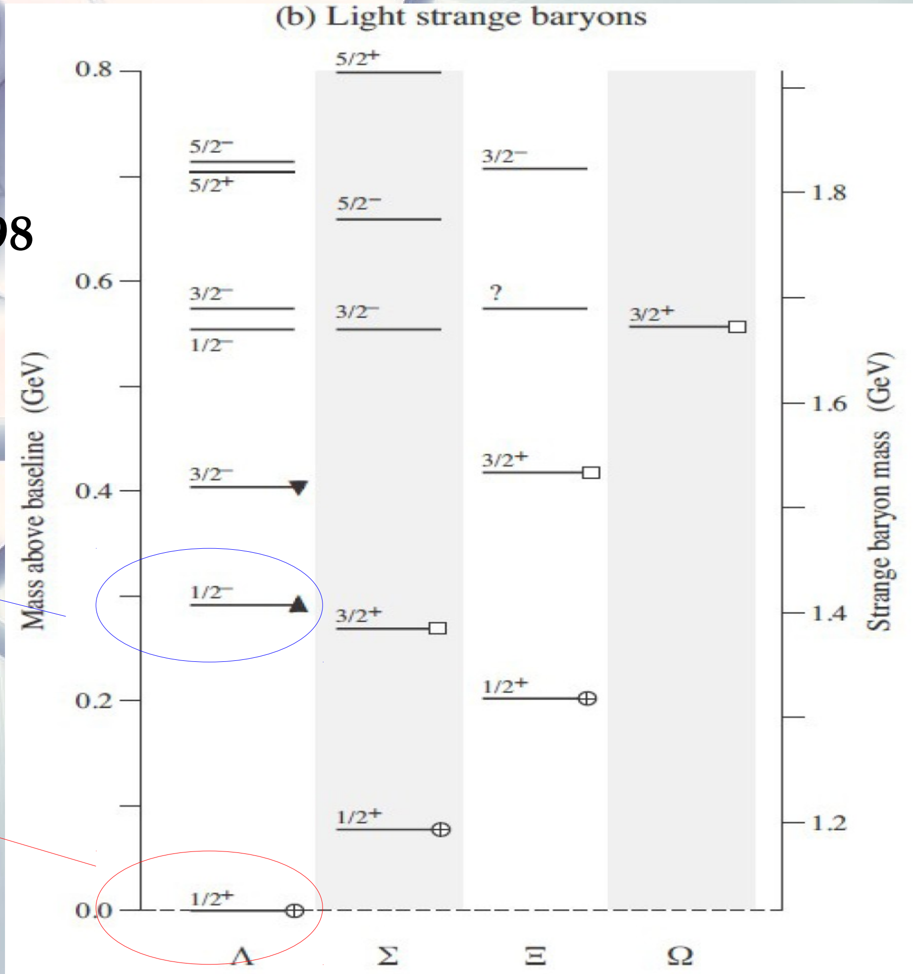

Scientific case Λ(1405)

Λ(1405) is a negative parity baryon resonance (spin = 1/2, isospin = 0, strangeness = -1) located slightly below the KN threshold, decaying into the Σπ channel through the strong interaction.

The three quark model picture has some difficulties to reproduce the Λ(1405). According to its negative parity, one of the quarks has to be excited to the *l* = 1 orbit. Similar to the nucleon sector, where one of the lowest negative parity baryon is the N(1535), the expected mass of the Λ^* is around 1700 MeV (since it contains one strange quark). Another difficulty is the energy splitting observed between the Λ(1405) and the Λ(1520), if is interpreted as the spin-orbit partner ($J^p = 3/2^-$).

R. Dalitz and collaborators first suggested to interpret Λ(1405) as an KN quasibound state.

R.H. Dalitz, T.C. Wong and G. Rajasekaran, Phys. Rev. **153** (1967) 1617.

Scientific case $\Lambda(1405)$

- Chiral unitary models: $\Lambda(1405)$ is an $I = 0$ quasibound state emerging from the coupling between the $\bar{K}N$ and the $\Sigma\pi$ channels. Two poles in the neighborhood of the $\Lambda(1405)$:

4) *two poles*: $(z_1 = 1424^{+7}_{-23} - i\, 26^{+3}_{-14}$; $z_1 = 1381^{+18}_{-6} - i\, 81^{+19}_{-8})$ MeV (Nucl. Phys. A881, 98 (2012))

mainly coupled to $\bar{K}N$ mainly coupled to $\Sigma\pi$ → line-shape depends on production mechanism

- Akaishi-Esmaili-Yamazaki phenomenological potential

Phys. Lett. B 686 (2010) 23-28 Confirmation of single pole ansatz?

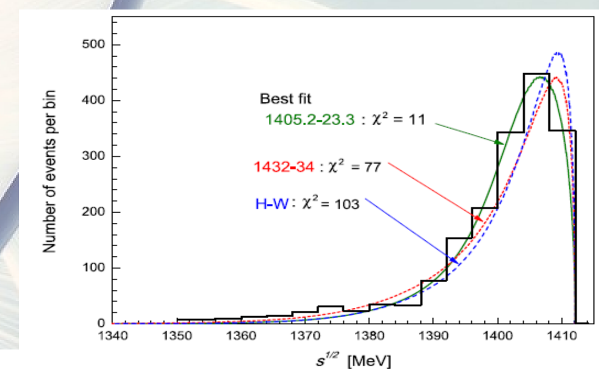

Fig. 6. Detailed differences in $M_{\Sigma\pi}$ spectra among the Hyodo–Weise prediction and the present model predictions.

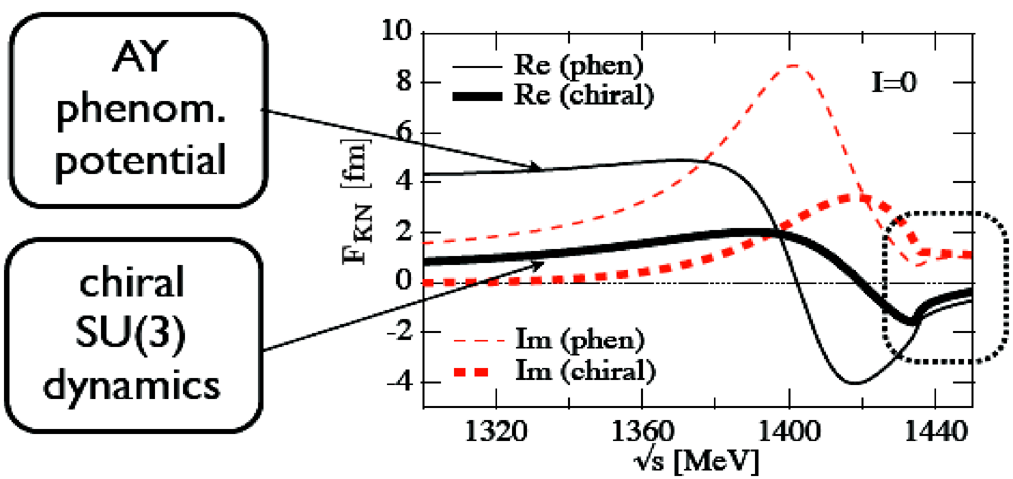

large differences in **subthreshold** extrapolations

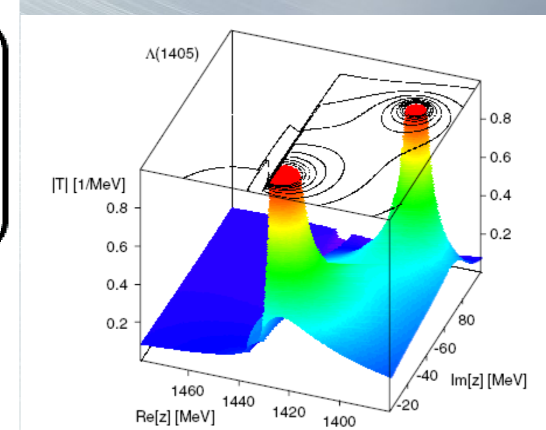

- **Chiral dynamics** predicts significantly **weaker attraction** than AY (local, energy independent) potential in **far-subthreshold** region

Scientific case Λ(1405)

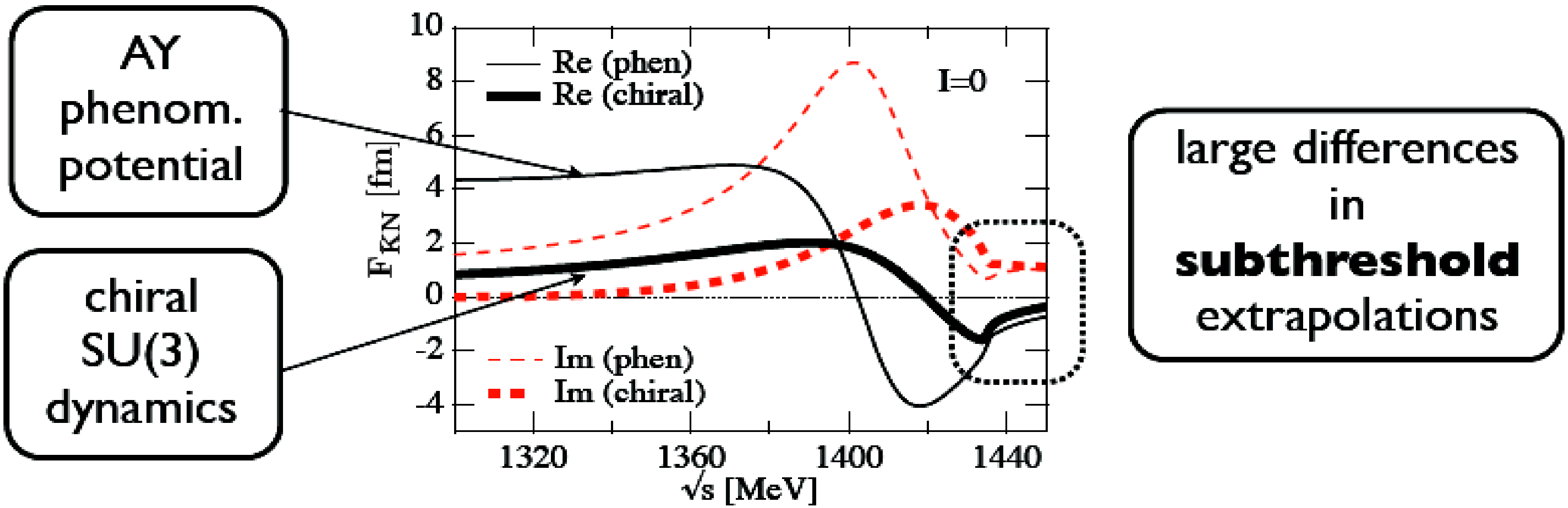

- **Chiral dynamics** predicts significantly **weaker attraction** than AY (local, energy independent) potential in **far-subthreshold** region

TO TEST THE HIGHER POLE:

- **production in $\bar{K}N$ reactions** (only chance to observe the high mass pole)
- **decaying in $\Sigma^0\pi^0$** (free from Σ(1385) background I=1)

Distribution shape depends

on the decay channel:

$$\frac{d\sigma(\Sigma^-\pi^+)}{dM} \propto \frac{1}{3}\left|T^0\right|^2 + \frac{1}{2}\left|T^1\right|^2 + \frac{2}{\sqrt{6}}Re(T^0T^{1*})$$

$$\frac{d\sigma(\Sigma^+\pi^-)}{dM} \propto \frac{1}{3}\left|T^0\right|^2 + \frac{1}{2}\left|T^1\right|^2 - \frac{2}{\sqrt{6}}Re(T^0T^{1*})$$

$$\frac{d\sigma(\Sigma^0\pi^0)}{dM} \propto \frac{1}{3}\left|T^0\right|^2$$

Scientific case $\Lambda(1405)$

K^- nuclear absorption experiments .. long history .. BUT

K^-

1) $m_{\pi\Sigma}$ spectra CUT AT THE ENERGY LIMIT AT-REST **2) $(\Sigma\pm\pi\mp)$ $\Sigma(1385)$ CONTAMINATION**

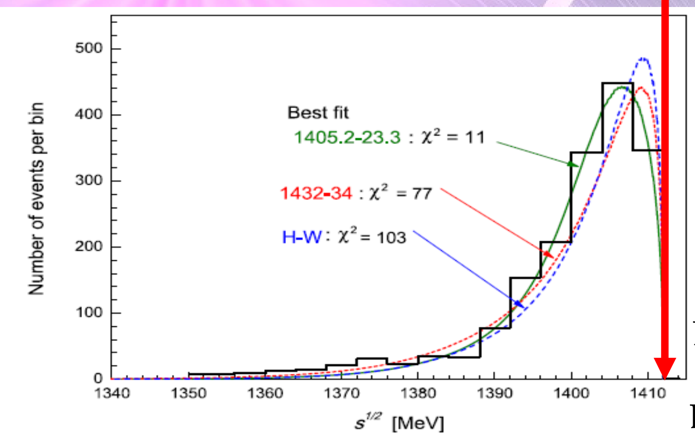

Fig. 6. Detailed differences in $M_{\Sigma\pi}$ spectra among the Hyodo–Weise prediction and the present model predictions.

"A study of K^- $^4He \rightarrow (\Sigma\pm\pi\mp) + {}^3H$ using slow instead of stopping K^- would be very useful in eliminating some of the uncertainties in interpretation"

D. Riley, et al. Phys. Rev. D11 (1975) 3065

Esmaili et el., Phys.Lett. B686 (2010) 23-28

P. J. Carlson, et al. Nucl. Phys. 74 642

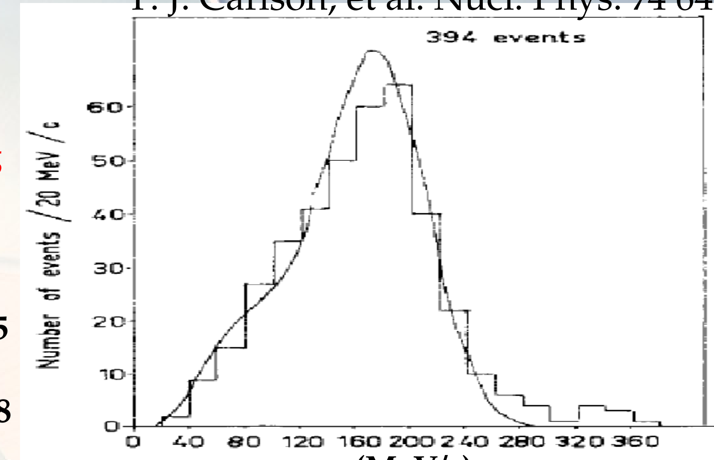

The $\Sigma^0\pi^0$ spectrum was only observed in 3 experiments … with different line-shapes !

I. Zychor et al., Phys. Lett. B 660 (2008) 167

K. Moriya, et al., (Clas Collaboration) Phys. Rev. C 87, 035206 (2013)

Magas et al. PRL 95, 052301 (2005) 034605 S. Prakhov, et al., Phys. Rev. C70 (2004)

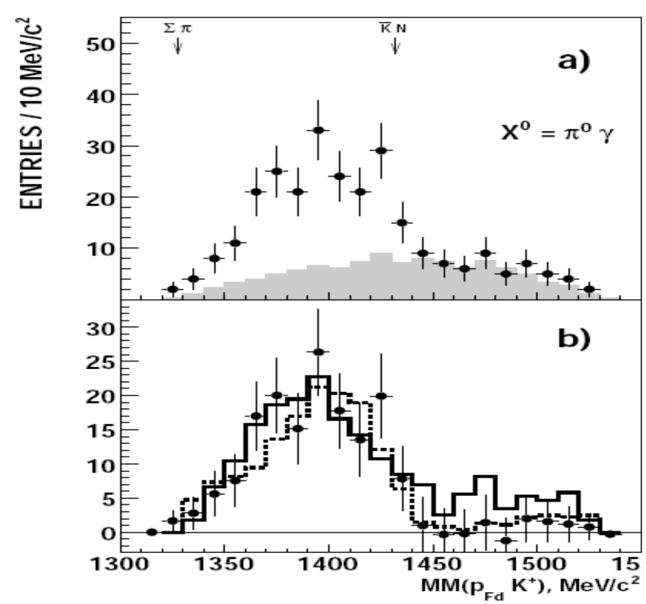

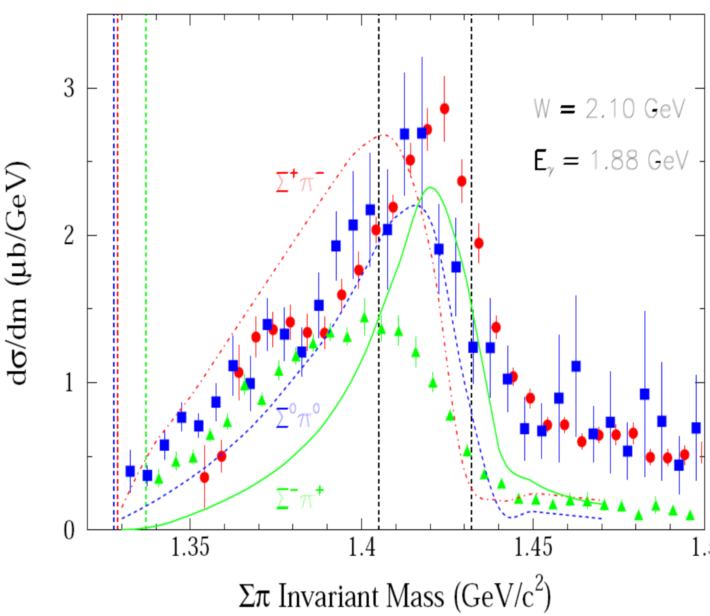

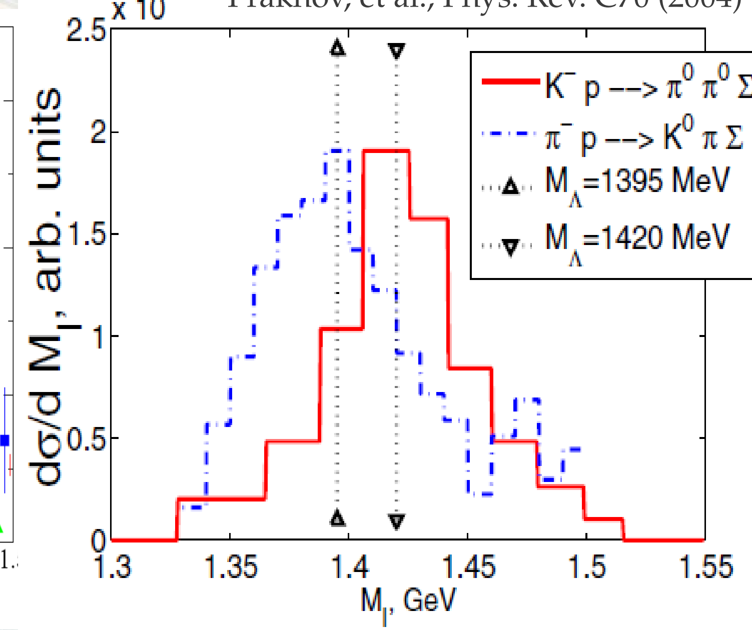

TWO SAMPLES OF DATA:

K^-

- 2004-2005 KLOE data (Analyzed luminosity of ~1.5 fb^{-1})

K^- absorbed in KLOE materials (H, ^4He, ^9Be, ^{12}C)
At-rest + In-flight

- Dedicated 2012 run with pure graphite Carbon target inside KLOE
(~90 pb^{-1}; analyzed 37 pb^{-1}, x1.5 statistics)

K^- ^{12}C absorptions At-rest

AMADEUS & DAΦNE with KLOE

K^-

DAΦNE

Double ring $e^+ e^-$ collider working in C. M. energy of ϕ, producing ≈ 600 $K^+ K^-$ /s

$\phi \rightarrow K^+ K^-$ (BR = (49.2 ± 0.6)%)

- low momentum Kaons ≈ 127 Mev/c
- back to back $K^+ K^-$ topology

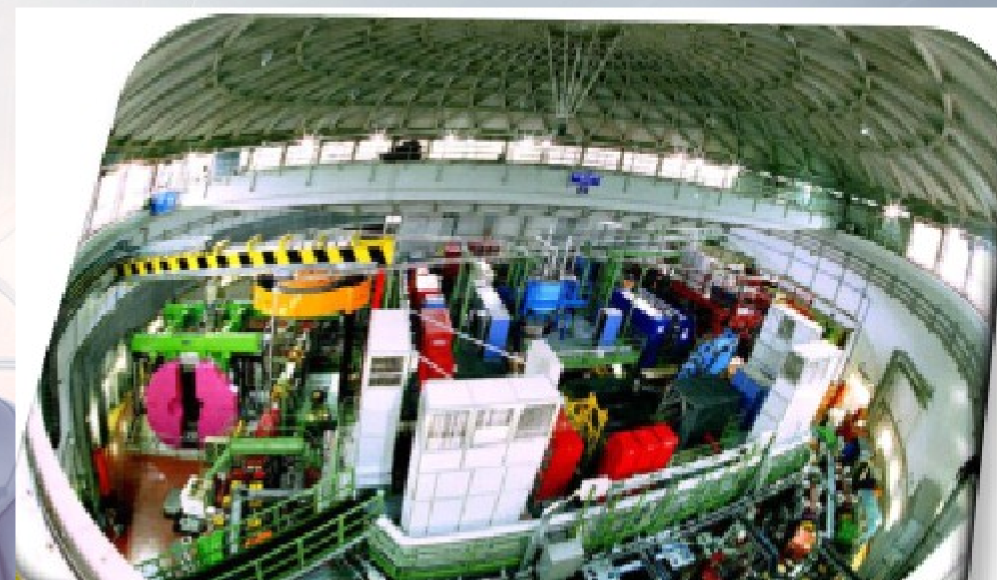

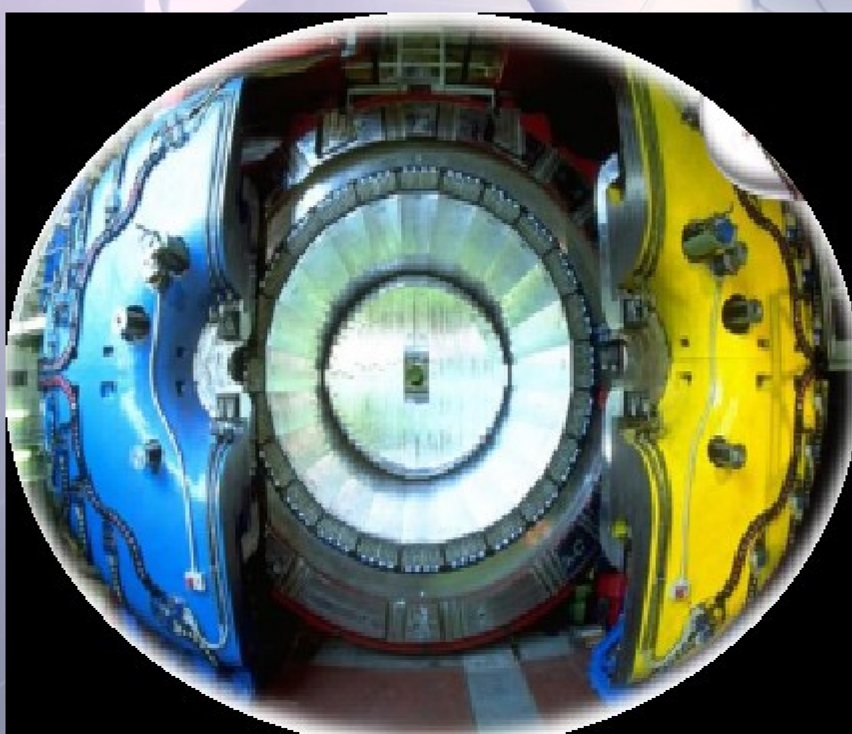

KLOE

- 96% acceptance,
- optimized in the energy range of all charged particles involved
- good performance in detecting photons (and neutrons checked by kloNe group (M. Anelli et al., Nucl Inst. Meth. A 581, 368 (2007)))

Low-energy K^- hadronic interactions studies with KLOE, why?

MC simulations show that :

- ~ 0.1 of K^- stopped in the DC gas (90% He, 10% C_4H_{10})
- ~2% of K^- stopped in the DC wall (750 μm c. f. , 150 μm Al foil).

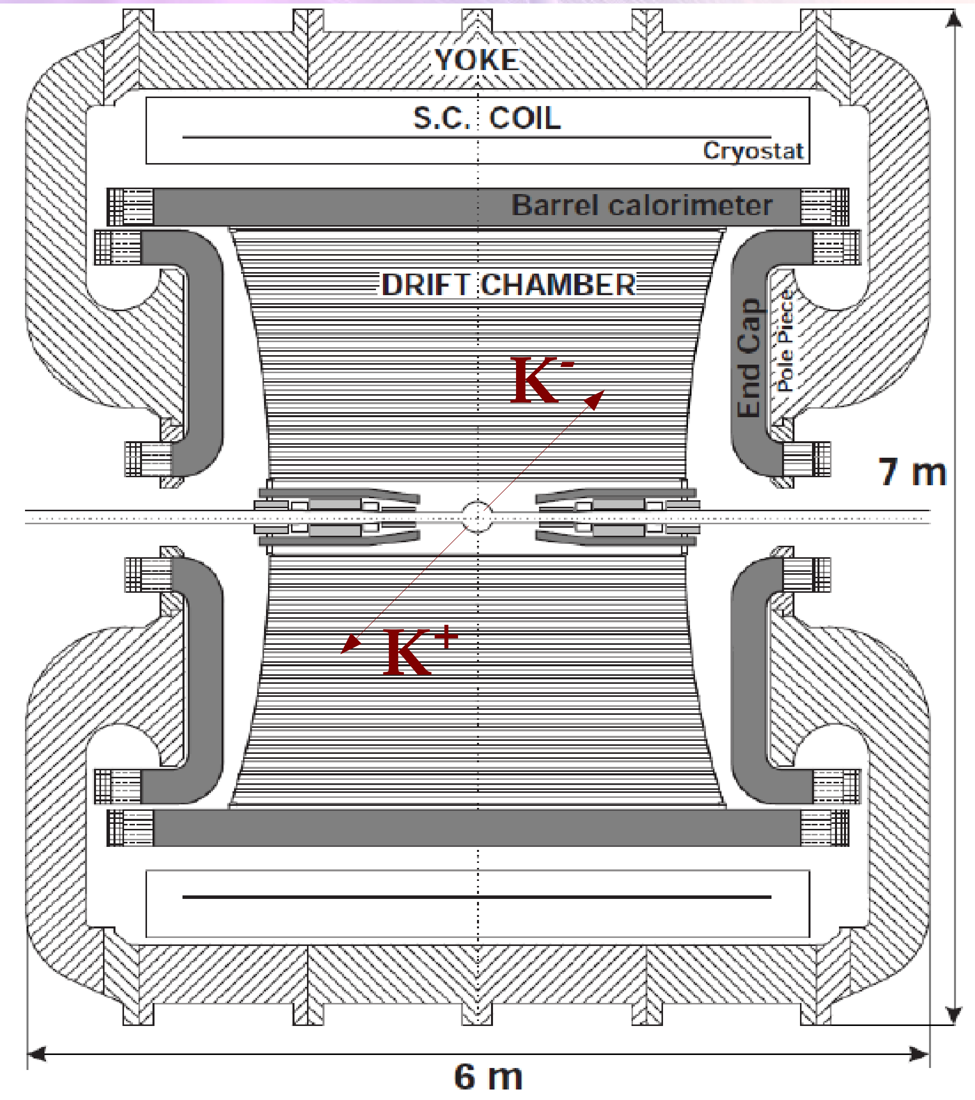

Possibility to use KLOE materials as an active target

Advantage:
excellent resolution ..

$\sigma_{p\Lambda}$ = 0.49±0.01 MeV/c in DC gas

$\sigma_{m\gamma\gamma}$ = 18.3±0.6 MeV/c^2

Disadvantage:
Non dedicated target → different nuclei contamination → complex interpretation ..
but → new features .. K^- in flight absorption.

Carbon target inside KLOE

K^-

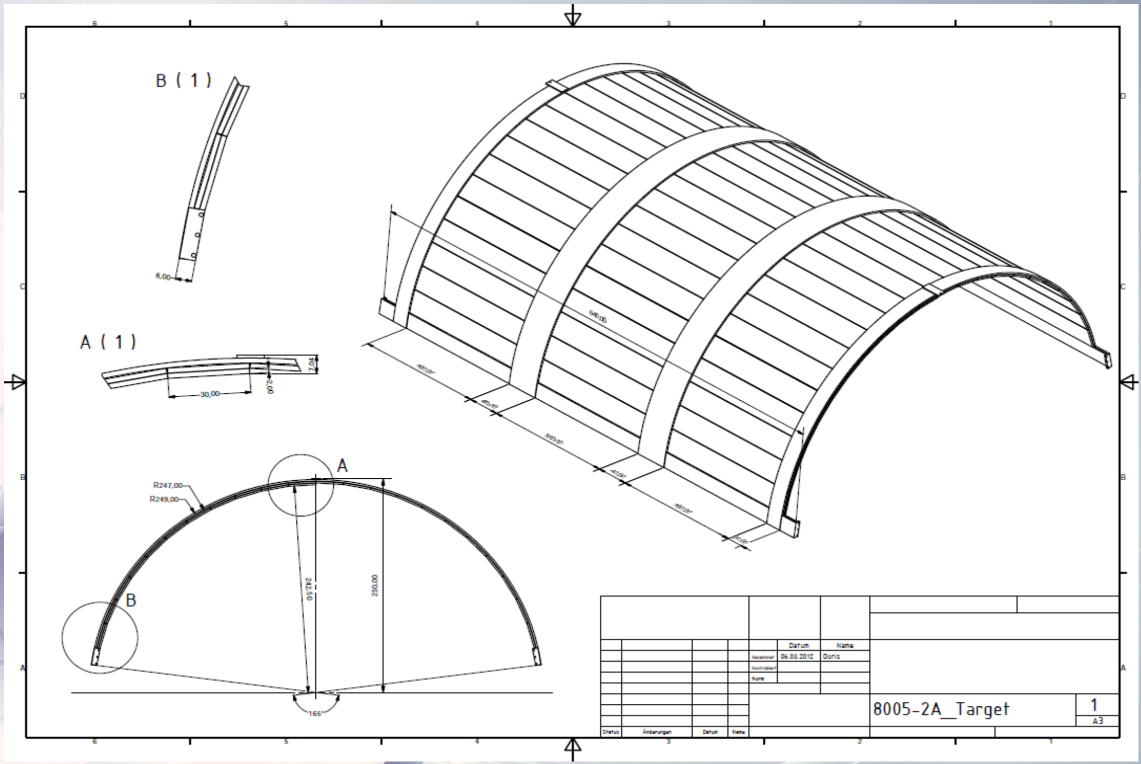

Advantages:

- gain in statistics
- K^- absorptions occur in Carbon
- absorptions at-rest.

- MC simulation: 26% of K^- stopped in C, 2% of K^- stopped in Al hence aluminium contamination from 19% → 7% !

- Thickness optimazied (based on MC simulations) to maximize the number of stopping K^- in the targed, minimizing the charged particles energy loss.

(~90 pb^{-1}; analyzed 37 pb^{-1}, x1.5 statistics)

Carbon target inside KLOE

K⁻

Advantages:

- gain in statistics
- K^- absorptions occur in Carbon
- absorptions at-rest.

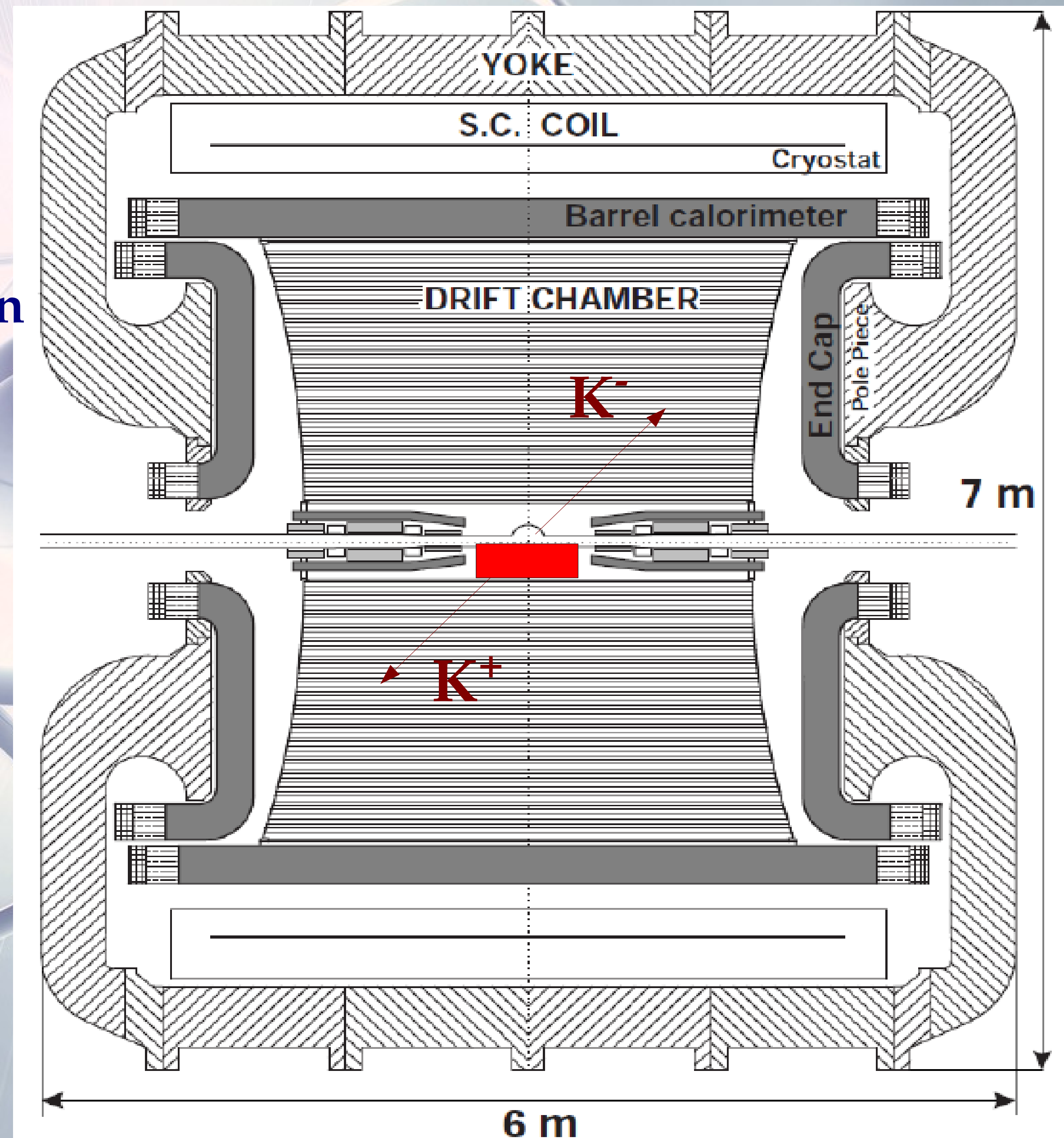

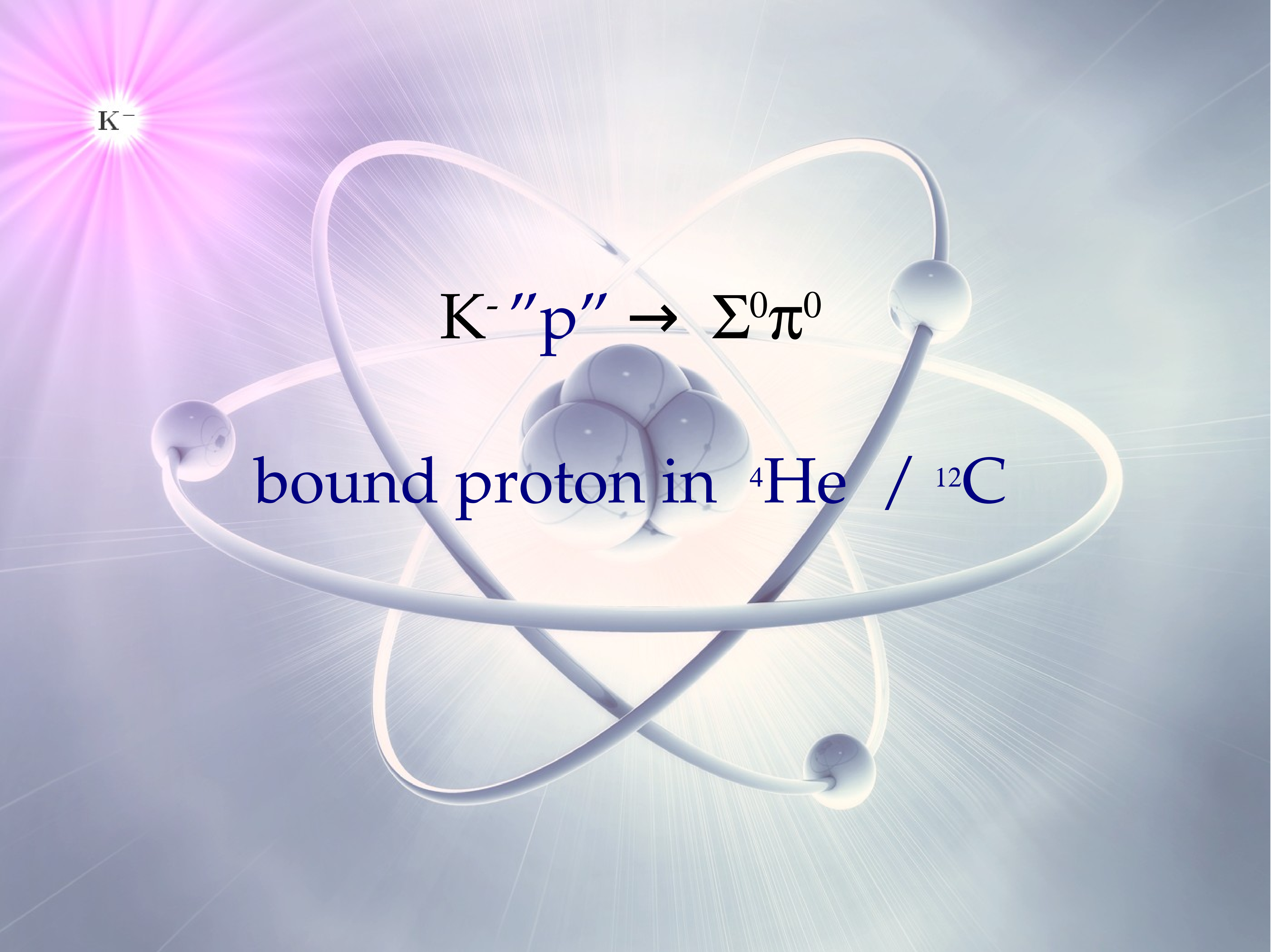

K⁻
K⁻ "p" → Σ⁰π⁰
bound proton in ⁴He / ¹²C

$\Sigma^0 \pi^0$ channel

K⁻ $\Lambda(1405)$ signal searched by K^- interaction with a bound proton in Carbon

$K^- p \rightarrow \Sigma^0 \pi^0$ detected via: $(\Lambda\gamma)$ $(\gamma\gamma)$

Strategy : K^- absorption in the DC entrance wall, mainly ^{12}C with H contamination (epoxy)

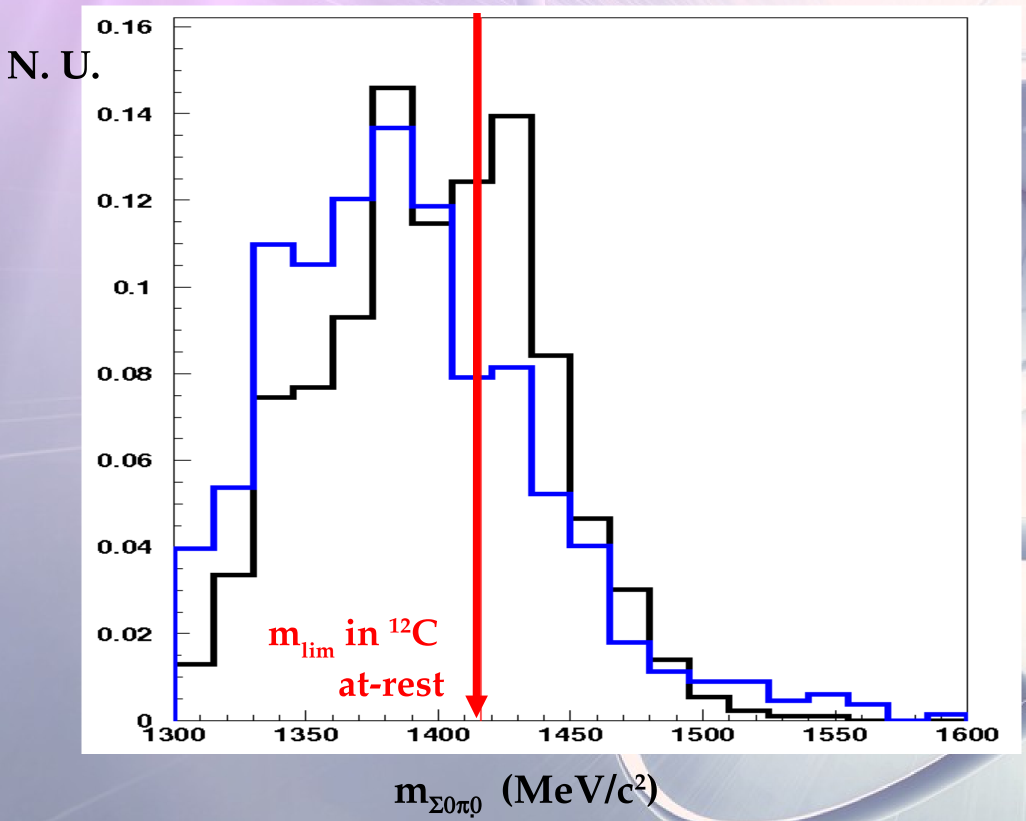

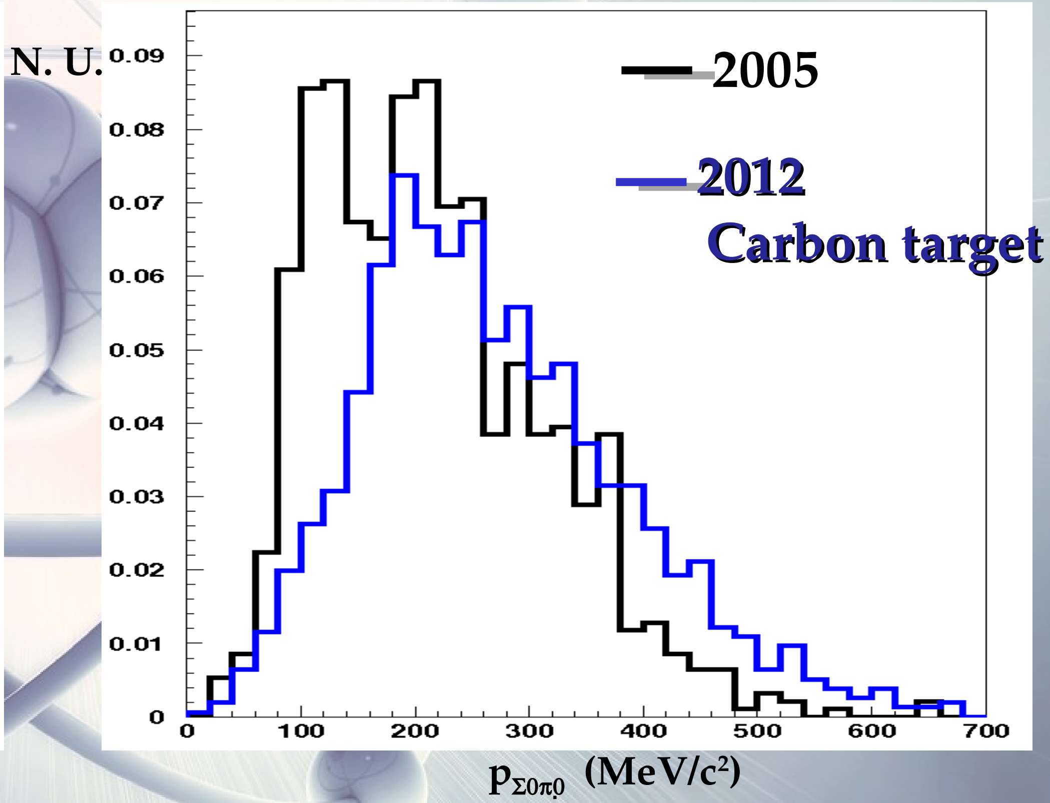

$m_{\pi0\Sigma0}$ resolution $\sigma_m \approx 32$ MeV/c² ; $p_{\pi0\Sigma0}$ resolution: $\sigma_p \approx 20$ MeV/c.

Negligible $(\Lambda\pi^0$ + internal conversion) background = (3±1) % → no I=1 contamination

$\Sigma^0\,\pi^0$ channel

K⁻ nuclear absorption experiments .. long history .. BUT

K⁻

1) $m_{\pi\Sigma}$ spectra always cut at the **at-rest limit** 2) ($\Sigma\pm\pi\mp$) spectra suffer $\Sigma(1385)$ contamination

P. J. Carlson, et al. Nucl. Phys. 74 642

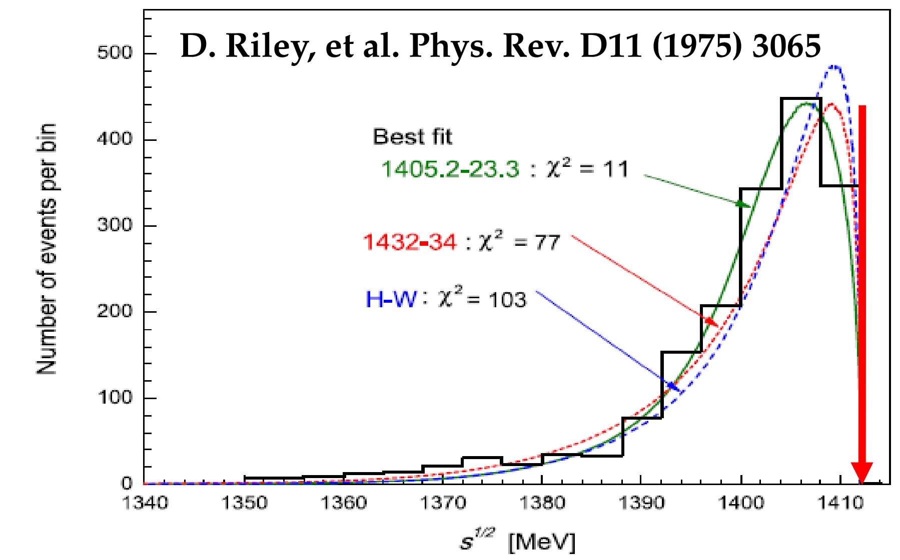

Fig. 6. Detailed differences in $M_{\Sigma\pi}$ spectra among the Hyodo–Weise prediction and the present model predictions.

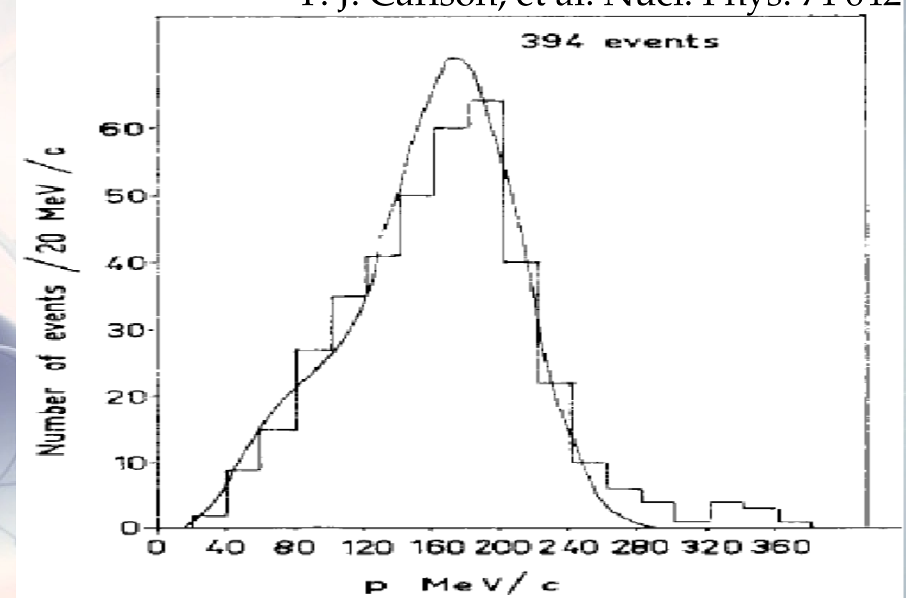

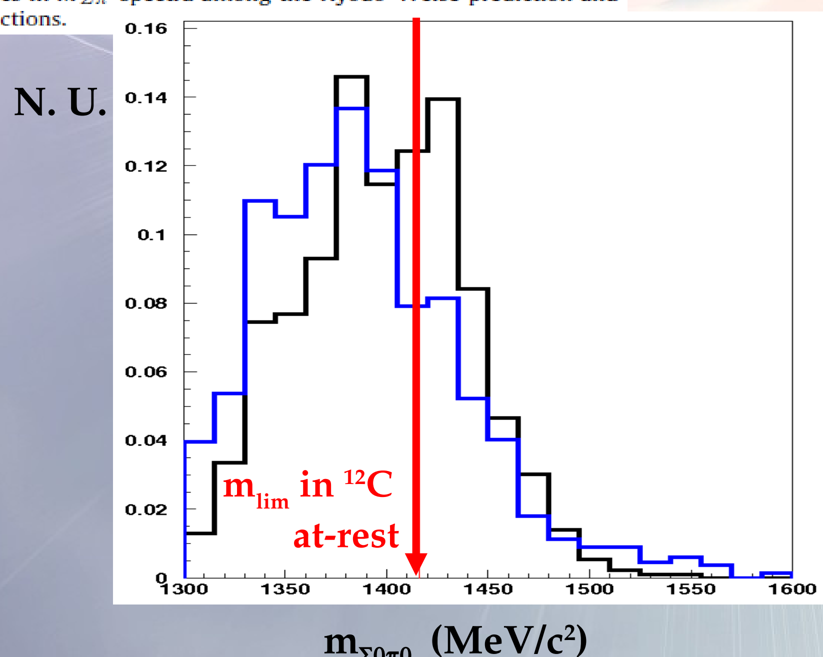

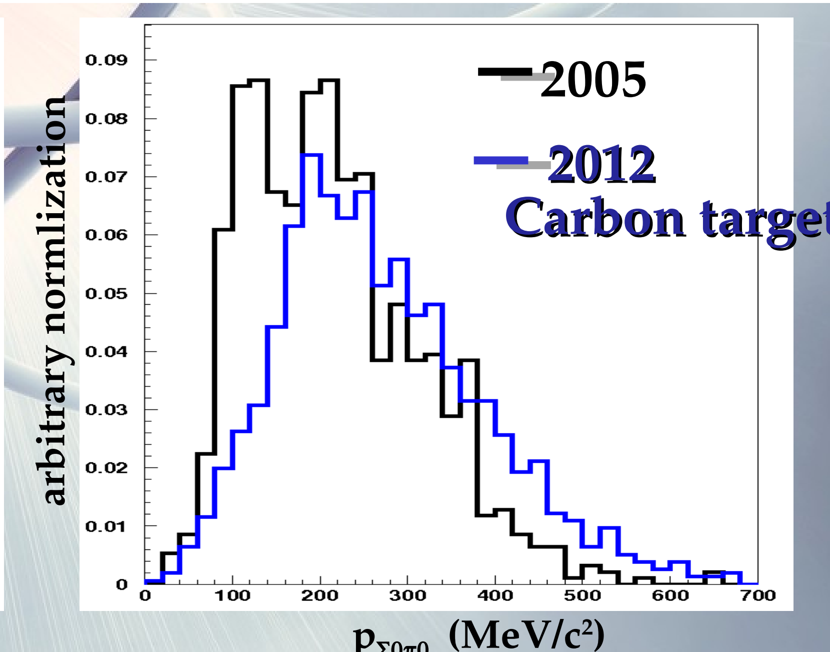

$\Sigma^0 \pi^0$ channel

In-flight component … FIRST EVIDENCE IN K^- ABSORPTION MASS SPECTROSCOPY

open a higher invariant mass region

$p_{\pi 0}$ resolution: $\sigma_p \approx 12$ MeV/c

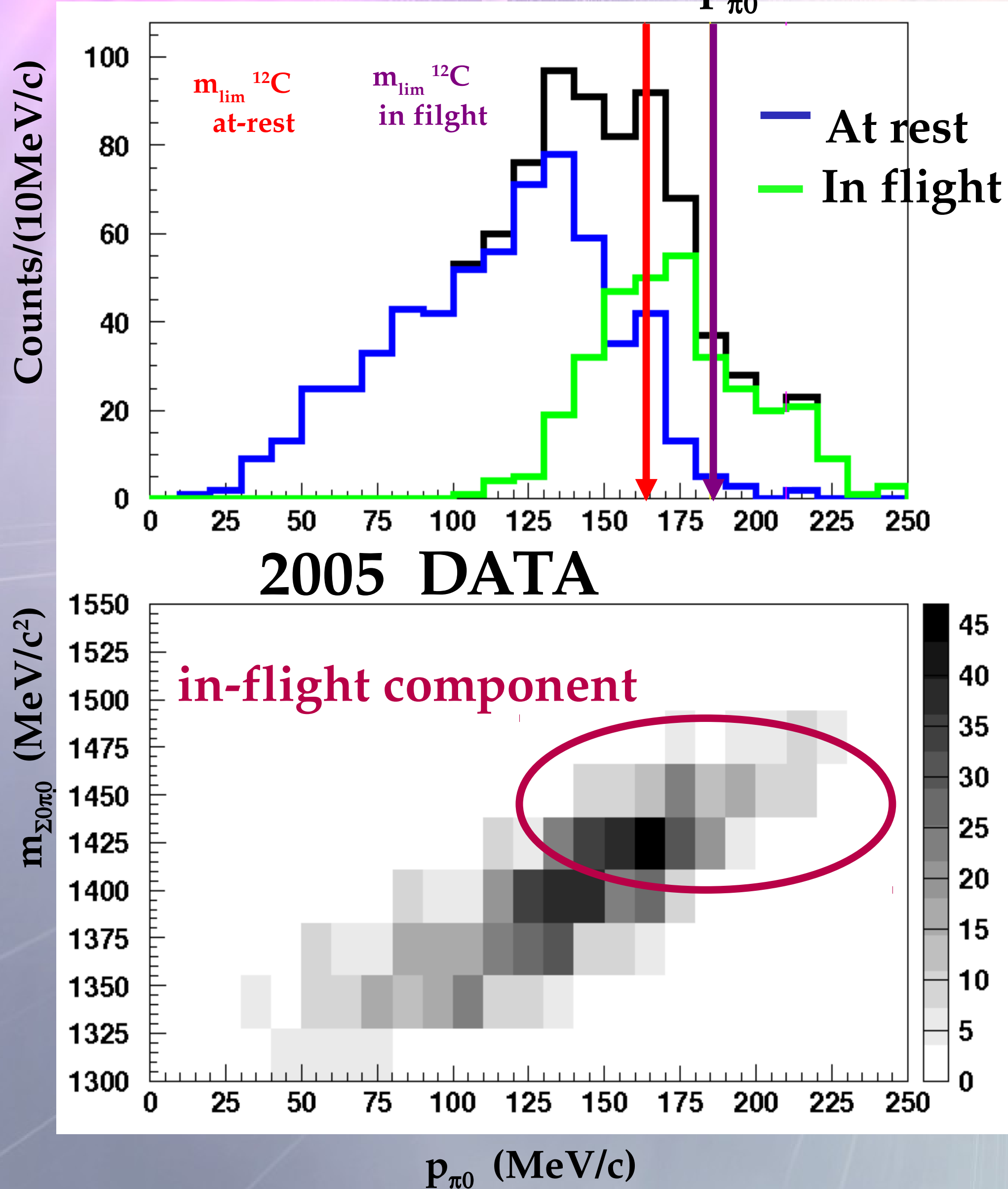

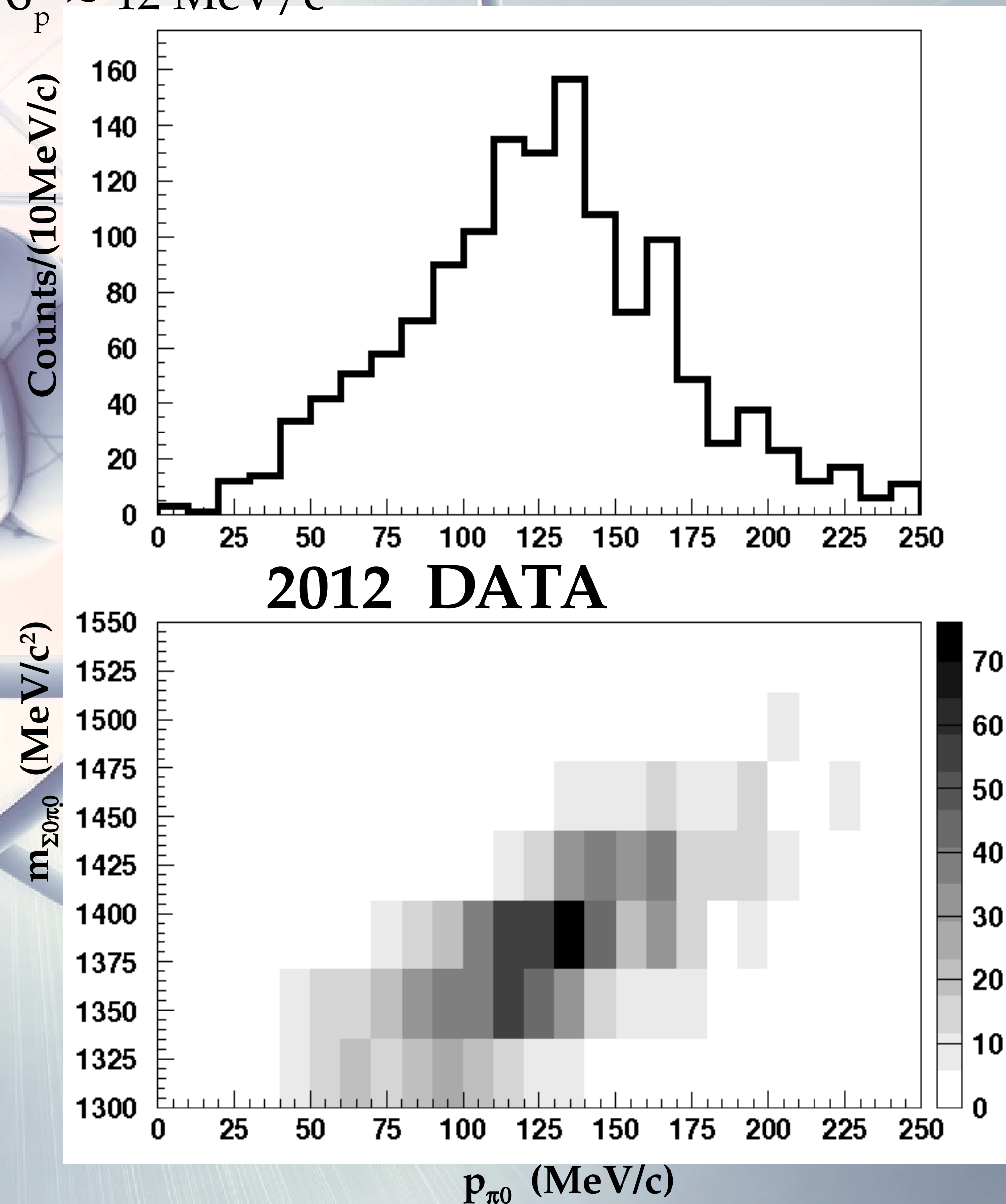

$\Sigma^0 \pi^0$ channel

K$^-$

Invariant mass spectra with mass hypotesis on Σ^0 and π^0 ***non resonant misidentification background subtracted (right)***

$\sigma_m \approx$ *17 MeV/c^2* (^{12}C) $\sigma_m \approx$ *15 MeV/c^2* (^{4}He)

Similar $m_{\pi 0 \Sigma 0}$ shapes due to the similar kinematical thresholds for ^{4}He and ^{12}C.

2005 DATA

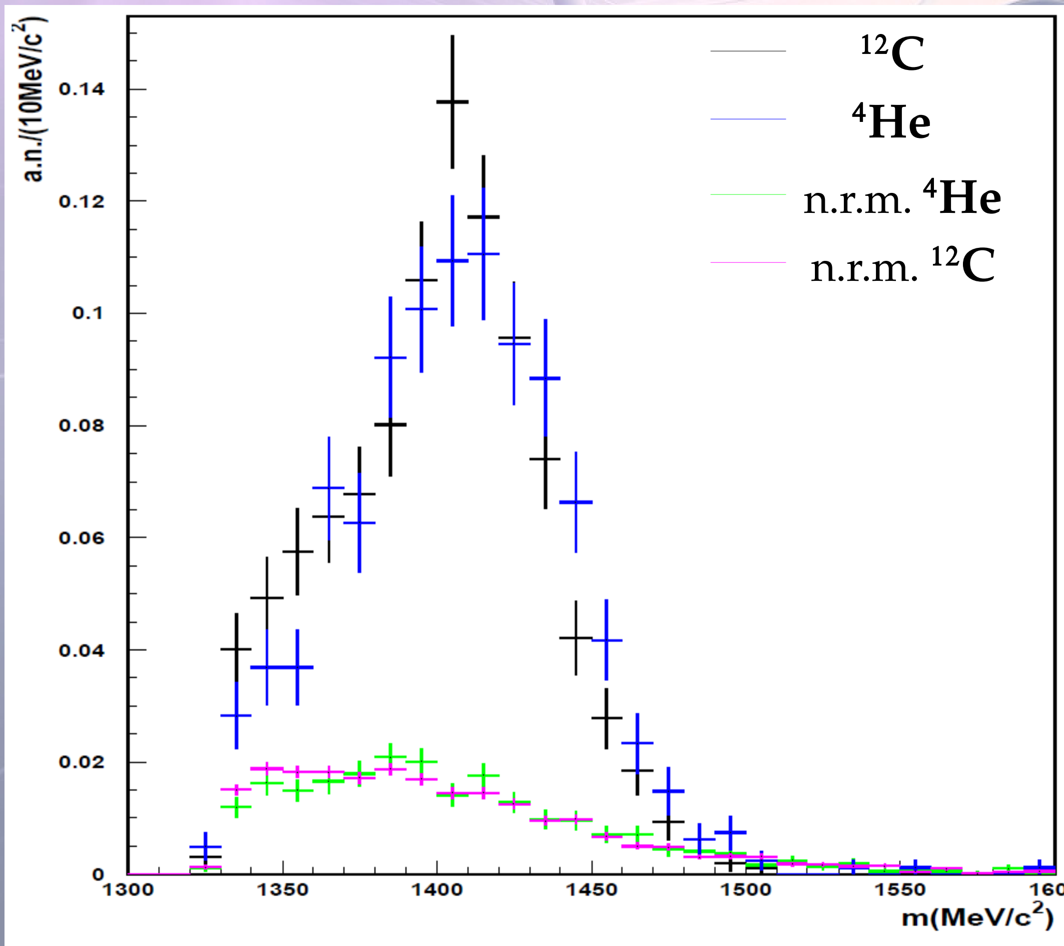

$m_{\Sigma^0\pi^0}$ *spectrum*

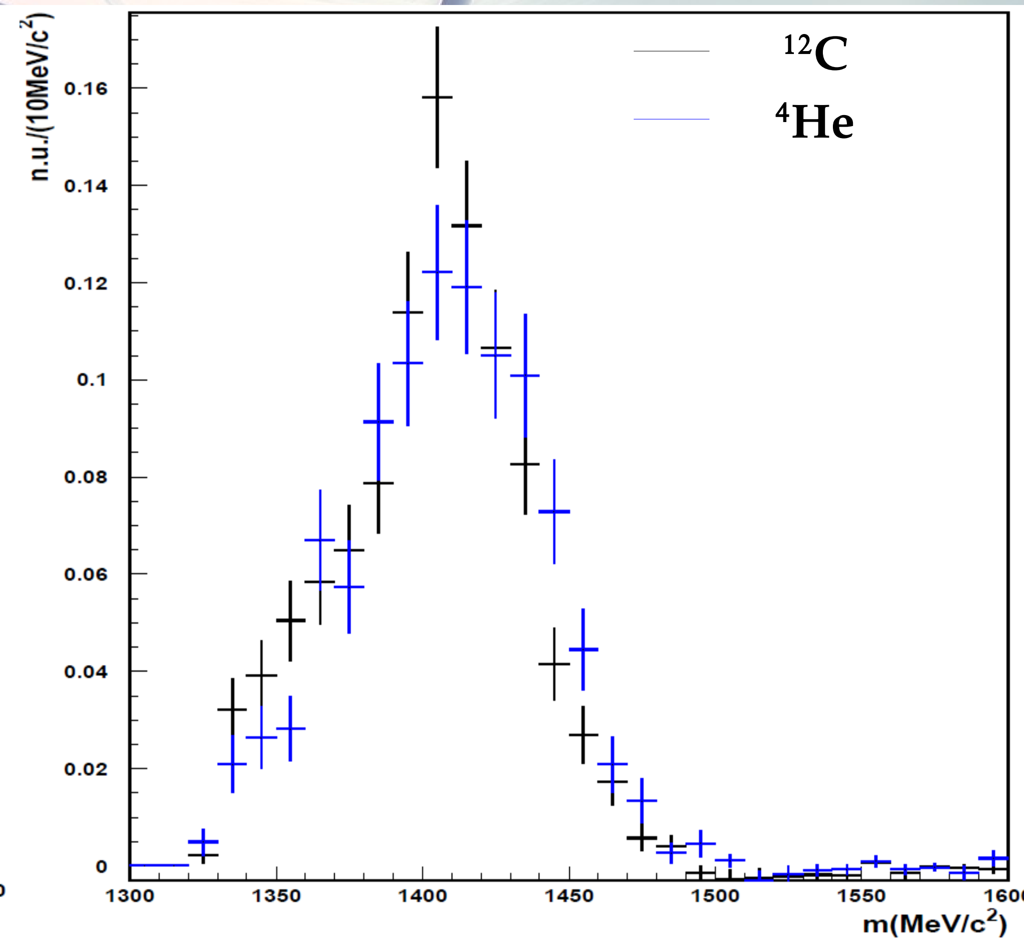

$m_{\Sigma^0\pi^0}$ *spectrum*

$\Sigma^0\ \pi^0$ channel

Acceptance corrected $m_{\pi0\Sigma0}$ spectra, DC wall (left) DC gas (right)

K^-

Acceptance function evaluated in 8 intervals of $p_{\pi0\Sigma0}$ (between 0 and 700 MeV/c) 8 intervals of $\theta_{\pi0\Sigma0}$ (between 0 and 3.15 rad) 30 intervals of $m_{\pi0\Sigma0}$ (between 1300 and 1600 MeV/c^2)

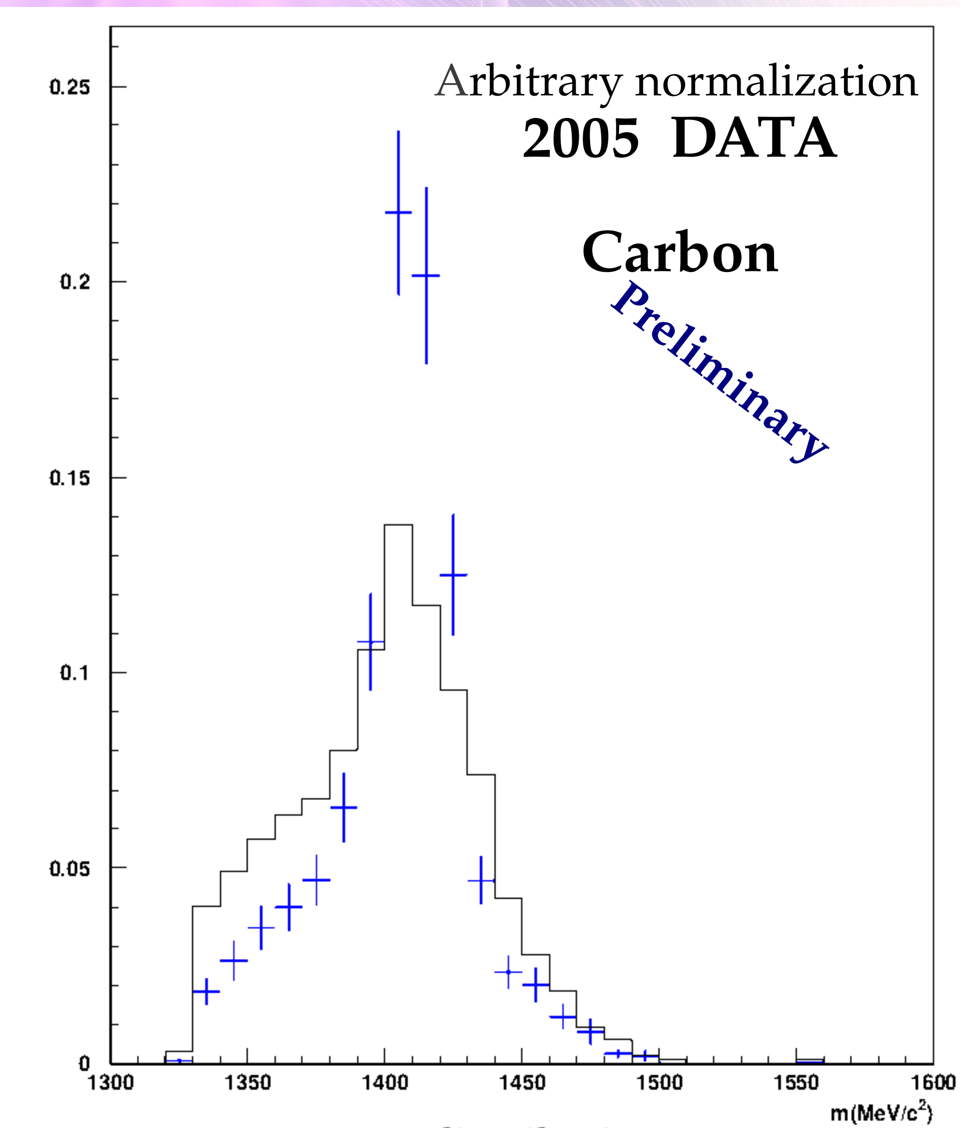

$m_{\Sigma^0\pi^0}$ *distribution*

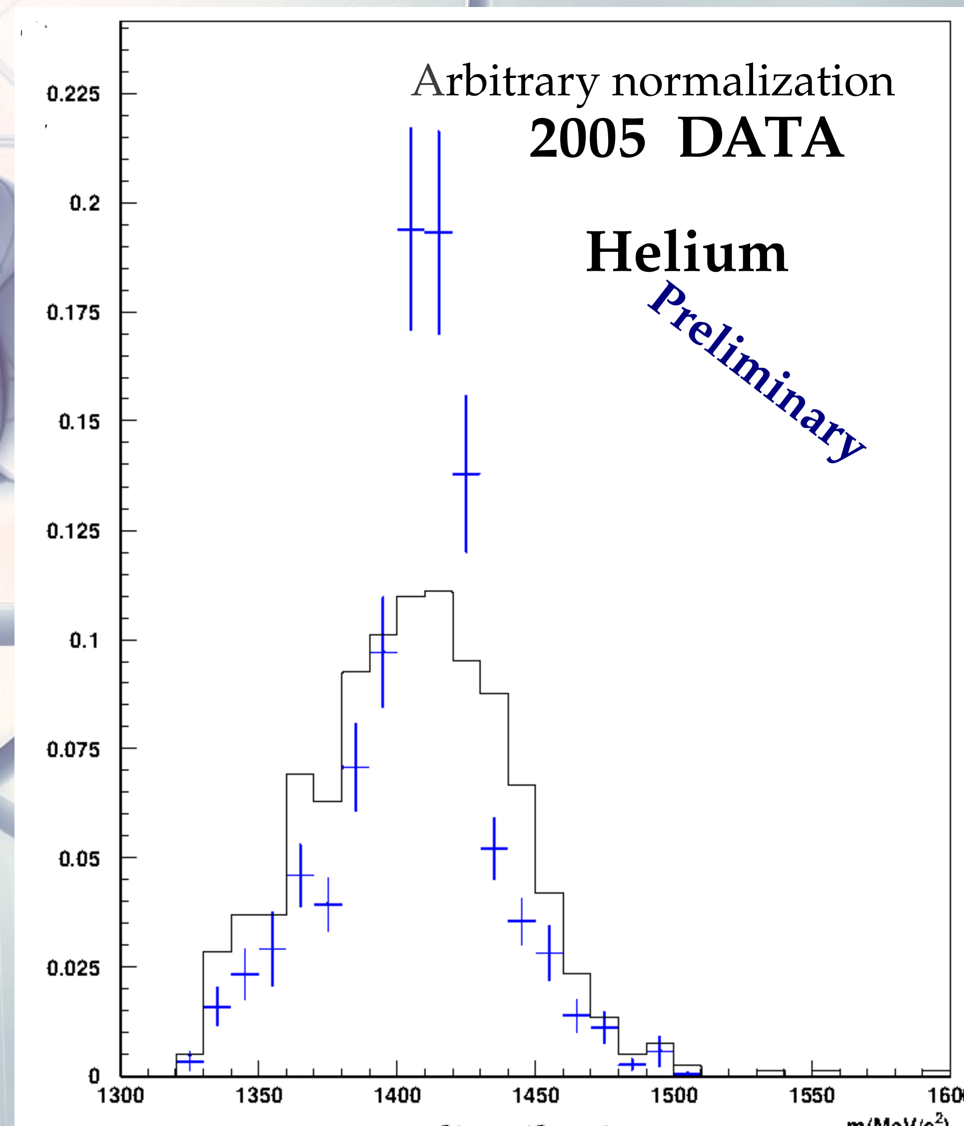

$m_{\Sigma^0\pi^0}$ *distribution*

Fit of $\Sigma^0\pi^0$ spectrum in C

K^-

8 component fit, simultaneously $m_{\Sigma0\pi0}$ & $p_{\Sigma0\pi0}$:

- Breit-Wigner resonant component K^- C at-rest/in-flight. $(M,\Gamma) = (1405 \div 1430\ ,\ 5 \div 52\ )$
- Non resonant $\Sigma^0\pi^0$ K^- H production at-rest/in-flight
- Non resonant $\Sigma^0\pi^0$ K^- C production at-rest/in-flight
- $\Lambda\pi^0$ background ($\Sigma(1385)$ + I.C.)
- non resonant misidentification (*n.r.m.*) background

$K^-\ {}^{12}C \rightarrow \Sigma^0\pi^0 + {}^{11}B$ (Boron spectator, left in ground state)

secondary interactions not taken into account.

Fit of $\Sigma^0\pi^0$ spectrum in C

K^-

χ^2_{min} /ndf ~ 1.7 corresponding to $(M_{min}, \Gamma_{min}) = (1426, 52)$ MeV/c^2

- **Global fit** (red)
- **Resonant component $K^- C$ at-rest** (green)
- **n. r. $K^- C$ at-rest** (blue)
- **n. r. $K^- C$ in-flight** (yellow)
- **n. r. $K^- H$ in-flight** (cyan)
- **$\Lambda^0\pi^0$ background + n. r. m.** (magenta)

Preliminary ..

more next weeks

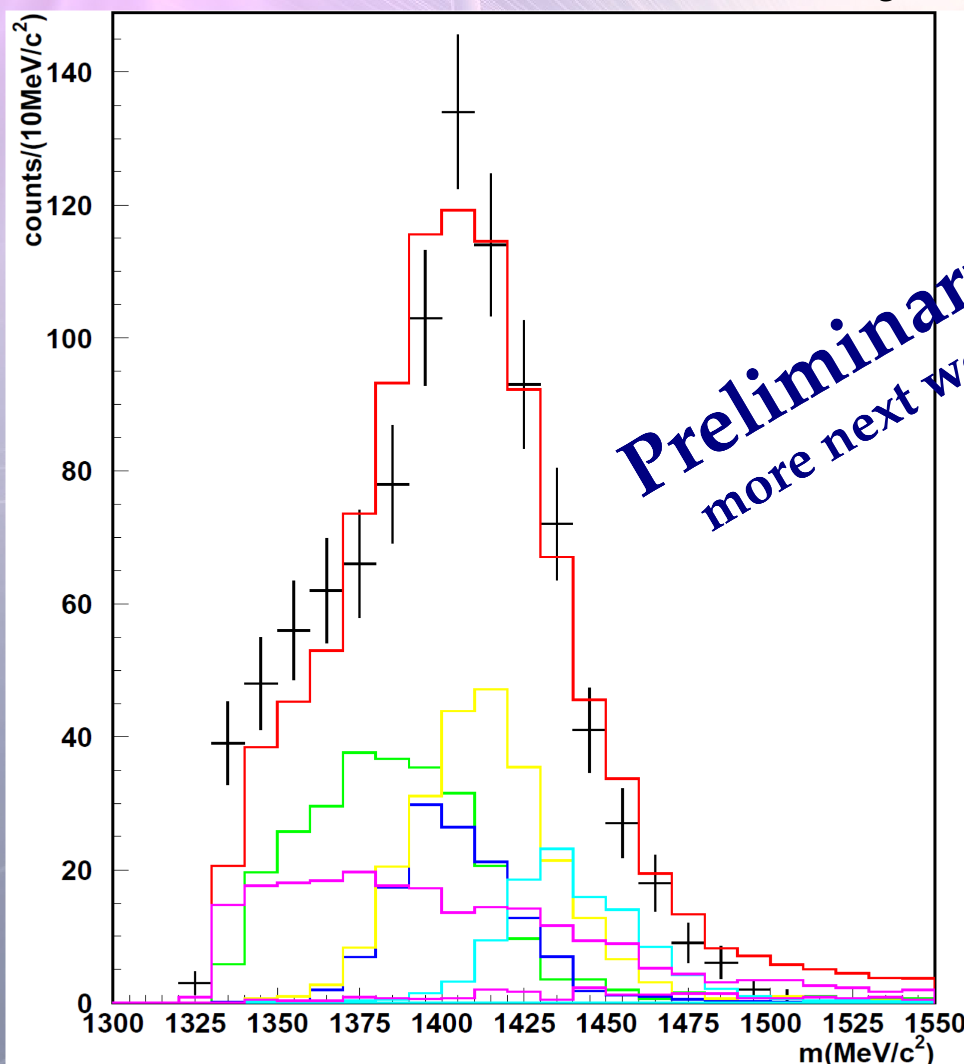

$m_{\Sigma 0\pi 0}$

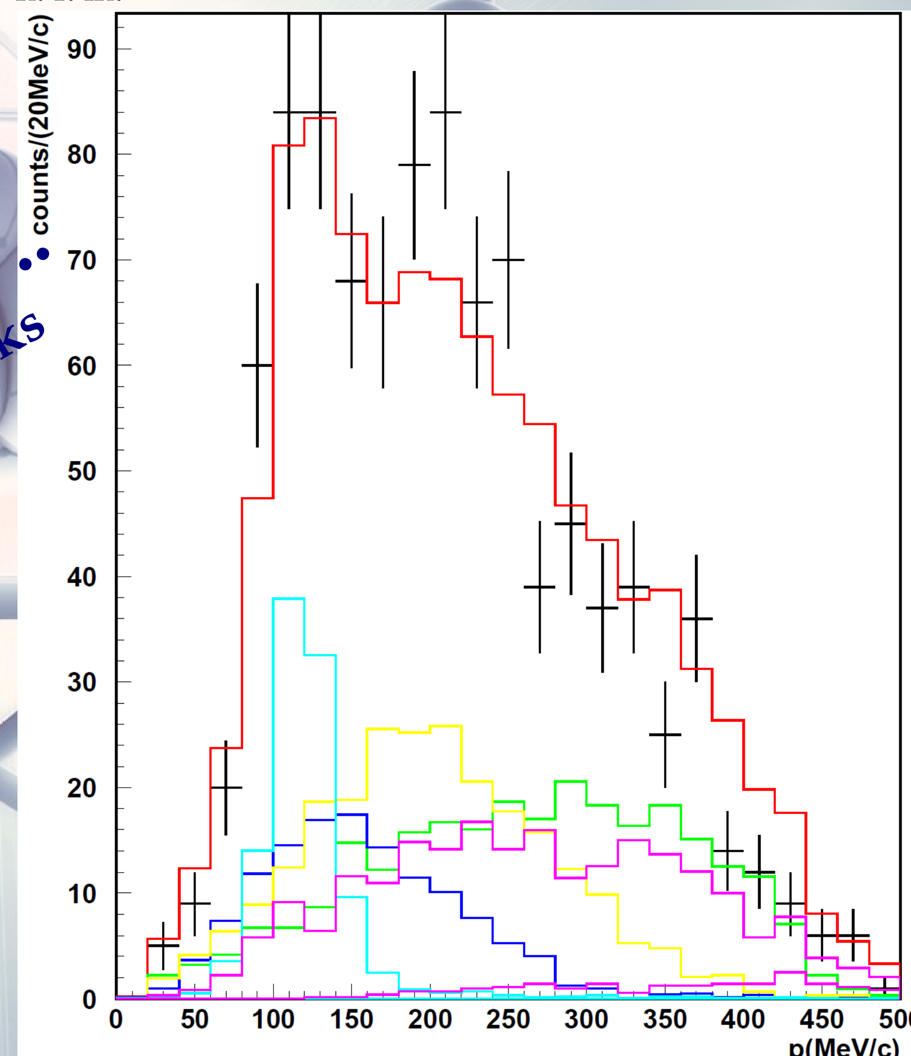

$p_{\Sigma 0\pi 0}$

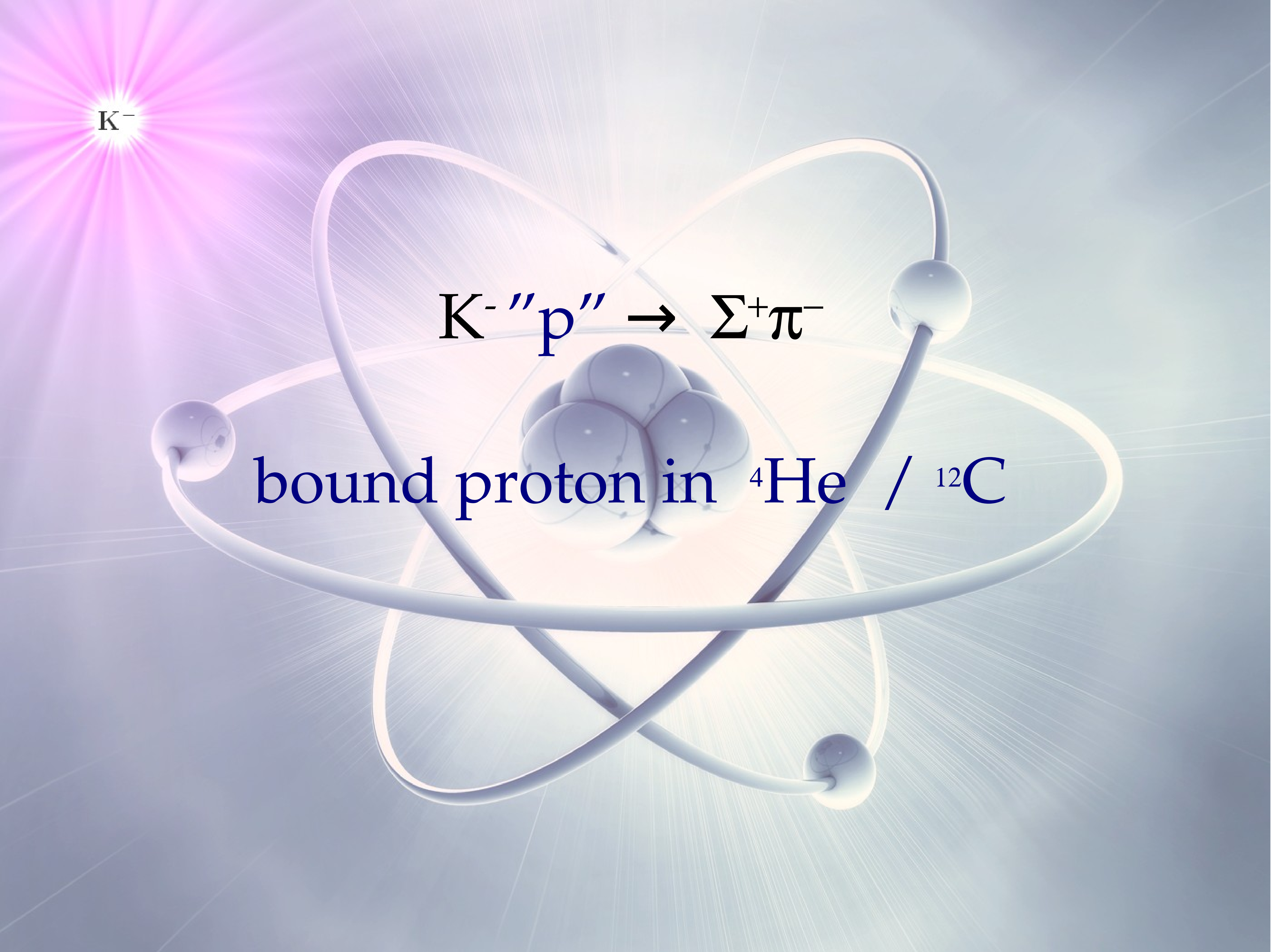

K^- "p" $\rightarrow$ $\Sigma^+\pi^-$

bound proton in ^{4}He / ^{12}C

$\Sigma^+\pi^-$ invariant mass spectra

K^-

$K^- p \rightarrow \Sigma^+ \pi^-$ detected via: $(p\pi^0)\, \pi^-$

The excellent momentum resolution for π^- enables to disentangle in-flight from at-rest K^- capture

Hint: if resonant production contribution is important a high mass pole appears!

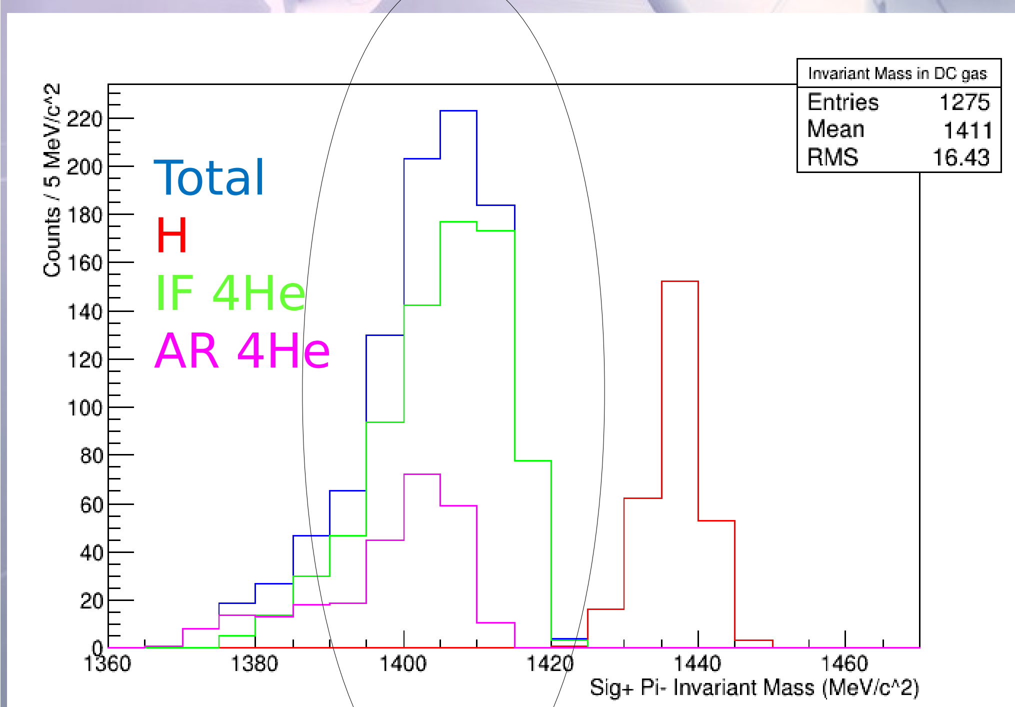

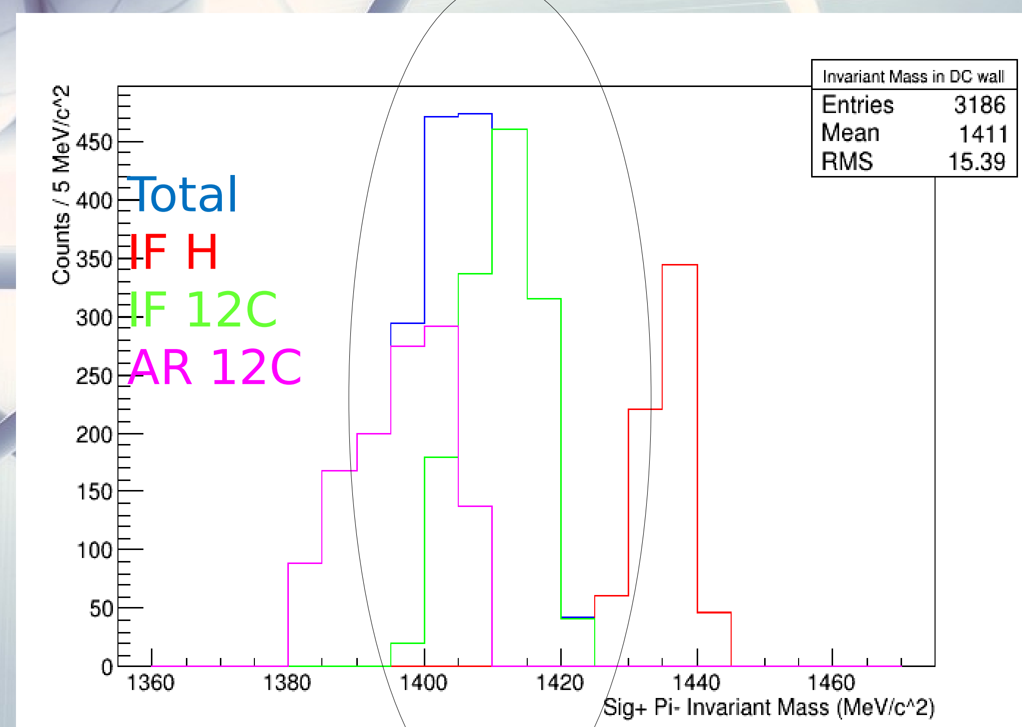

K^-

Resonant VS non-resonant

Another unsolved question ..

$$K^- N \rightarrow (Y^* ?) \rightarrow Y \pi$$

how much comes from resonance ?

Investigated using:

K^- "n" $\rightarrow \Lambda\pi^-$ direct formation in ^{4}He

Channel: $K^- \; ^4He \rightarrow \Lambda \, \pi^- \; ^3He$ … the idea

$K^-(s=0)$ $^4He(s=0)$ $n(s=1/2)$ $\Sigma^{*-}(s=3/2) \rightarrow$ resonance p-wave only

atomic s-state capture:

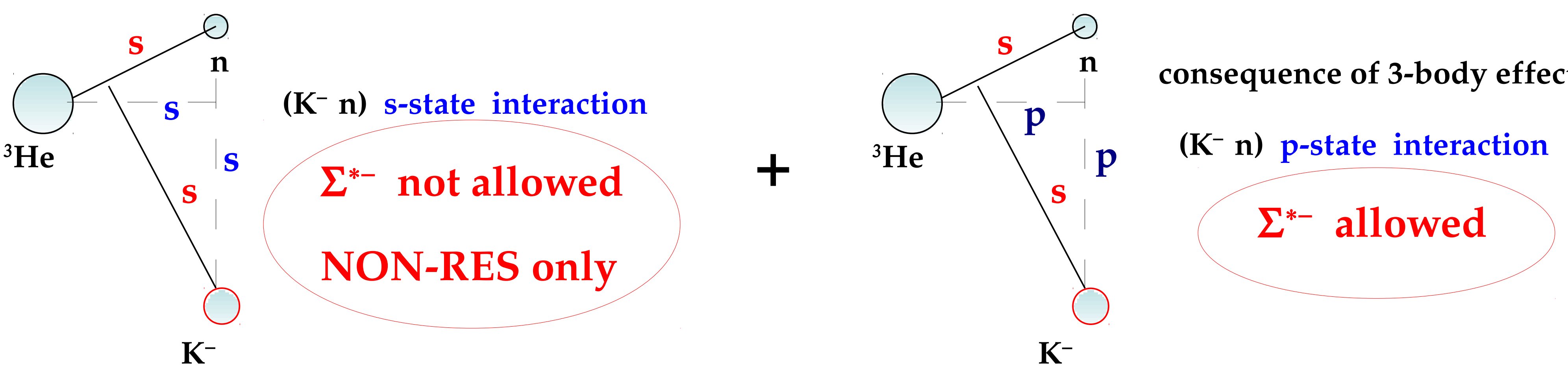

- ($K^- \; ^4He \rightarrow \Lambda \, \pi^- \; ^3He$) absorptions from (n s) - atomic states are assumed $\rightarrow$

^4He bubble chamber data (Fetkovich, Riley interpreted by Uretsky, Wienke)

- Coordinates recupling enables for P-wave resonance formation

Channel: $K^- \; {}^4He \rightarrow \Lambda \, \pi^- \; {}^3He$ … <u>the strategy</u>

K^-

- **Fit of the $p_{\Lambda\pi^-}$ observed distribution using calculated distributions :**

$$P_s^{\,s}\,(p_{\Lambda\pi}) = |\Psi_N\,(p_{\Lambda\pi})|^2 \;|f^{\,s}\,(p_{\Lambda\pi})|^2 \;\rho$$ **non-resonant**

$$P_s^{\,p}\,(p_{\Lambda\pi}) = |\Psi_N\,(p_{\Lambda\pi})|^2 \;c^2 \;|2f^{\,\Sigma*}\,(p_{\Lambda\pi})|^2 \;\rho/3 \;\,(k p_{\Lambda\pi})^2$$ **resonant**

- **To determine *for the first time* the ratio resonant/non-res.**

↓

$|f^{\,N\text{-}R}_{\;\Lambda\pi}|$ given the fairly well known $|f^{\,\Sigma*}_{\;\Lambda\pi}|$

$K^- \; {}^4He \rightarrow \Lambda \pi^- \; {}^3He$ fit

Simultaneous fit ($p_{\Lambda\pi^-}$ - $m_{\Lambda\pi^-}$ - $\theta_{\Lambda\pi^-}$) leaving the ratio At-rest /In-flight and ^{12}C contamination to vary around the estimated values within errors:

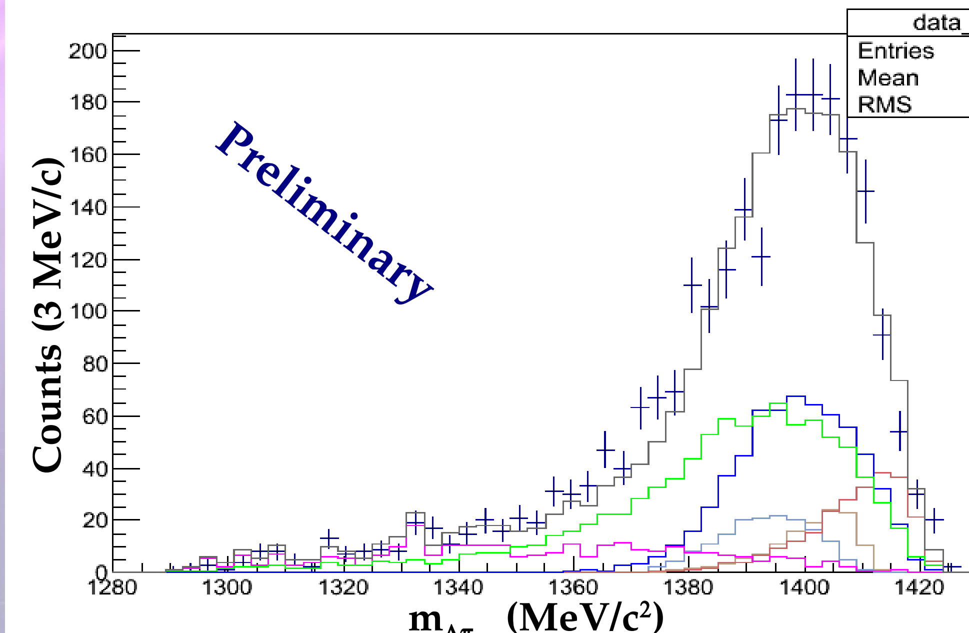

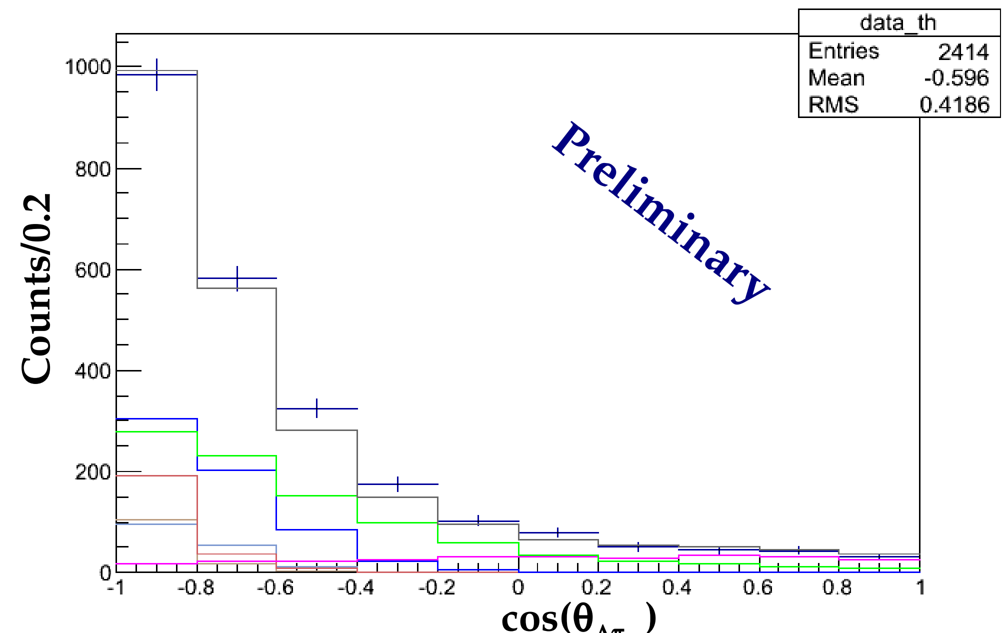

Global fit

$\Lambda \pi^-$ At-rest N-R

$\Lambda \pi^-$ At-rest RES

$\Lambda \pi^-$ In-flight N-R

$\Lambda \pi^-$ In-flight RES

$\Lambda \pi^-$ events from $K^- \; {}^{12}C$

Σ p/n $\rightarrow$ Λ p/n conversion

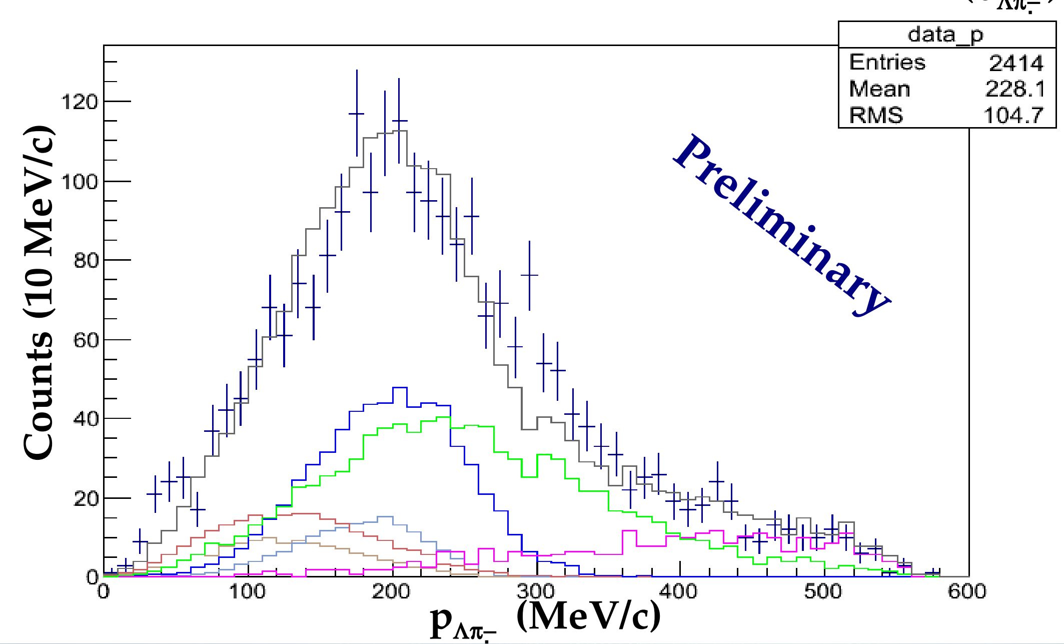

$K^- \ ^4He \rightarrow \Lambda \pi^- \ ^3He$ fit

Simultaneous fit ($p_{\Lambda\pi^-}$ - $m_{\Lambda\pi^-}$ - $\theta_{\Lambda\pi^-}$) leaving the ratio At-rest /In-flight and ^{12}C contamination to vary around the estimated values within errors:

- χ^2/ (ndf – np) = 1.2
- **(At-rest RES)/(At-rest N-R) = 1.26 ± 0.06**
- **(In-flight RES)/(In-flight N-R) = 2.59 ± 0.3**

Preliminary

- (In-flight) / (At-rest) = 2.9 ± 0.5 → consistent with the estimate in $\Sigma^+\pi^-$
- Σ p/n → Λ p/n conversion = (12.2 ± 0.8)%
- $\Lambda \pi^-$ events from $K^- \ ^{12}C$ = (38 ± 1)%

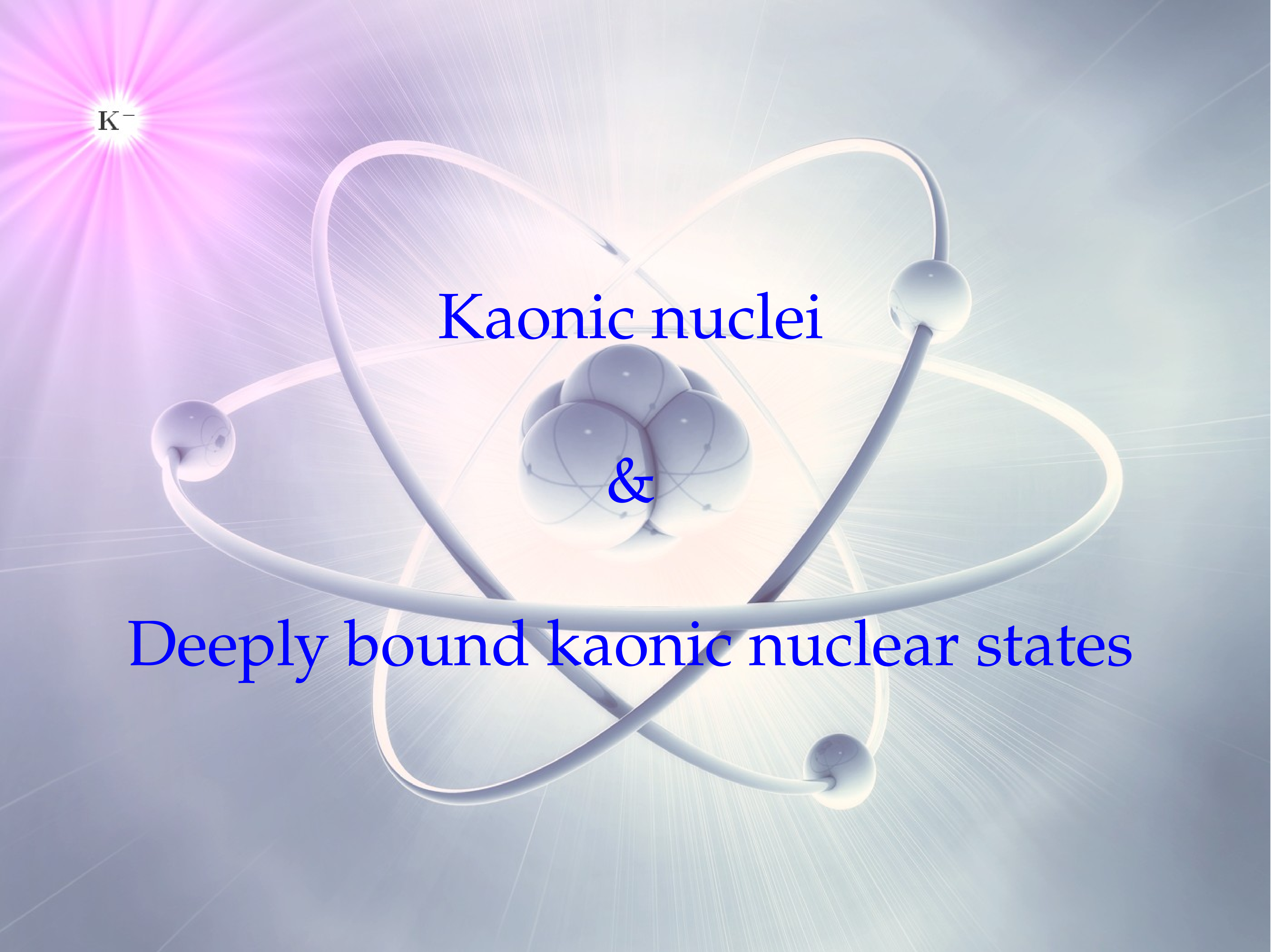

Kaonic nuclei

&

Deeply bound kaonic nuclear states

Kaonic nuclei

How deeply is bound a kaon in a nucleus?

Strong attractive I=0 $\bar{K}$N interaction favors discrete nuclear states **high B** and **small Γ**.

Different theoretical approaches:

- Few-body calculations solving Faddeev equations
  - Variational calculations with phenomenological KN potential
  - KN effective interactions based on Chiral SU(3) dynamics

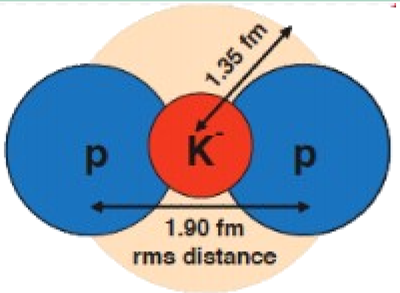

Experimental studies in the Λp decay channel

- pp collisions: DISTO (published), FOPI, HADES (ongoing analysis)
- Absorption experiments:

FINUDA

K- stopped + X -> Λp X'

6Li
X = 7Li
9Be

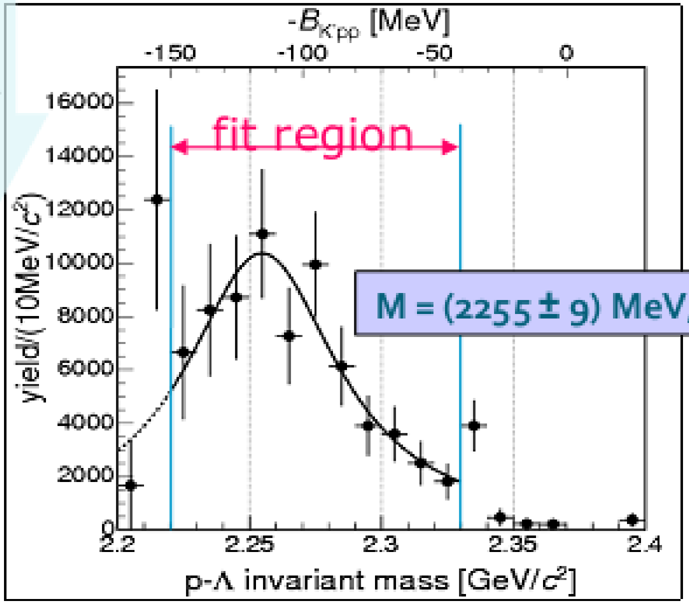

PRL94 (2005) 212303

B = 115$^{+6}_{-5}$(stat)$^{+3}_{-4}$(sys) MeV
Γ = 67$^{+14}_{-11}$(stat)$^{+2}_{-3}$(sys) MeV

Kaonic nuclei

How deeply is bound a kaon in a nucleus?

Strong attractive I=0 $\bar{K}$N interaction favors discrete nuclear states **high B** and small **Γ** .

Different theoretical approaches:

- Few-body calculations solving Faddeev equations
  - Variational calculations with phenomenological KN potential
  - KN effective interactions based on Chiral SU(3) dynamics

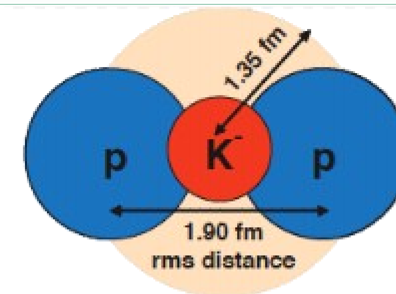

Experimental studies in the Λp decay channel

- pp collisions: DISTO (published), FOPI, HADES (ongoing analysis)
- Absorption experimei

@KEK E-549

K- stopped + 4He -> Λp X

arXiv:0711.4943v1

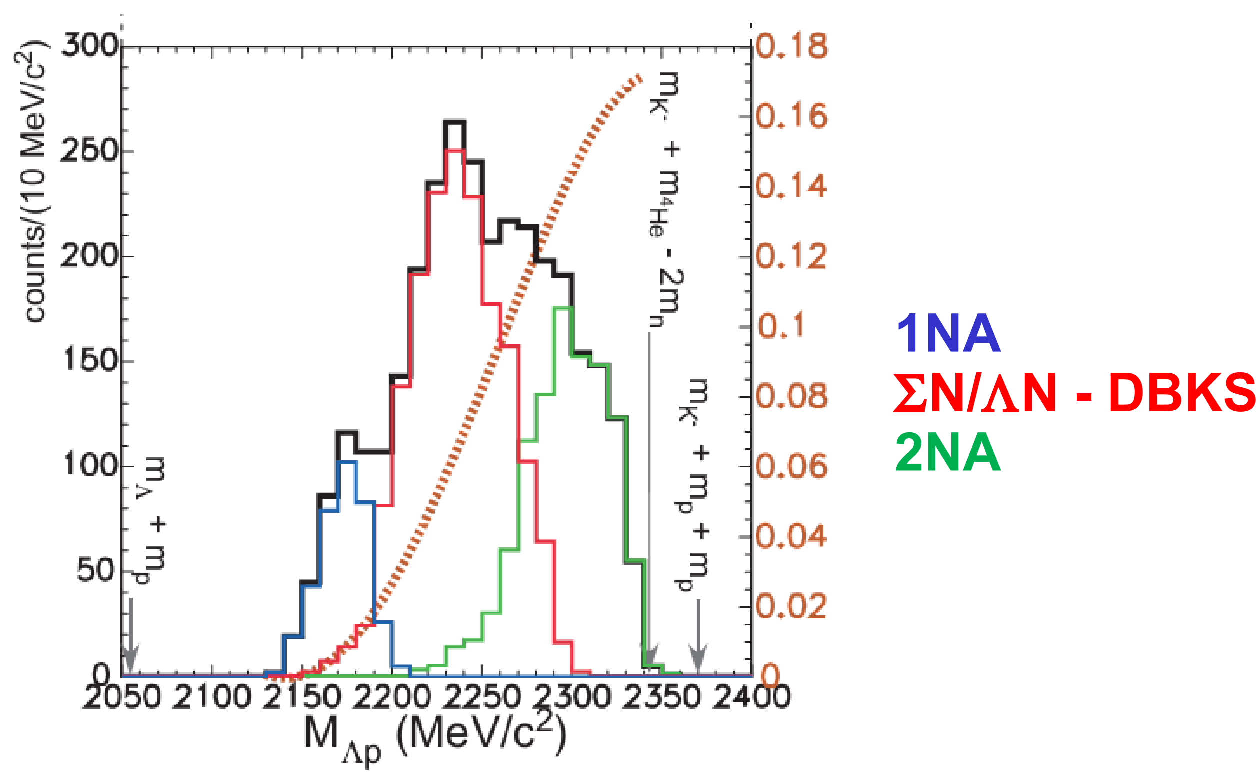

Kaonic nuclei

How deeply is bound

Different theo

- Few-b
  - Varia
  - KN e

Experimen

- pp c
  ar
- Abs

@KEK E-5

K- stoppe

$\bar{K}$N **interaction** favors
B and small **Γ**.

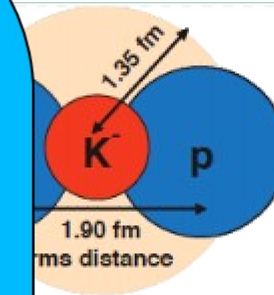

ing

NA
N/ΛN - DBKS
NA

Slide by J. Mares @ Trento ECT* Workshop

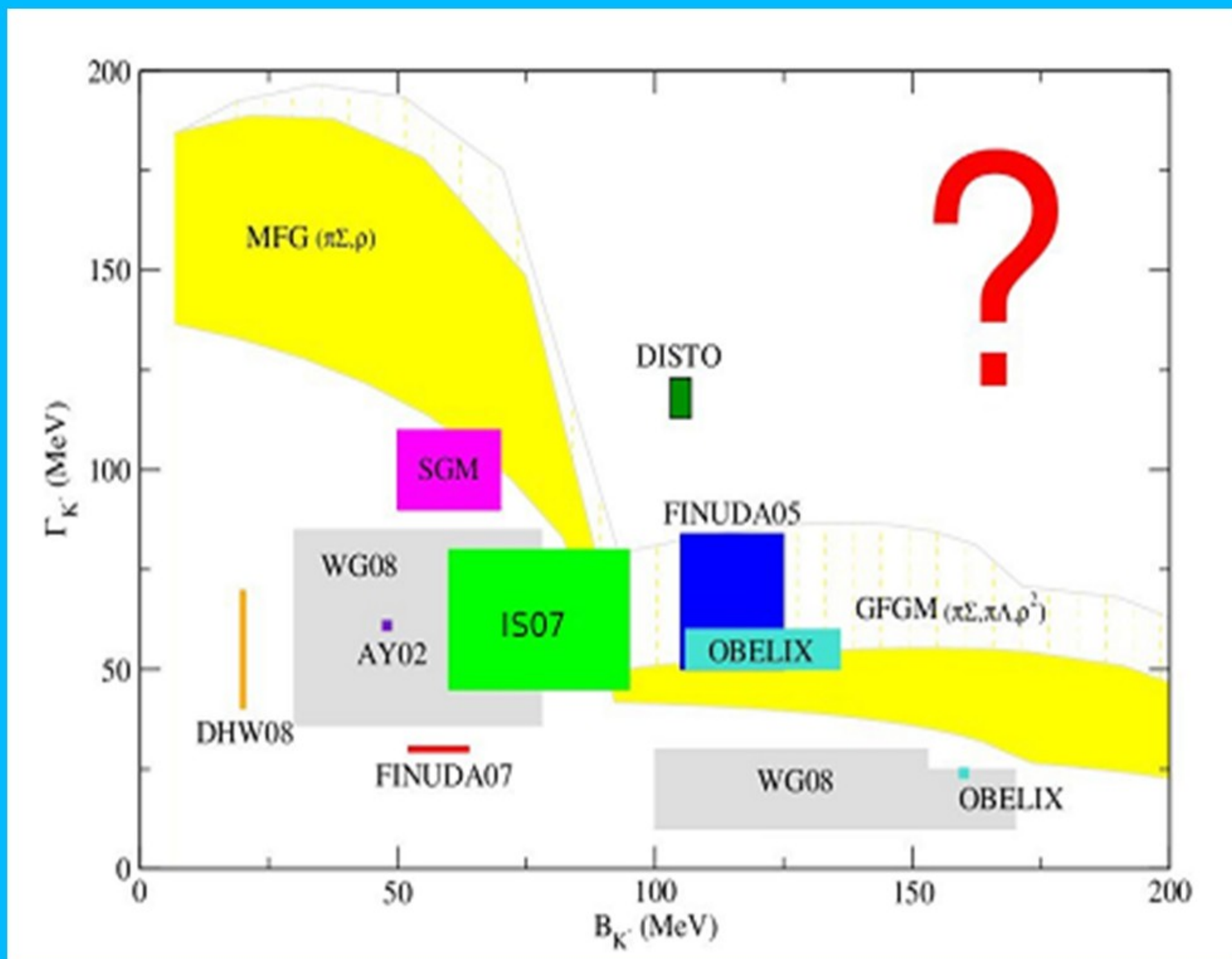

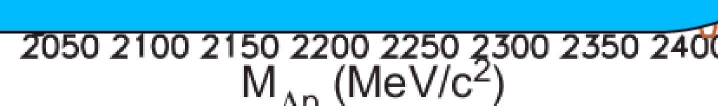

Kaonic nuclei

- Deeply bound state by strong interaction.
- Strong attraction of the I =0 $\bar{K}N$ interaction ($\bar{K}N^{I=0}$) plays an important role in kaonic nuclei.

K^-pp bound state

- The simplest kaonic nuclei.
- Theoretical prediction of B.E. and Γ depend on the $\bar{K}N$ interaction and the calculation method .

	Theoretical prediction	B.E (MeV)	Γ (MeV)
PRC76, 045201 (2002)	T. Yamazaki and Y. Akaishi	48	61
arXiv:0512037v2[nucl-th]	A. N. Ivanov, P. Kienle, J. Marton, E. Widman	118	58
PRC76, 044004 (2007)	N. V. Shevchenko, A. Gal, J. Mares, J. Revai	50~70	~100
PRC76, 035203 (2007)	Y. Ikeda and T. Sato	60~95	45~80
NPA804, 197 (2008)	A. Dote, T. Hyodo, W. Weise	20±3	40~70
PRC80, 045207 (2009)	S. Wycech and A. M. Green	56.5~78	39~60
PRL B712, 132-137 (2012)	Barnea et al.	15.7	41.2

KLOE data: Λp analysis

Analysis of events in the DC gas volume

K- stopped / in-flight abs. **+ 4He → Λp X**

→ pπ–

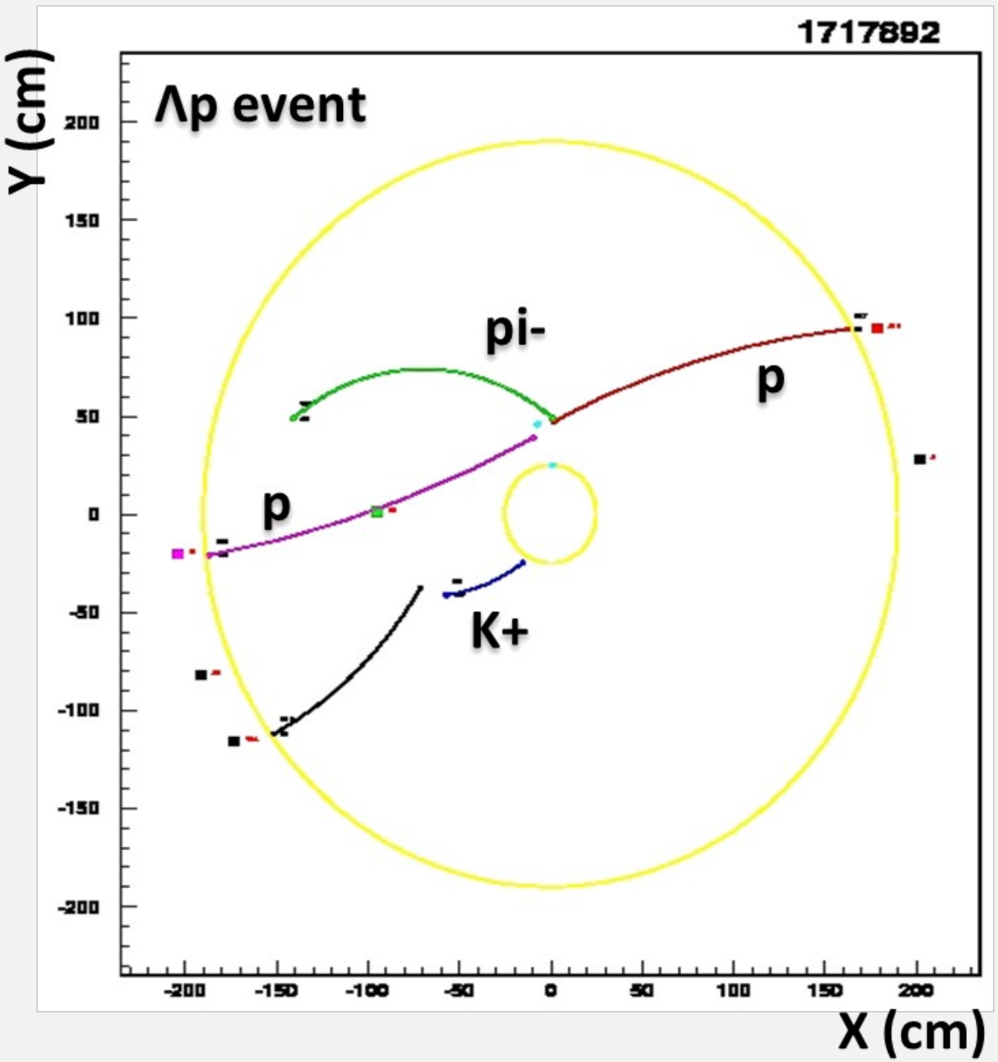

KLOE data: Λp analysis

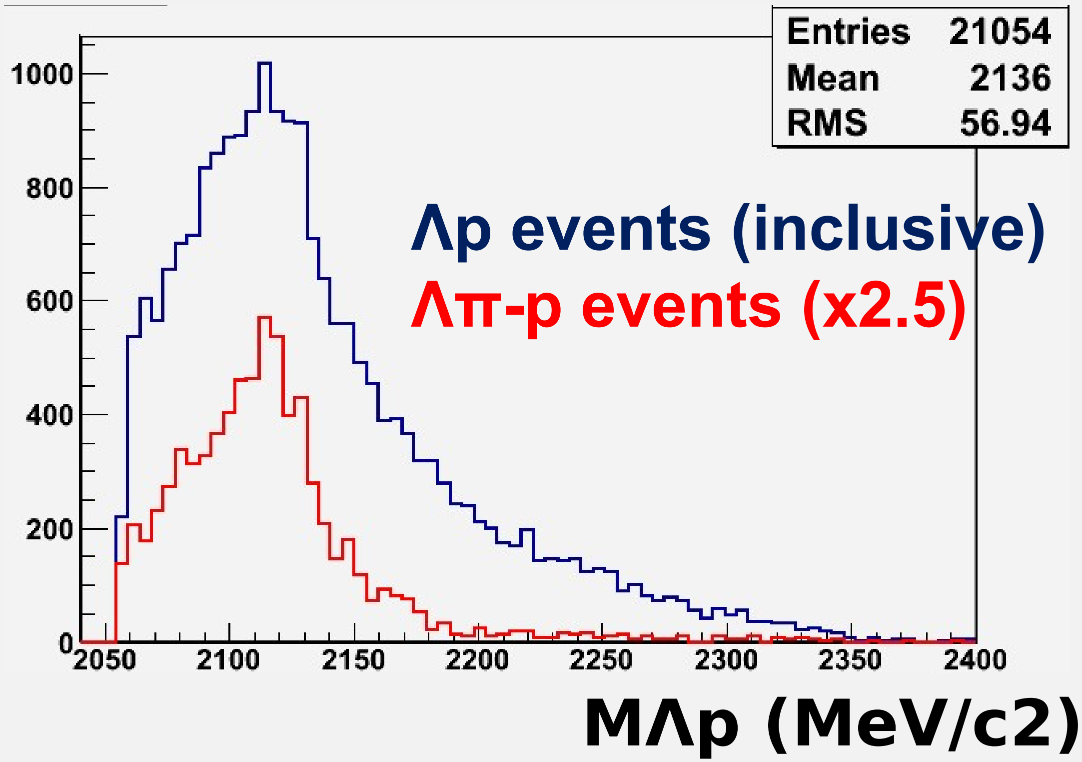

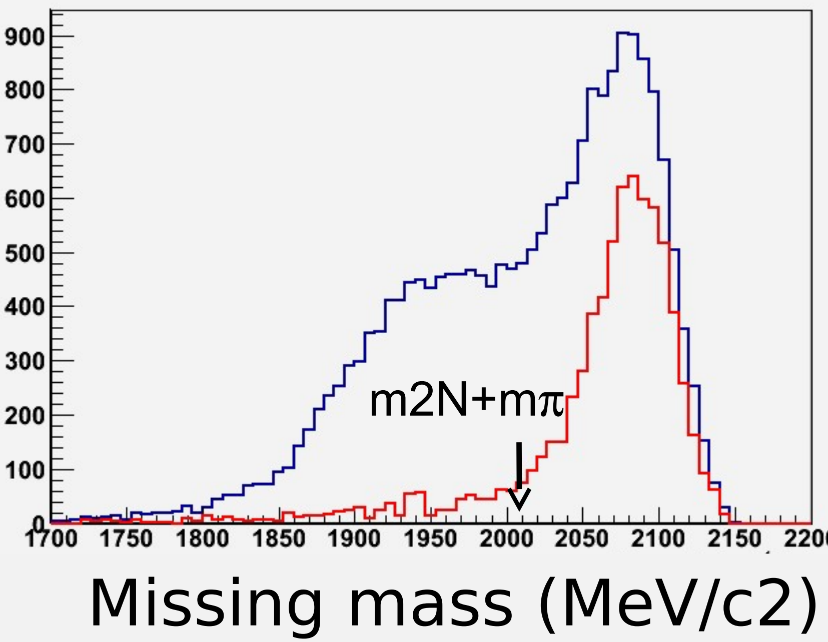

·1NA: **K-N→Λπ-** (N from residual nucleus)

·2NA: **K-NN→ΛN** (pionless)

alternative process: **<u>ΣN/ΛN conversion</u>**

1NA: **K-N→Σπ**

→ **ΣN→ΛN**

KLOE data: Λp analysis

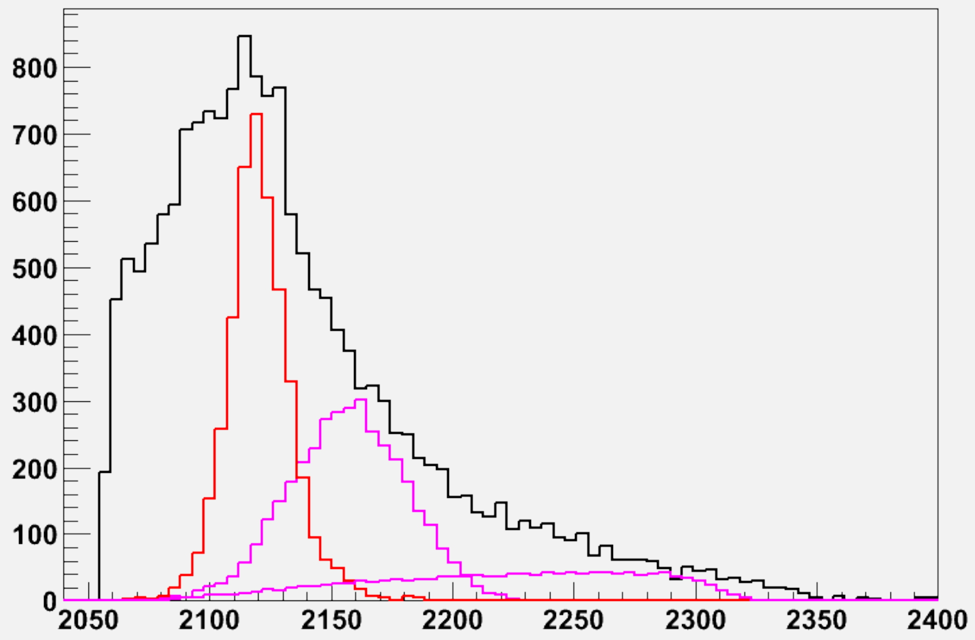

— **Λp events (inclusive)**

Simulations:

— **1NA + conversion Σ+n→Λp**
K-p →Σ+π-→Λpπ-

— **2NA + conversion Σ0p→Λp**
K-pn →Σ0n→Λ(p)n

— **2NA + conversion Σ0n→Λn**
K-pp →Σ0p→Λ(n)p

KLOE data: Λp analysis

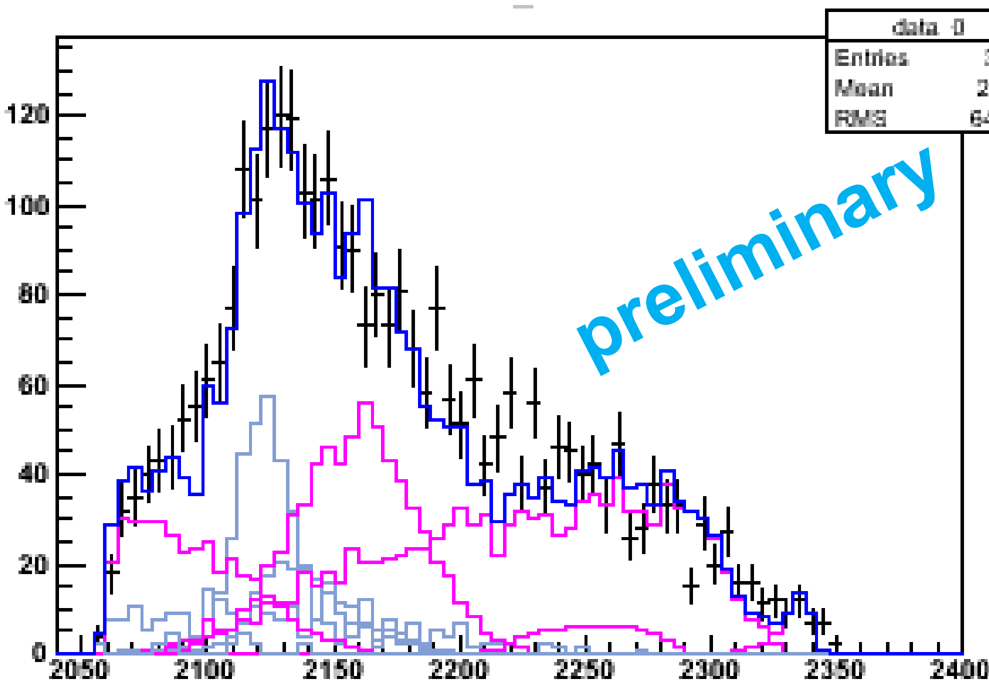

MΛp (MeV/c2)

Fit 3D (PΛ, Pp, θΛp)
for Λp inclusive selection with proton mass calculated by TOF (calorimeter hit)

DATA
Total simulation
1NA simulation
2NA (in absorption or conversion) sim.

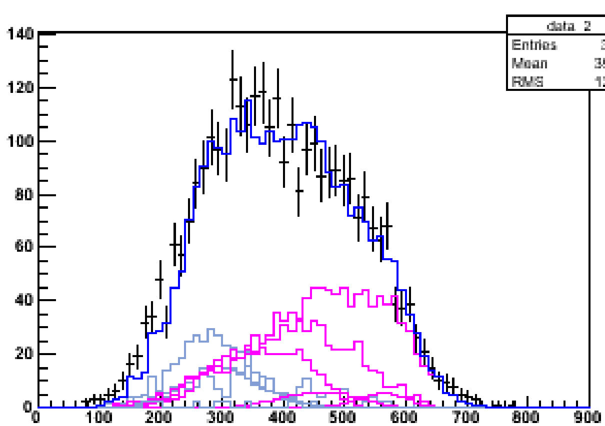

PΛp (MeV/c)

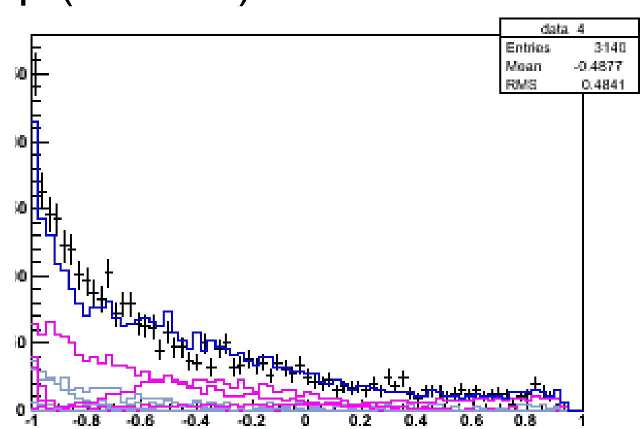

Cos(θΛp)

Conclusions and perspectives ..

- $m_{\Sigma\pi^-}$ spectra show a high invariant mass component → associated to in-flight K^- capture
- PRELIMINARY $\Lambda\pi^-$ first measurement of RES/N-R ratio in nuclear K^- absorption.

Next steps …

- Same analysis is ongoing for $\Sigma^0\pi^-$ → extraction of $|f^{N\text{-}R}_{\Sigma 0\pi-}(I=1)|$
- Similar description of $\Sigma^+\pi^-$ and $\Sigma^-\pi^+$ production → extraction of $|f^{N\text{-}R}_{\Sigma+\pi-}|$ and $|f^{N\text{-}R}_{\Sigma-\pi+}|$, a comparison of these could give an estimate of

  $|f^{N\text{-}R}_{\Sigma+\pi-}(I=0) + f^{N\text{-}R}_{\Sigma+\pi-}(I=1)|$ against $|f^{N\text{-}R}_{\Sigma+\pi-}(I=0) - f^{N\text{-}R}_{\Sigma+\pi-}(I=1)|$
- Branching ratio modifications in different targets (see A. Ohnishi et al., Phys. Rev. C 56 5 (1997) 2767) & Density dependence of $m_{\Sigma\pi}$ and $p_{\Sigma\pi}$ (see L. R. Staronski, S. Wycech, Nucl. Phys. 13 (1987) 1361 / A. Cieplý, E. Friedman, A. Gal, V. Krejčiřík - Phys.Lett.B698 (2011) 226-230)

Sheding light on the nature of the $\Lambda(1405)$ and its behaviour in nuclear matter is crucial to understand the role of strangeness in our universe.

K^-
Thanks

K^-

SPARE SLIDES ...

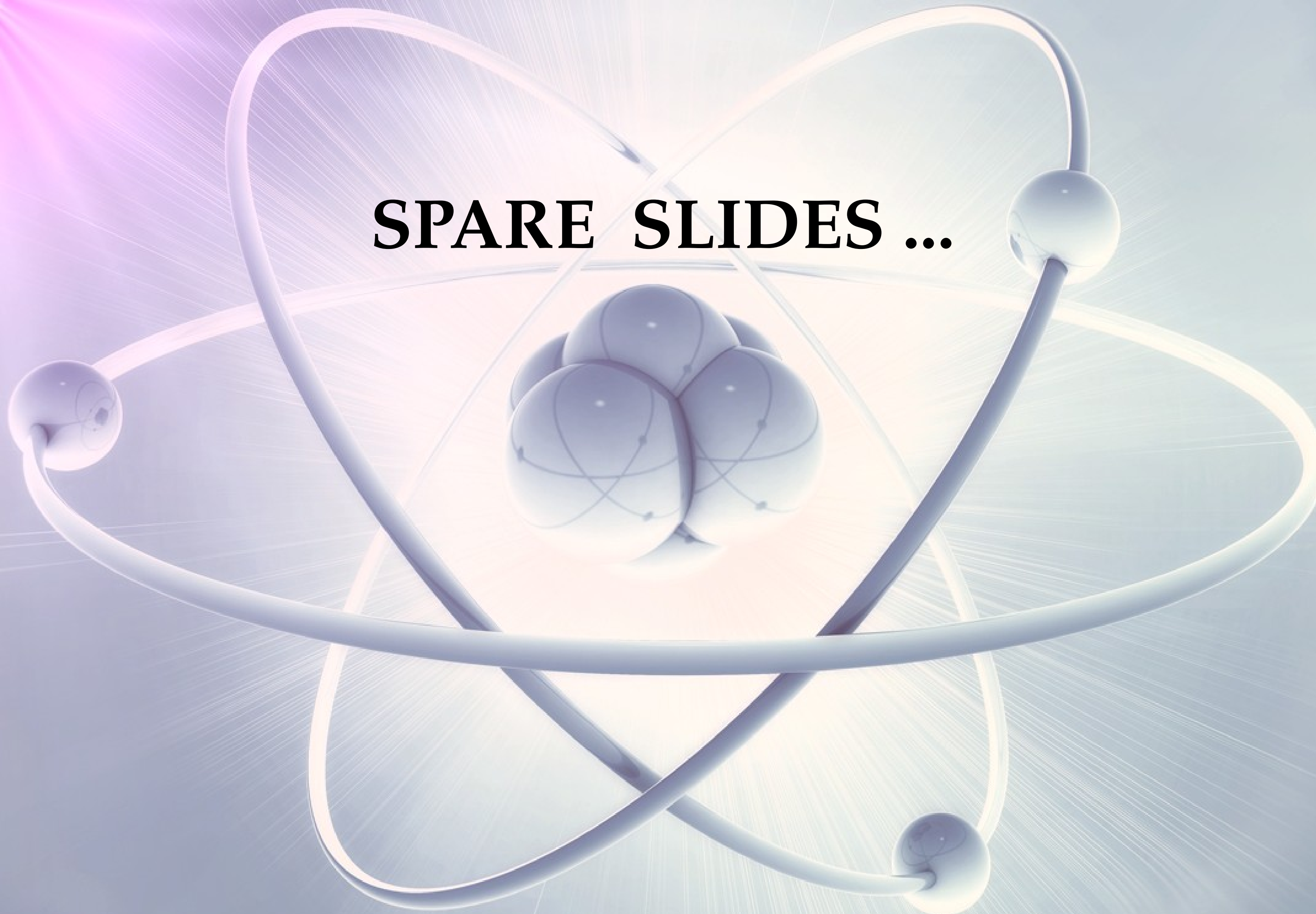

AMADEUS & DAΦNE

K^-

Completely neutral channel:

$\Lambda \rightarrow n\ \pi^0$

Possibility to detect neutrons!

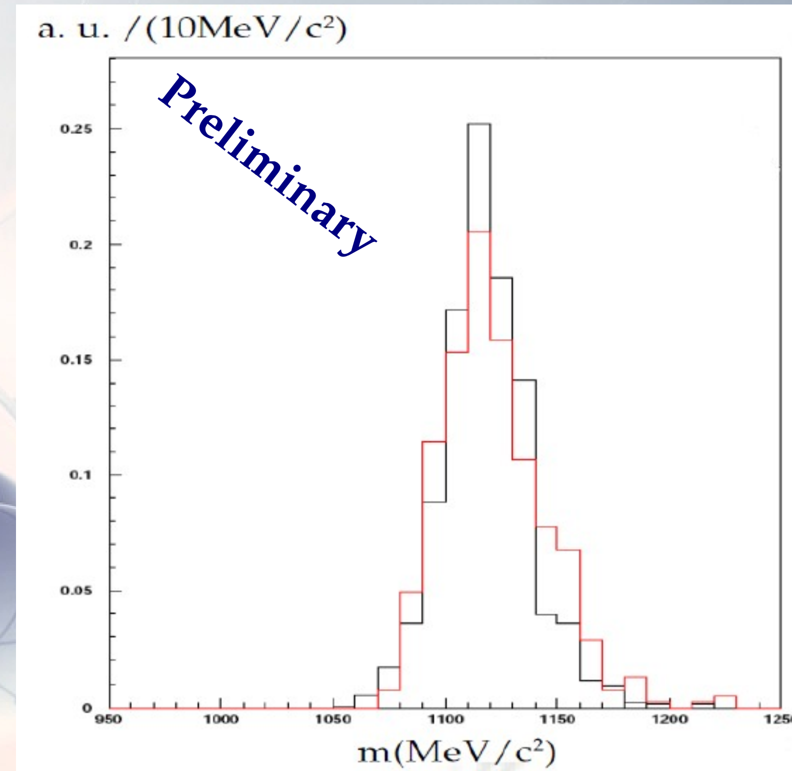

black MC **red data**

Perspective: $\Sigma^-\pi^+ \rightarrow (n\pi^-)\ \pi^+$

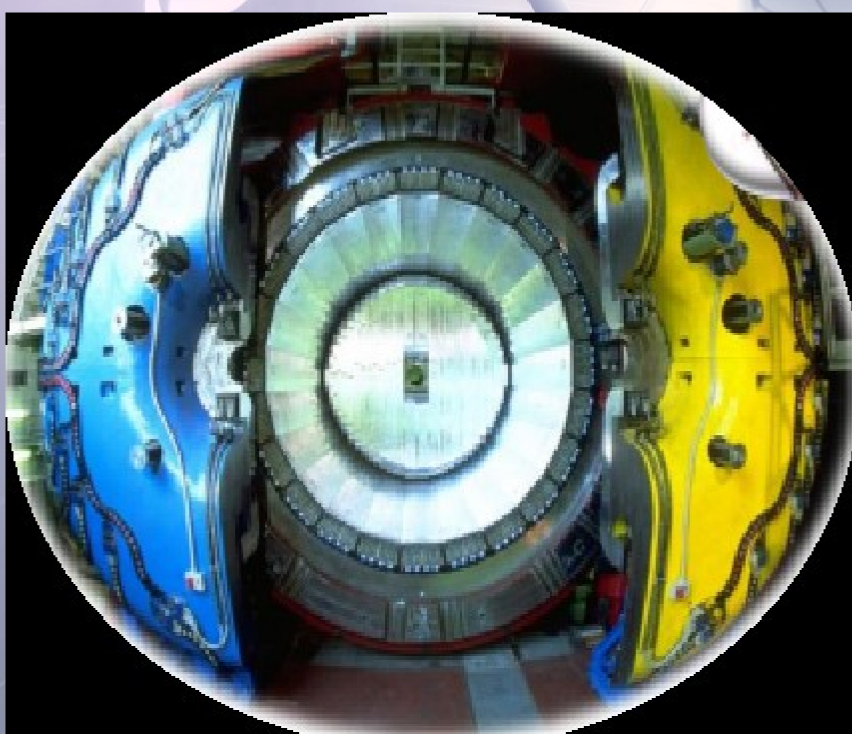

KLOE

- **96% acceptance,**
- **optimized in the energy range of all charged particles involved**
- **good performance in detecting photons (and neutrons checked by kloNe group (M. Anelli et al., Nucl Inst. Meth. A 581, 368 (2007)))**

KLOE data on K^- nuclear absorption

Use of two different data samples:

- KLOE data from 2004/2005 (2.2 fb^{-1} total, 1.5fb^{-1} analyzed)

- Dedicated run in november/december 2012 with a Carbon target 4/6 *mm* thickness (~90 pb^{-1}; analyzed 37 pb^{-1}, x1.5 statistics)

Position of the K^- hadronic interaction inside KLOE:

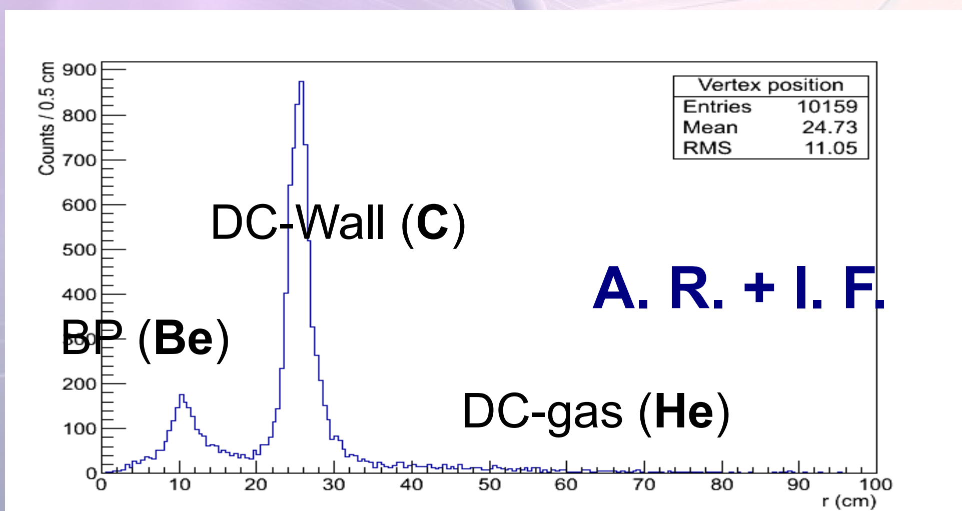

2005 data

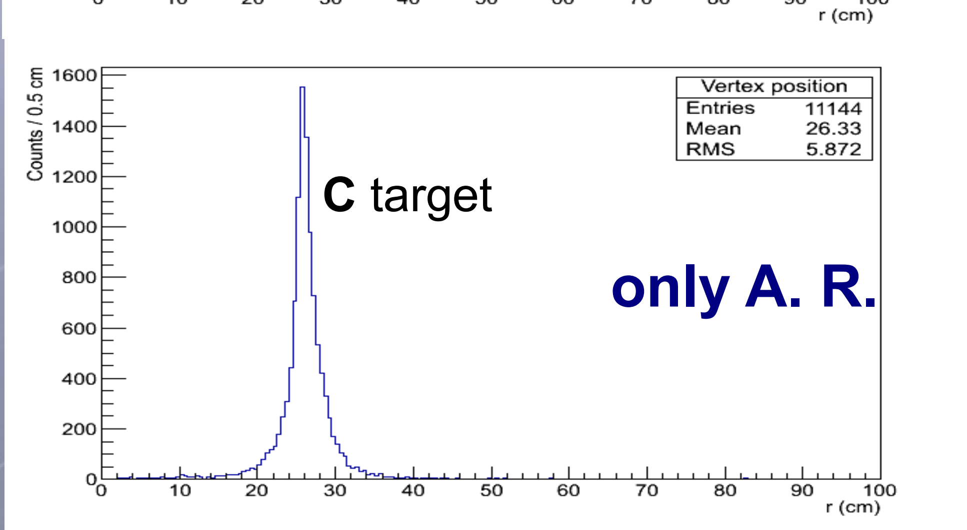

2012 with Carbon target

Photon clusters identification

K$^-$

$$K^- \text{"p"} \rightarrow \Sigma^0\pi^0 \rightarrow (\Lambda(1116)\,\gamma_3)\,(\gamma_1\gamma_2) \rightarrow (p\pi^-)\,3\gamma$$

1) 3 neutral clusters selection (E_{c1} > 20 MeV) not from K^+ decay ($K^+ \rightarrow \pi^+\pi^0$)

2) photon clusters selection: $\chi_t^2 = t^2/\sigma_t^2$ **where** $t = t_i - t_j$

time of flights in light speed hypothesis.

Three photons in time from the Λ decay vertex r_Λ

3) photon clusters identification: γ_3 from $\pi^0 \rightarrow \gamma_1\gamma_2$

$$\chi^2_{\pi\Sigma} = \frac{(m_{\pi^0} - m_{ij})^2}{\sigma^2_{ij}} + \frac{(m_{\Sigma^0} - m_{k\Lambda})^2}{\sigma^2_{k\Lambda}}$$

i,j and *k* candidate photon cluster.

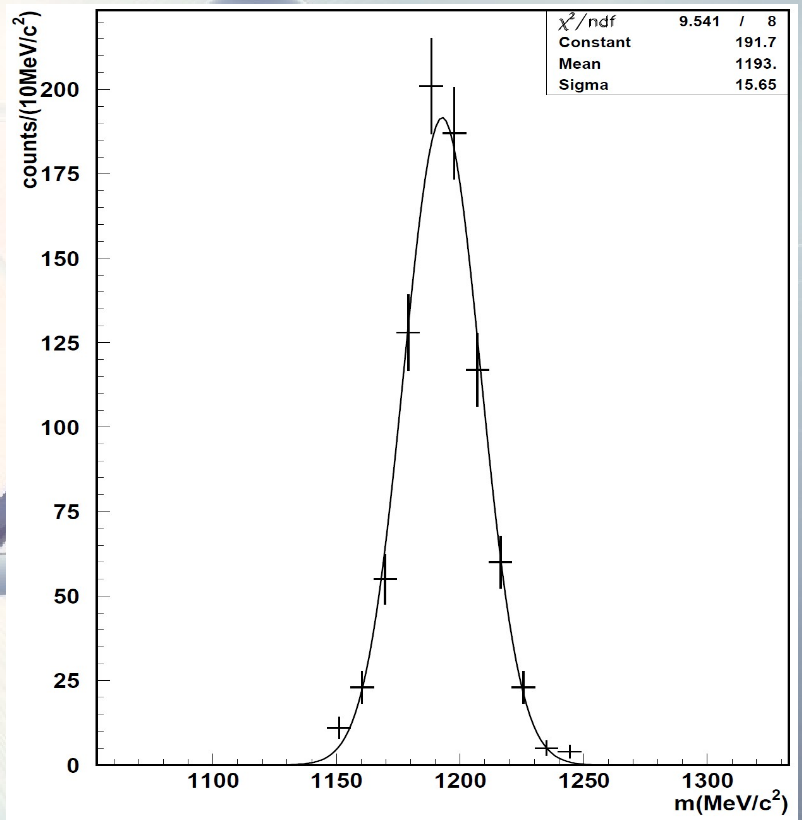

4) Cuts on χ_t^2 and $\chi_{\pi\Sigma}^2$ optimized on MC simulations & splitted clusters rejection

Efficiency (98±1)% to identify photons and (78±2)% to select the correct triple of neutral clusters.

Resolution for neutral clusters

K^-

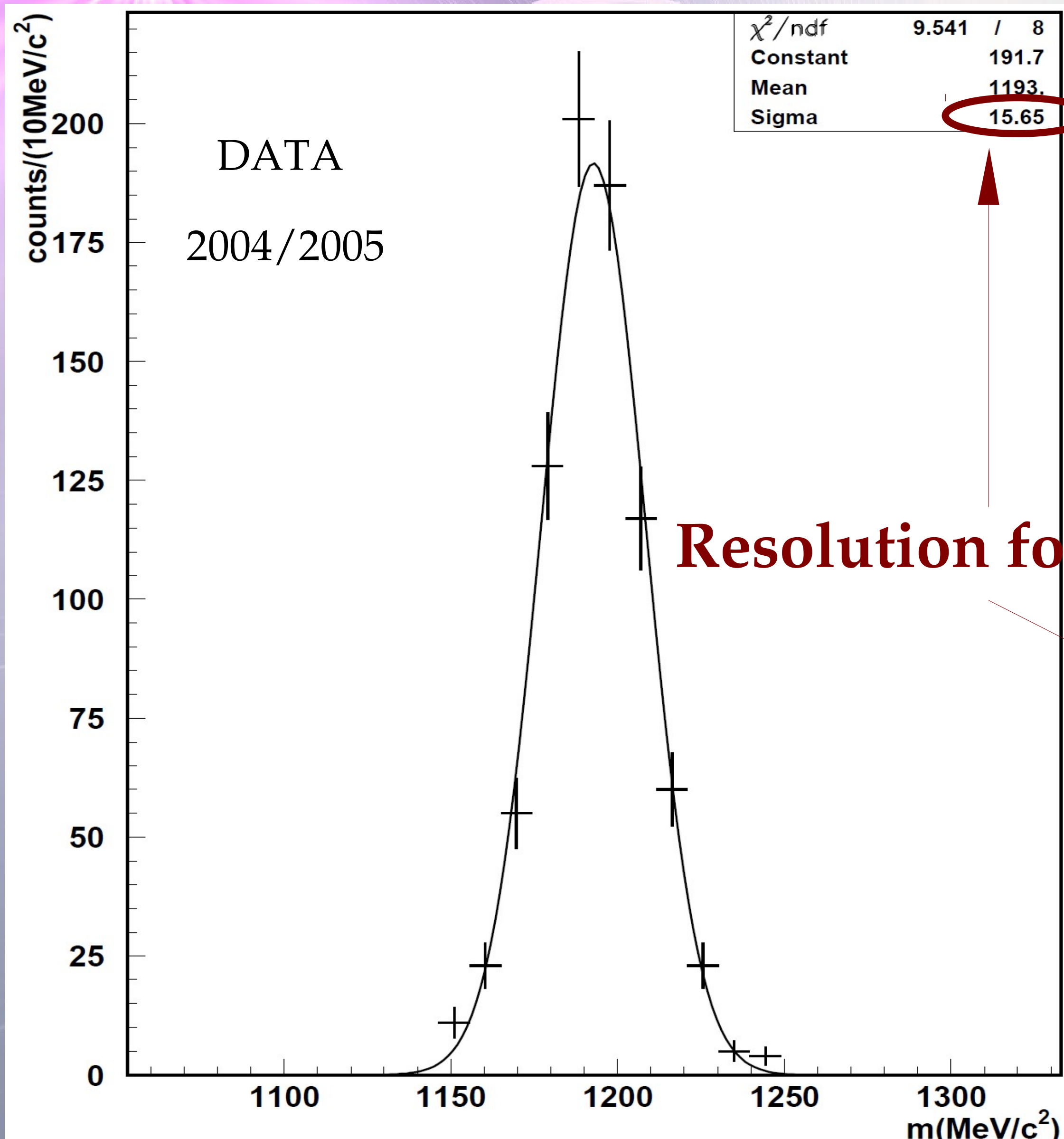

$m_{\Lambda\gamma 3}$

Resolution for neutrals !

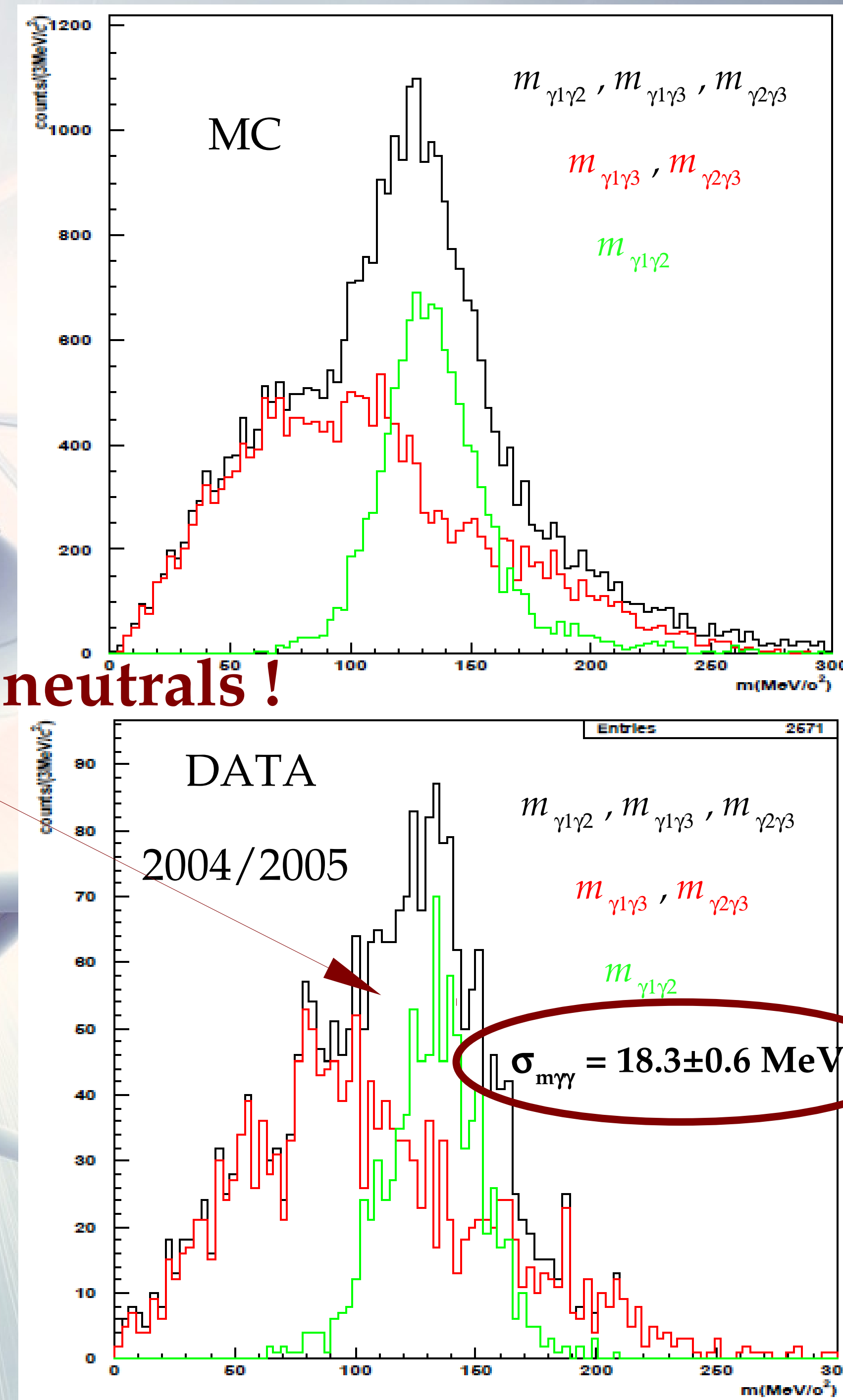

$\Sigma^+ \pi^-$ channel … A NEW POWERFUL TOOL (A. Scordo) !

$K^- p \rightarrow \Sigma^+ \pi^-$ detected via: $(p\pi^0)\,\pi^-$

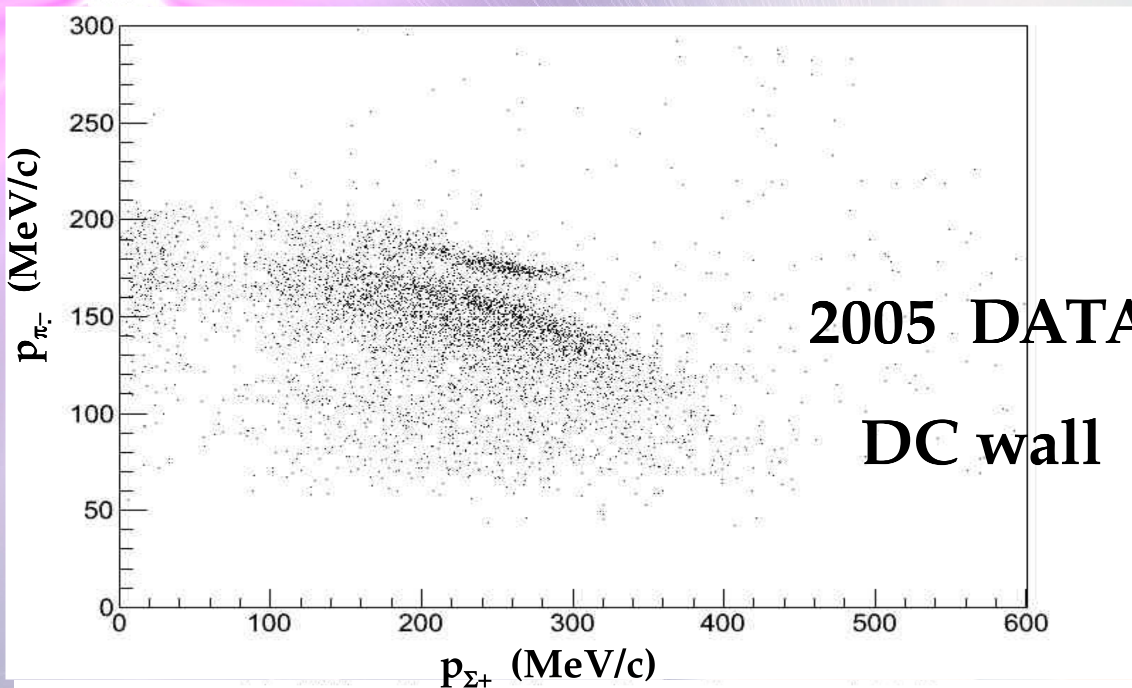

2005 DATA

DC wall

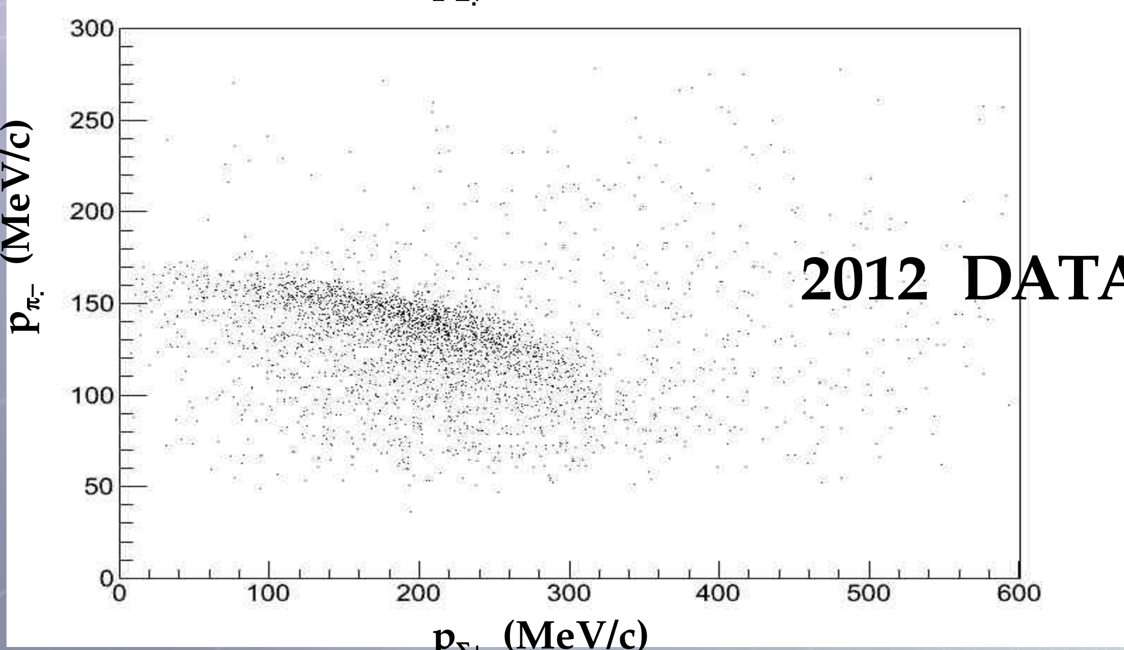

2012 DATA

BEFORE …

K^-H interaction probability estimate based on K^- interaction AT-REST in hydrocarbons mixture data (Lett. Nuovo Cimento, C 1099 (1972))

order of 1% !!!

NOW

Thanks to the excellent p_{π^-} resolution

…

$\Sigma^+ \pi^-$ channel … A NEW POWERFUL TOOL (A. Scordo) !

$K^- p \rightarrow \Sigma^+ \pi^-$ detected via: $(p\pi^0)\, \pi^-$

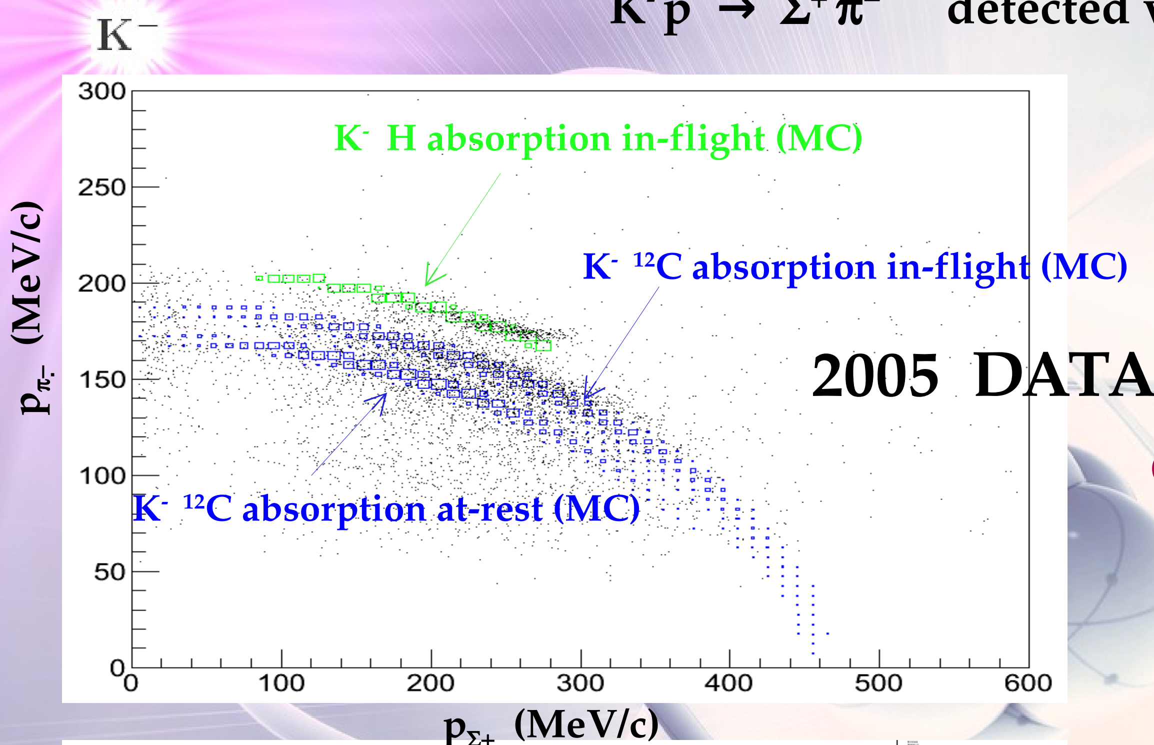

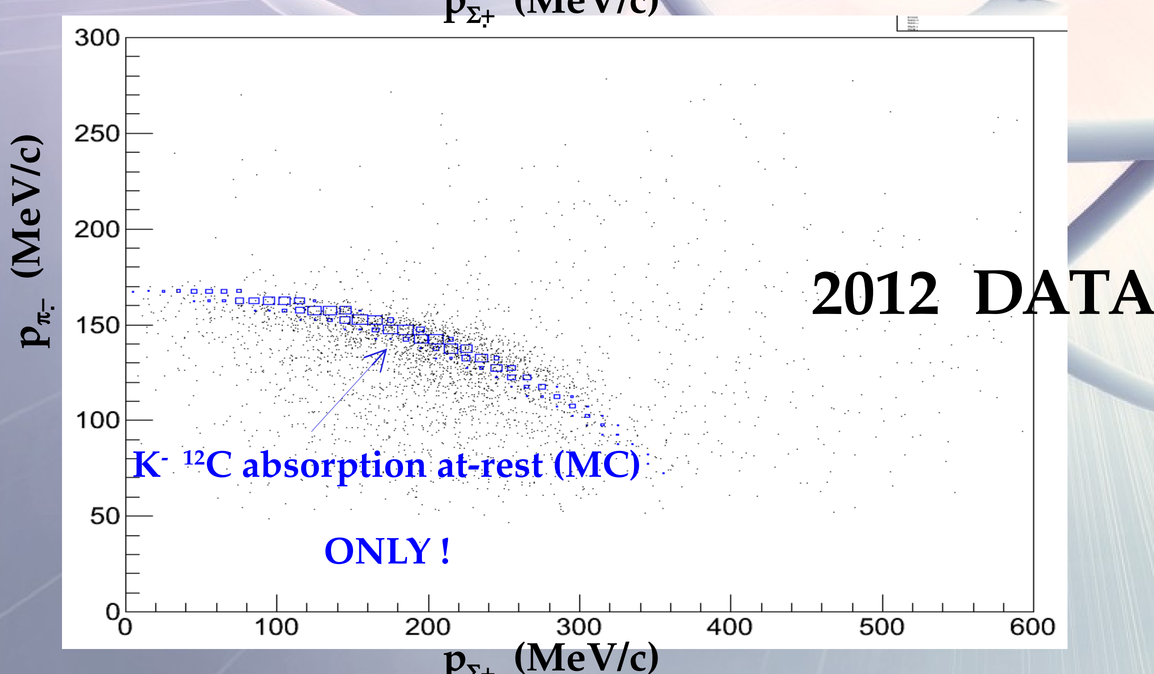

Complete understanding of different nuclear targets in different KLOE materials

AND

K^- H contribution ~ 20%

… in-flight the situation is extremely different

Concluding, a fit of $\Sigma^0\pi^0$ spectrum requires ...

K^-

9 components:

- Resonant component K^- C at-rest/in-flight.
- Non resonant $\Sigma^0\pi^0$ K^- H production at-rest/in-flight
- Non resonant $\Sigma^0\pi^0$ K^- C production at-rest/in-flight
- $\Lambda\pi^0$ background (Σ(1385) + I.C.)
- non resonant misidentification (*n.r.m.*) background

a careful model of K^- - nuclear interaction is required

in Helium and Carbon!

Channel: $K^- \, {}^4He \rightarrow \Lambda \pi^- \, {}^3He$ … the idea

Bubble chamber experiments exhibit two components:

- Low momentum $\Lambda \pi^-$ pair → S-wave, I=1, non-resonant transition amplitude.
- High momentum $\Lambda \pi^-$ pair → P-wave resonant formation ?

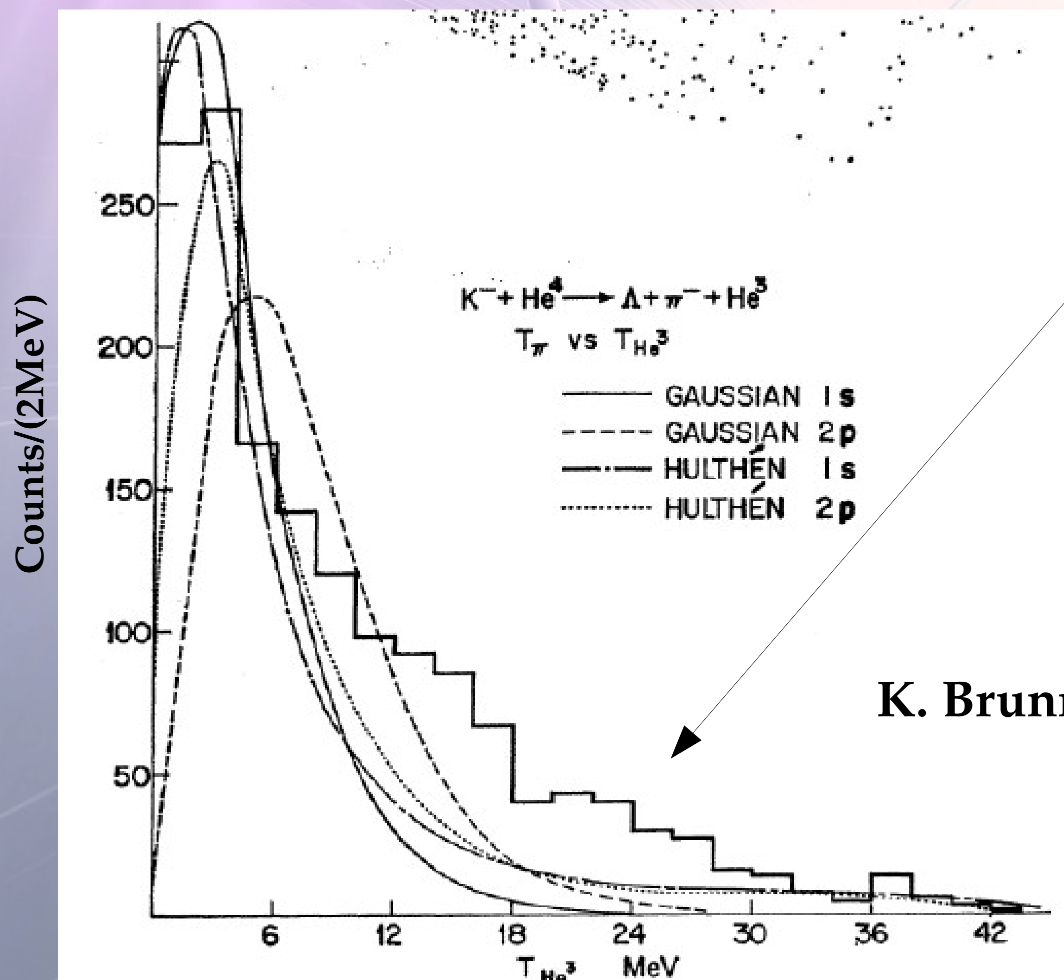

Also exsists in S-state K-mesic atom

as a result of the

three body structure of the system

(K = 1, n=2, ^{3}He = 3)

K. Brunnel et al., Phys.Rev. D2 (1970) 98

Channel: $K^- \; {}^4He \rightarrow \Lambda \pi^- \; {}^3He$ … the strategy

K^-

- Fit of the $p_{\Lambda\pi^-}$ observed distribution using calculated distributions :

$$P_s^{\,s}\,(p_{\Lambda\pi}) = |\Psi_N\,(p_{\Lambda\pi})|^2 \; |f^{\,s}\,(p_{\Lambda\pi})|^2 \;\rho$$

where $\rho = k\, p_{\Lambda\pi}^{\,2}$

$$P_s^{\,p}\,(p_{\Lambda\pi}) = |\Psi_N\,(p_{\Lambda\pi})|^2 \; c^2 \; |2f^{\,\Sigma^*}\,(p_{\Lambda\pi})|^2 \;\rho/3 \;\; (kp_{\Lambda\pi})^2$$

The constant $c = M_K/(M_K+M_n) = 0.345$ re-couples the S x S waves to P x P waves

- To determine the ratio resonant/non-res.

↓

$|f^{\,N\text{-}R}{}_{\Lambda\pi}|$ given the fairly well known $|f^{\,\Sigma^*}{}_{\Lambda\pi}|$

Channel: $K^- \ {}^4He \rightarrow \Lambda \pi^- \ {}^3He$ … calculated reactions

Calculated primary hadronic interactions:

- $K^- \ {}^4He \rightarrow \Lambda \pi^- \ {}^3He$
  - **At-rest :** S-wave non-Res / P-wave $\Sigma(1385)$ Res
  - **In-flight :** S-wave non-Res / P-wave $\Sigma(1385)$ Res
- $K^- \ {}^4He \rightarrow \Sigma^0 \pi^- \ {}^3He$
  - **At-rest :** S-wave non-Res / P-wave $\Sigma(1385)$ Res
  - **In-flight :** S-wave non-Res / P-wave $\Sigma(1385)$ Res
- $K^- \ {}^4He \rightarrow (\Sigma \pi)^0 \ {}^3H$
  - **At-rest :** S-wave non-Res / S-wave $\Lambda(1405)$ Res / P-wave $\Sigma(1385)$ Res
  - **In-flight :** S-wave non-Res / S-wave $\Lambda(1405)$ Res / P-wave $\Sigma(1385)$ Res

Channel: $K^- \, ^4He \rightarrow \Lambda \, \pi^- \, ^3He$ … calculated reactions

Calculated secondary hadronic interactions:

EACH INTERNAL CONVERSION PROCESS:

$$\Sigma \; p/n \rightarrow \Lambda \; p/n$$

was calculated for both P-wave and S-wave produced Σs.

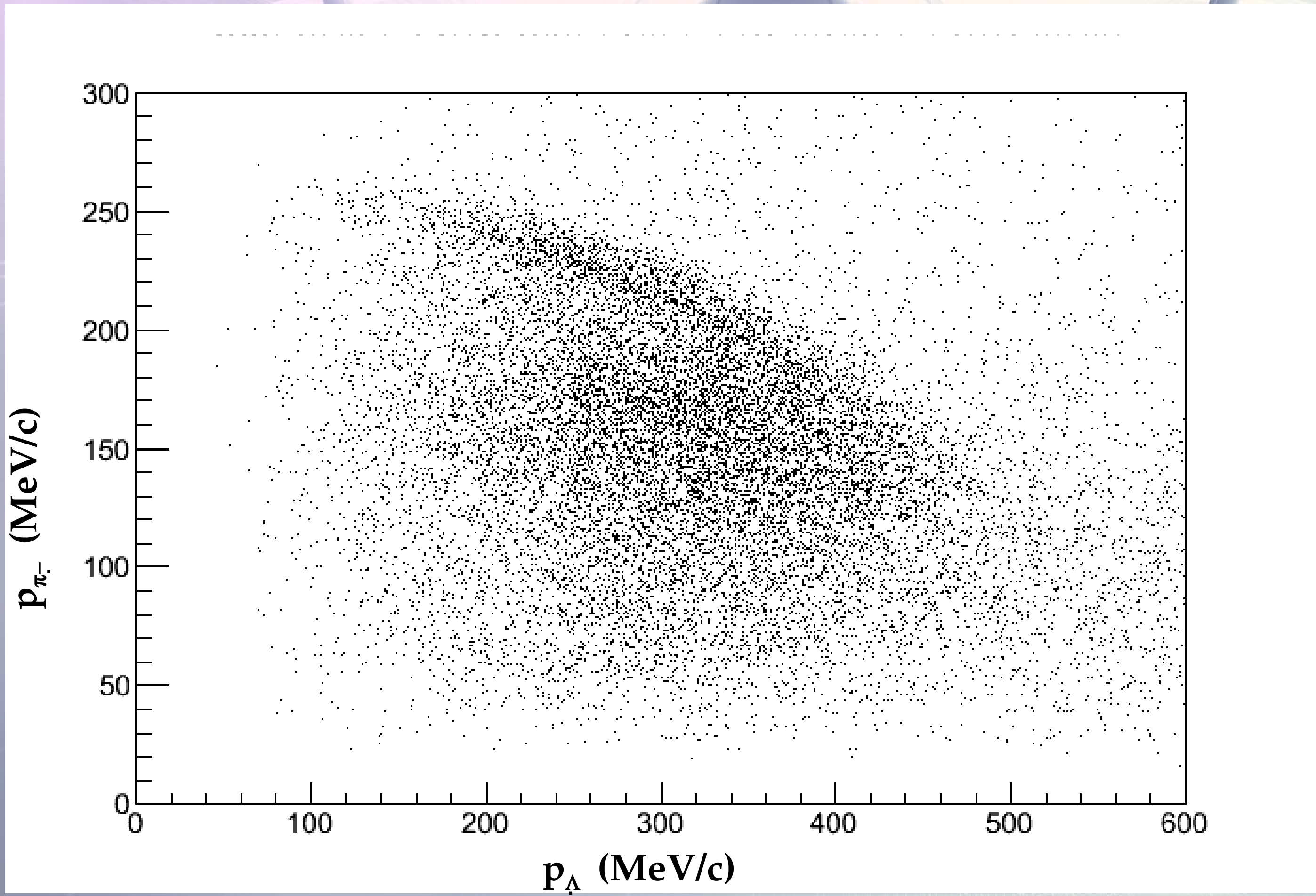

Channel: $K^- \ {}^4He \rightarrow \ \Lambda \pi^- \ {}^3He$ … calculated reactions

Calculated secondary hadronic interactions:

EACH INTERNAL CONVERSION PROCESS:

$$\Sigma \ p/n \ \rightarrow \ \Lambda \ p/n$$

was calculated for both P-wave and S-wave produced Σs.

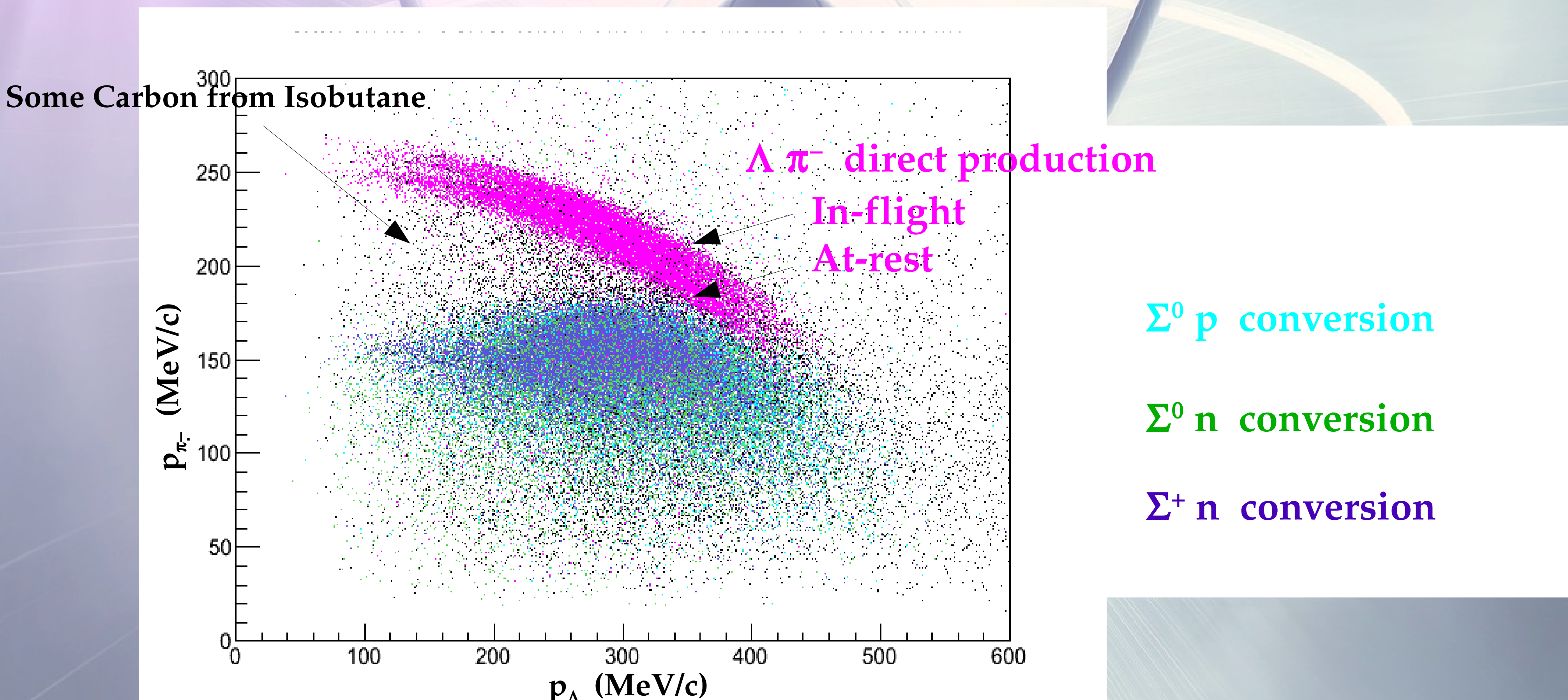

$K^- \ {}^4He \rightarrow \Lambda \pi^- \ {}^3He$ <u>events selection</u>

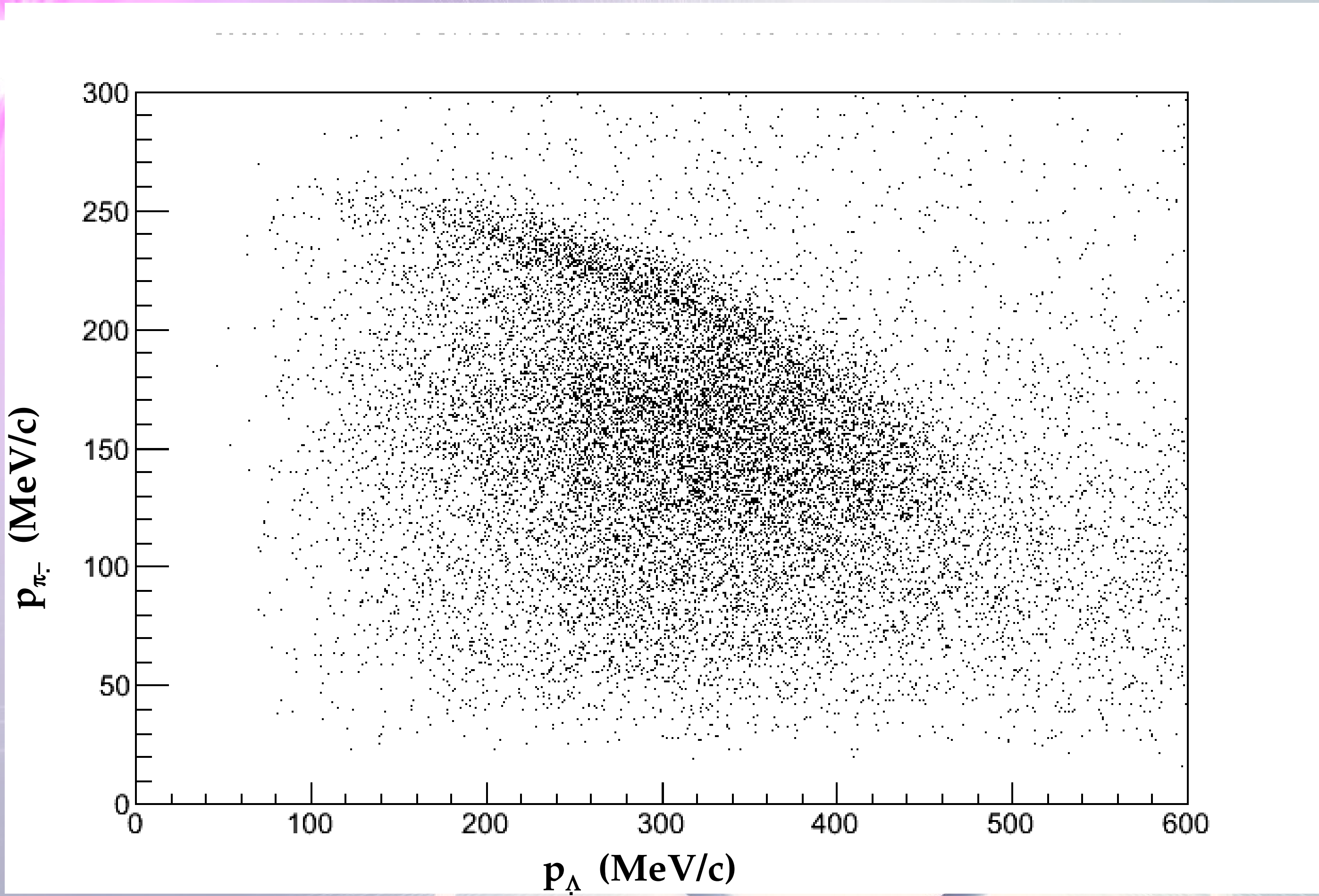

$K^- \ {}^4He \rightarrow \ \Lambda \pi^- \ {}^3He$ events selection

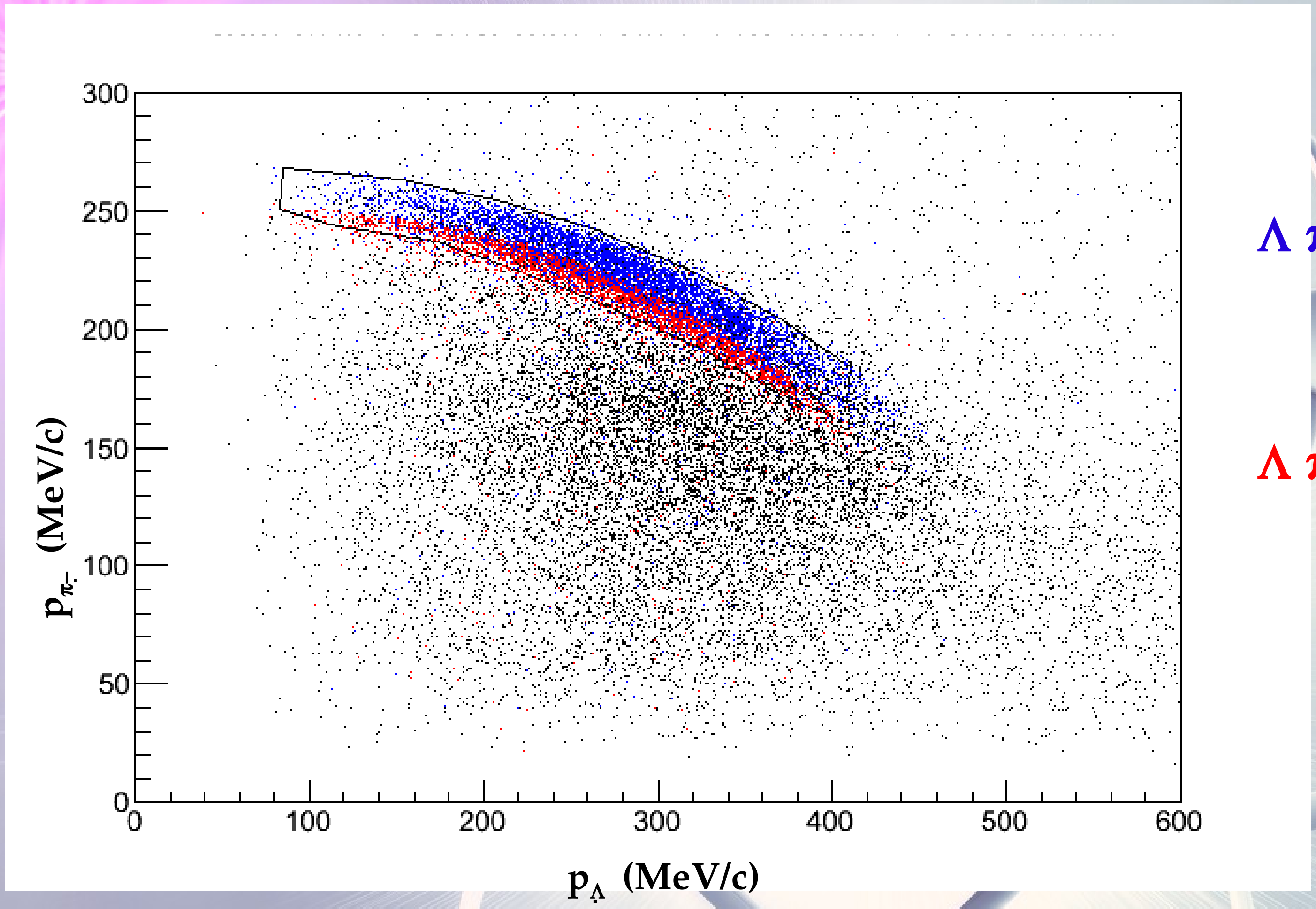

$\Lambda \pi^-$ direct production
In-flight RES + N-R

$\Lambda \pi^-$ direct production
At-rest RES + N-R

- CUT based on MC simulations used to select $\Lambda \pi^-$ direct production events
- At-rest CAN NOT be separated from In-flight → global fit performed
- Background sources: - $\Lambda \pi^-$ events from Σ p/n → Λ p/n conversion
  - $\Lambda \pi^-$ events from K^- ${}^{12}C$ absorptions in Isobutane

$K^- \ ^4He \rightarrow \Lambda \pi^- \ ^3He$ background

- **Σ p/n → Λ p/n conversion:**

  Each possible conversion channel was simulated

  Σ^0 p / Σ^0 n / Σ^+ n / At-rest / In-flight / from RES and N-R produced Σs

- **$\Lambda \pi^-$ events from $K^- \ ^{12}C$ absorptions in Isobutane (90% He, 10% C_4H_{10}):**

  $K^- \ ^{12}C$ DATA in the KLOE DC wall are used

  estimated contribution:

  $$N_{KHe}/N_{KC} = (n_{KHe}/n_{KC}) \cdot (\sigma_{KHe}/\sigma_{KC}) \cdot (BR_{KHe}(\Lambda \pi^-)/BR_{KC}(\Lambda \pi^-)) \sim 1.3 \pm 0.3$$

  Nuovo Cimento 39 A 338-347 (1977)

  $K^- \ ^{12}C$ still not calculated:

  - **uncertain initial state of K meson $l_K = 1, 2, 3$**
  - **4 nucleons in s-orbit , 8 nucleons in p-orbit**
  - **final state hyperon interactions**

Study of the background

The main background sources for this channel are (example in ^{12}C):

- $K^- \ ^{12}C \rightarrow \Sigma^0(1385) + {}^{11}B \rightarrow \Lambda\pi^0 + {}^{11}B$

Σ^0(1385) can not decay in $\Sigma^0 \pi^0$ for isospin conservation.

- **Internal conversion** $K^- \ ^{12}C \rightarrow \Lambda(1405) + {}^{11}B \rightarrow \mathbf{\Sigma^0}\pi^0 + {}^{11}B$, $\Sigma^0 N \rightarrow \Lambda N$
  competes with the decay $\Sigma^0 \rightarrow \Lambda \gamma$.

Both background sources were analized by different methods:

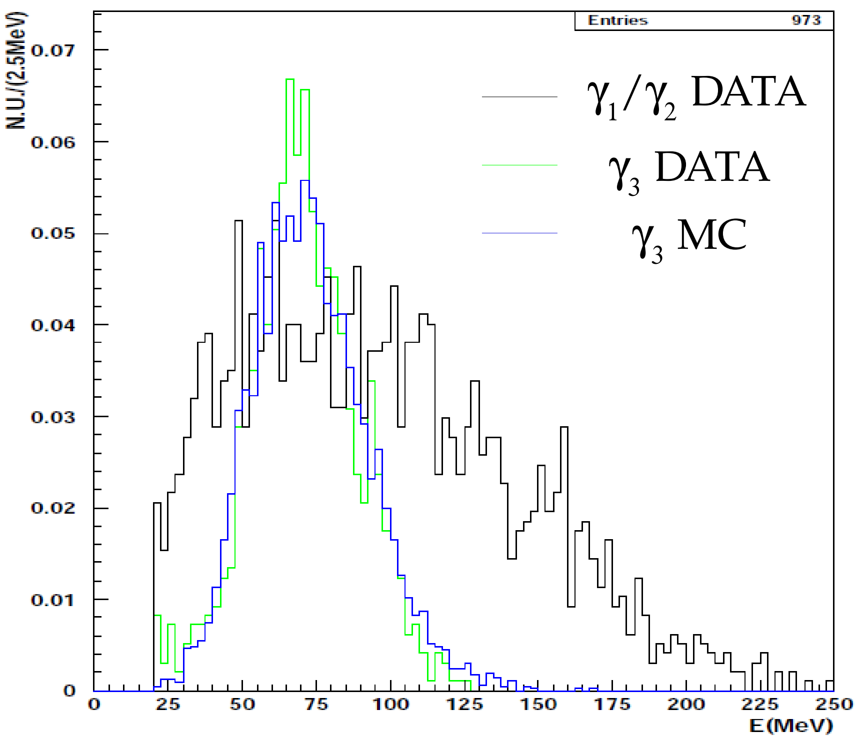

photons energy distribution

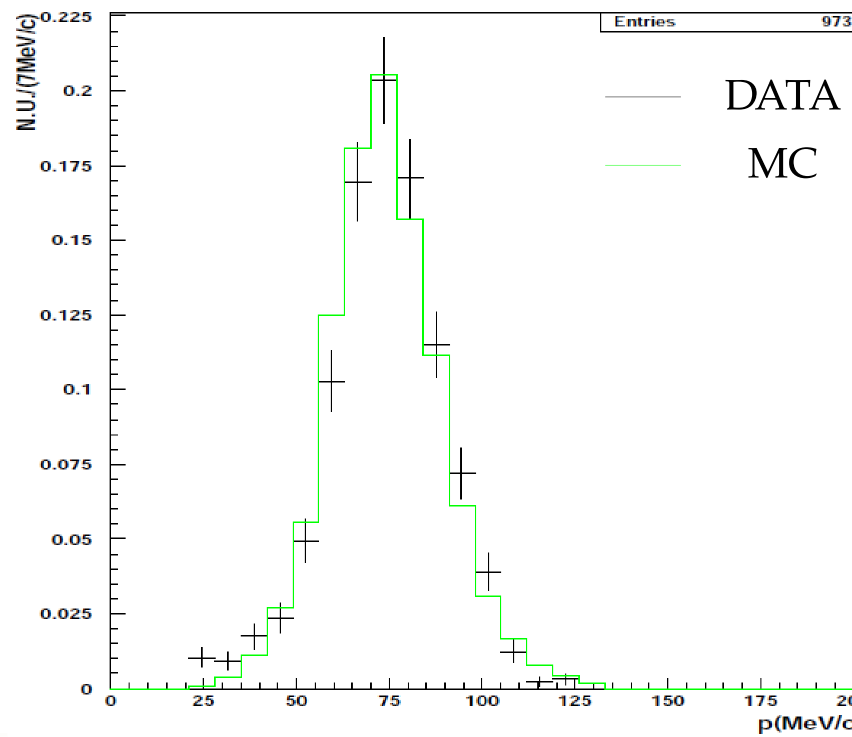

Λ momentum in the Σ^0 rest frame

Study of the background

In both cases γ_3 is not present, if a contamination is present, the neutral cluster which is associated to γ_3 by reconstruction should show differences.

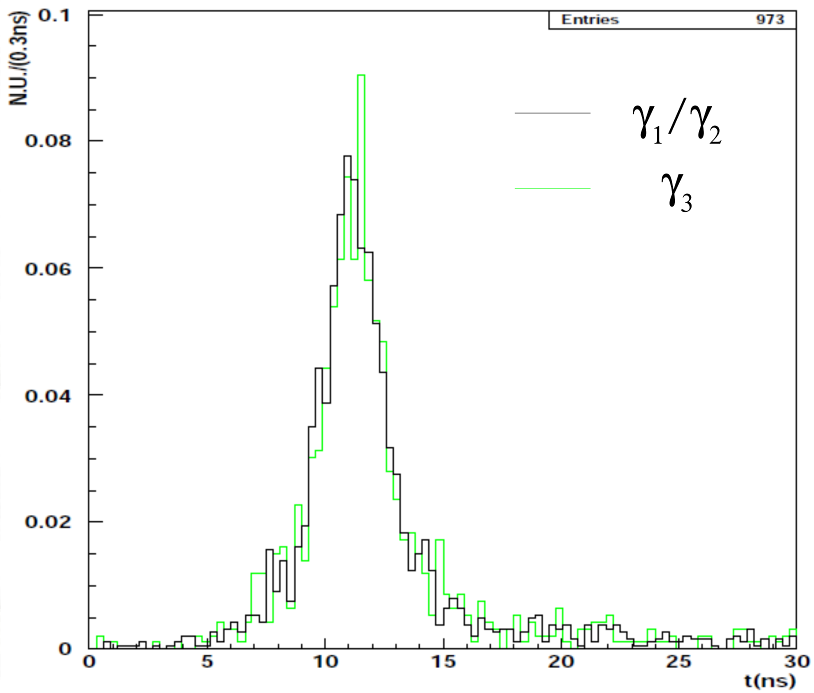

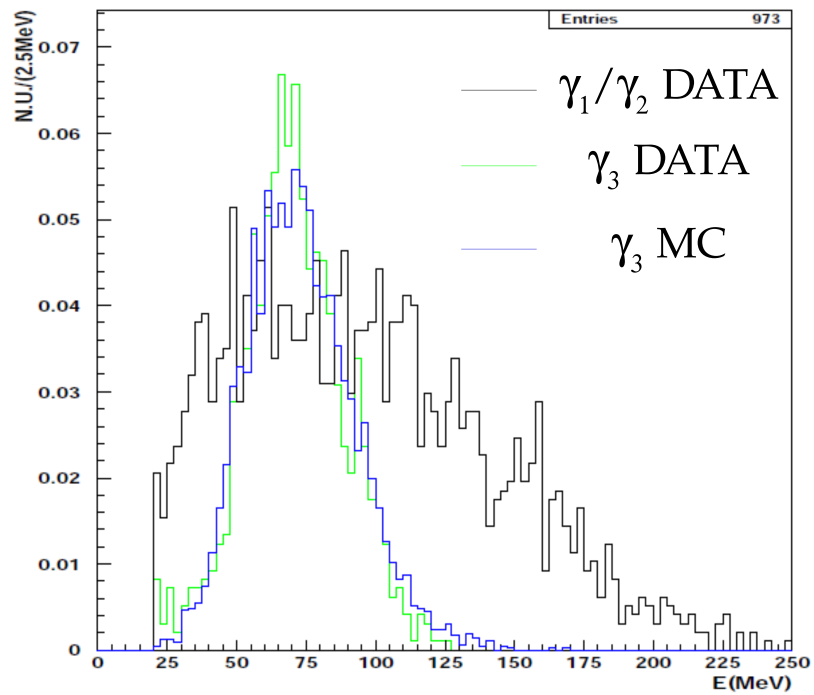

- Right: the energy distribution of γ_3 (green) is in perfect agreement with MC simulations of pure signal events (blue) (energy spectrum of $\gamma_1\gamma_2$ is shown in black).
- Left: the time distribution of γ_3 (green) is in agreement with the time distributions of the two photons coming from π^0 decay (black).

Study of the background

The numbers of pure background $\Sigma(1385)$ and $\Sigma^0 N \to \Lambda N$ events passing the analysis cuts are normalized to pure signal $\Lambda(1405)$ events, then weighted to the BRs for $\Lambda\pi^0$ direct production (D), internal conversion (IC) and $\Sigma^0\pi^0$ production due to K^- interaction in ^{4}He and C respectively :

P. A. Katz et al., Phys.Rev. D1 (1970) 1267

C. Vander Velde-Wilquet et al., Nuovo Cimento 39 A, (1977) 538

The percentages of background events entering the final selected samples are:

$$\frac{n_{\Lambda\pi^0\,D}\,\mathrm{norm} + n_{\Lambda\pi^0\,IC}\,\mathrm{norm}}{n_{\Sigma^0\pi^0} + n_{\Lambda\pi^0\,D}\,\mathrm{norm} + n_{\Lambda\pi^0\,IC}\,\mathrm{norm}} = 0.03 \pm 0.01$$

in DC wall (0.03 ± 0.02 in DC gas)

$p_{\pi^0\Sigma^0}$ spectrum for boost and anti-boost events

$p_{\Sigma^0\pi^0}$ distribution for lower (black) and higher (red) p_k values

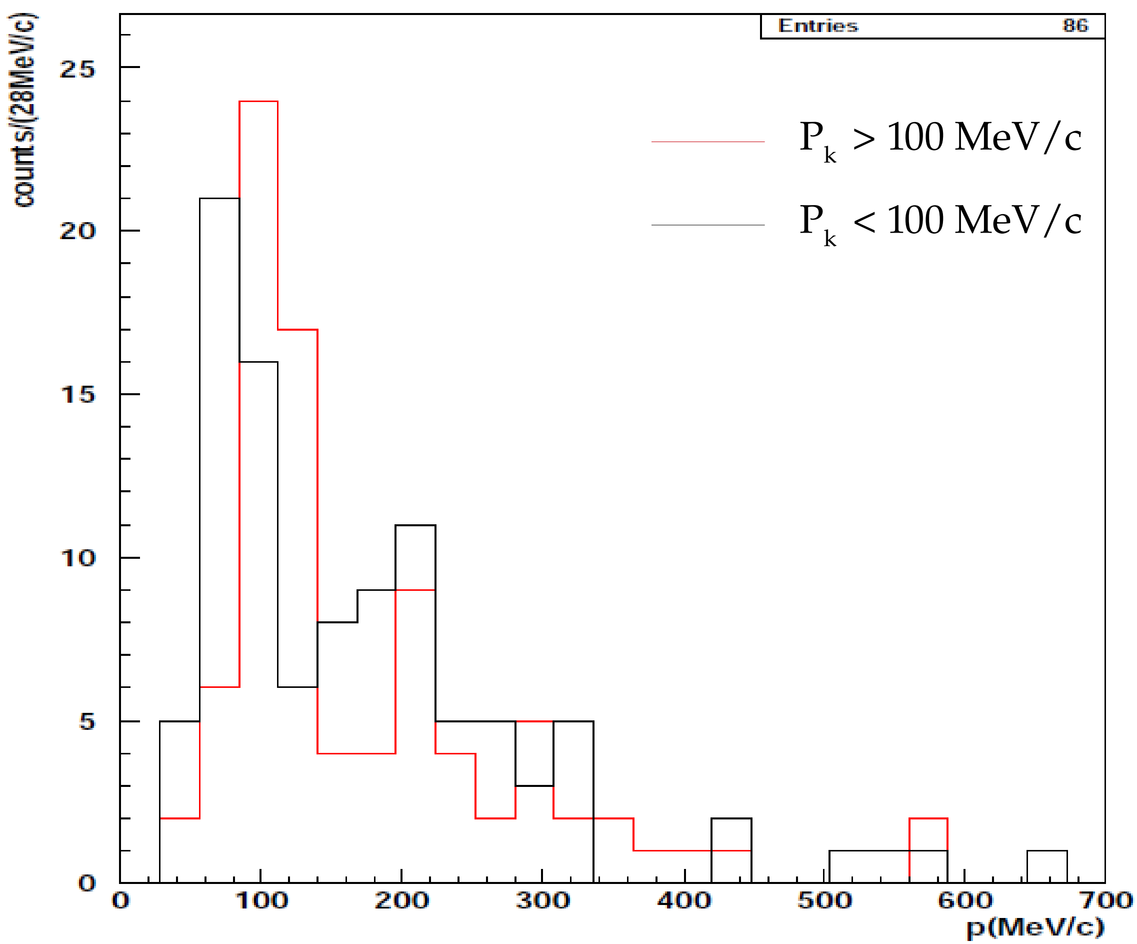

$\Sigma^0\,\pi^0$ channel

K^-

Mass momentum correlatation

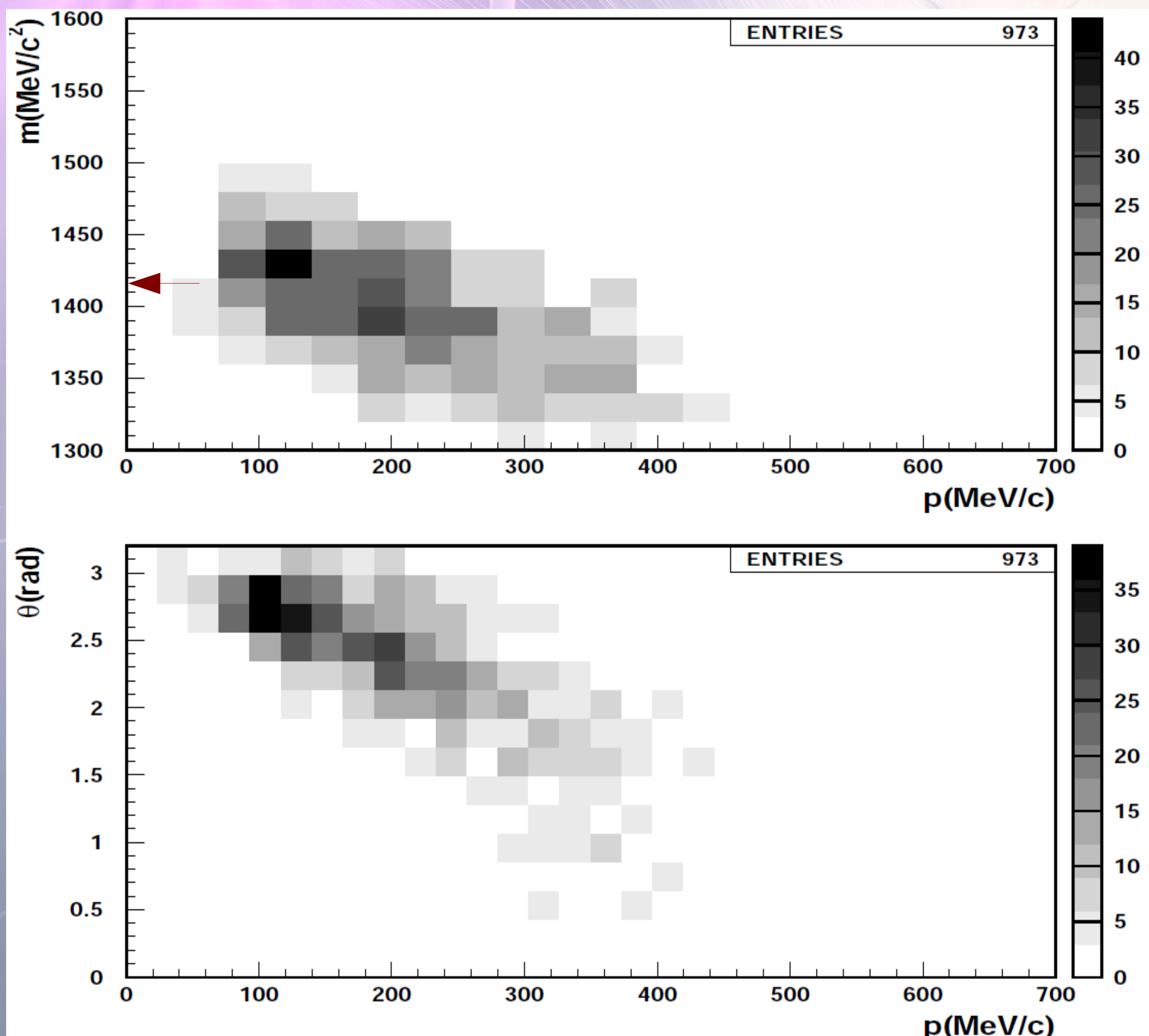

Top $m_{\Sigma^0\pi^0}$ vs $p_{\Sigma^0\pi^0}$, bottom $\theta_{\Sigma^0\pi^0}$ vs $p_{\Sigma^0\pi^0}$.

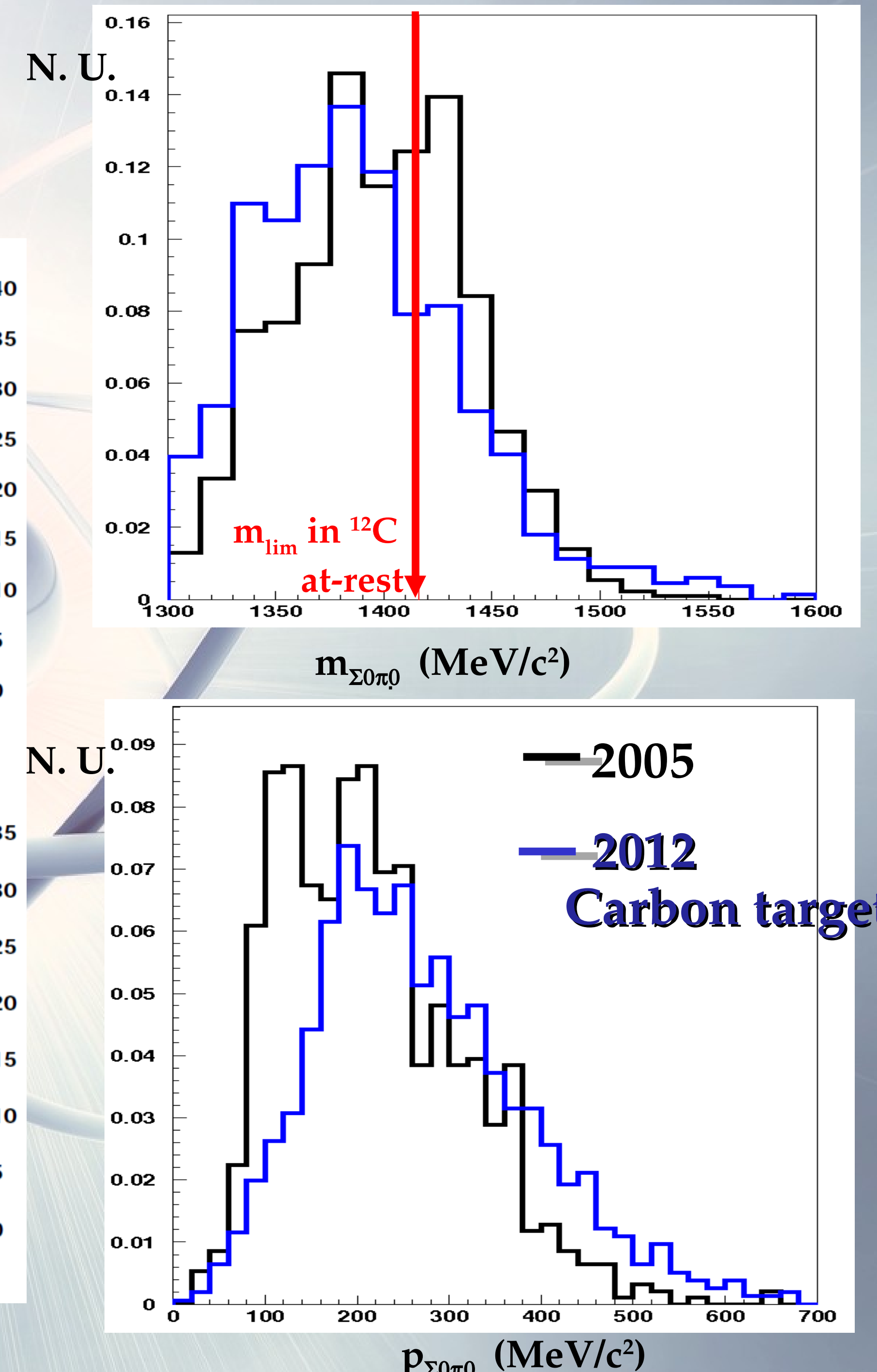

Fit of $\Sigma^0\pi^0$ spectrum in C

K^-

8 component fit, simultaneously $m_{\Sigma0\pi0}$ & $p_{\Sigma0\pi0}$:

- Breit-Wigner resonant component K^- C at-rest/in-flight. $(M,\Gamma) = (1405 \div 1430\ ,\ 5 \div 52\ )$
- Non resonant $\Sigma^0\pi^0$ K^- H production at-rest/in-flight
- Non resonant $\Sigma^0\pi^0$ K^- C production at-rest/in-flight
- $\Lambda\pi^0$ background ($\Sigma(1385)$ + I.C.)
- non resonant misidentification (*n.r.m.*) background

$K^-\ {}^{12}C \rightarrow \Sigma^0\pi^0 + {}^{11}B$ (Boron spectator, left in ground state)

secondary interactions not taken into account.

Fit of $\Sigma^0\pi^0$ spectrum in C

K^-

χ^2_{min} /ndf ~ 1.7 corresponding to $(M_{min}, \Gamma_{min}) = (1426, 52)$ MeV/c^2

- **Global fit** (red)
- **Resonant component K^- C at-rest** (green)
- **n. r. K^- C at-rest** (blue)
- **n. r. K^- C in-flight** (yellow)
- **n. r. K^- H in-flight** (cyan)
- **$\Lambda^0\pi^0$ background + n. r. m.** (magenta)

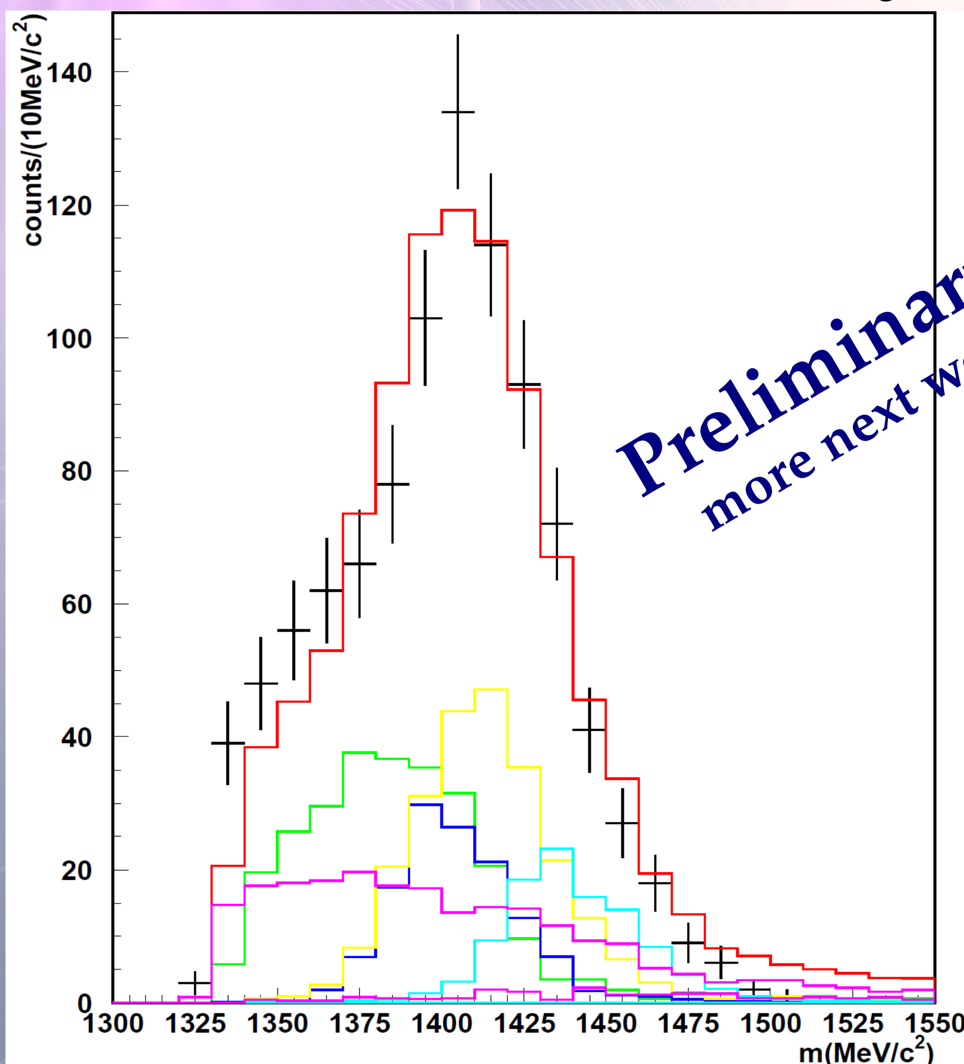

$m_{\Sigma 0\pi 0}$

Preliminary..
more next weeks

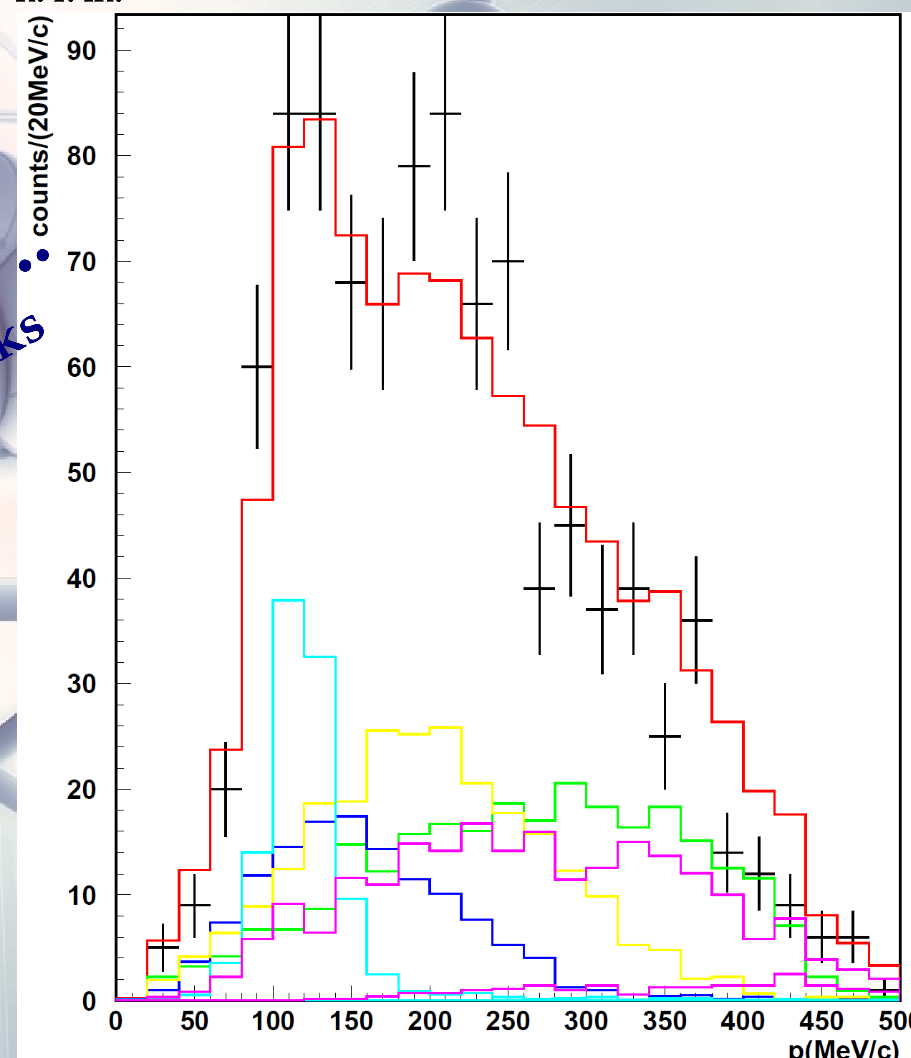

$p_{\Sigma 0\pi 0}$

$\Lambda\pi^-$ + extra-proton

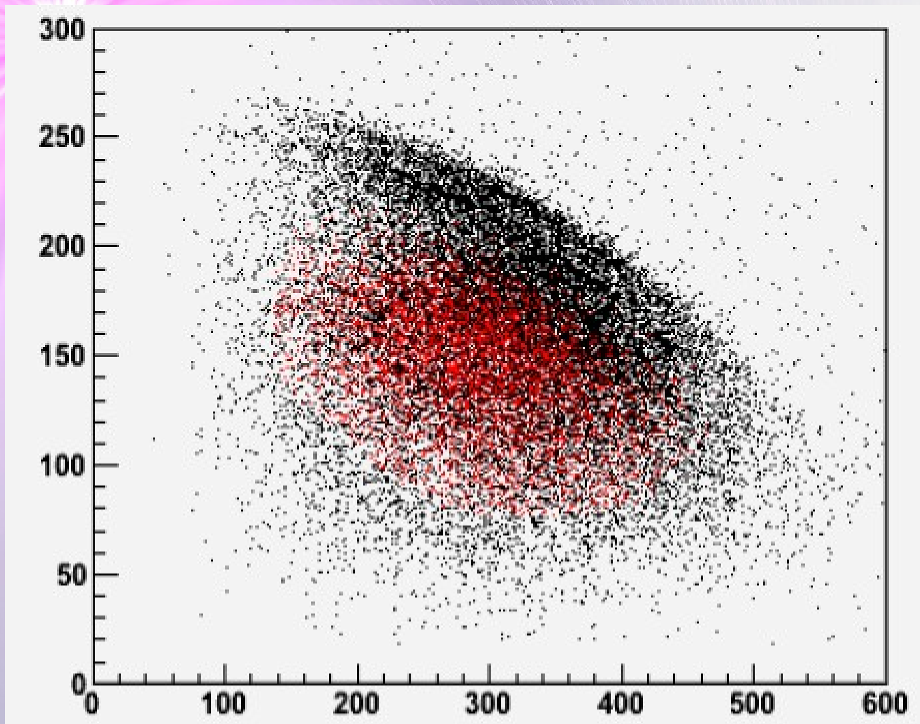

Black-> lambda + pi-
Red-> lambda + pi- **+ proton**

The extra-p indicates fragmentation of the residual nucleus (Σ / Λ conversion , Σ / Λ / π secondary interacions, multi-nucleon absorption) but ...

...

- if ($\Lambda\pi^-$ direct production) then 3% extra-p

- if ($\Lambda\pi^-$ in-direct production) then 25% extra-p